

Supplementary Materials

The macro-eco-evolutionary interplay between dispersal, competition, and landscape structure in generating biodiversity

Hagen O Viana SD Wiegand T Chase JM Onstein RE

Environment

We simulate 5 Myrs of environmental dynamics of four patches (i.e. A, B, C and D), inspired by a theoretical but realistic isolated island system placed in the south with a total area of 60X60 Km² with site area = 1 Km² and timestep=10'000 years and number of timesteps=501 (Animation 1). We consider dynamic topography, minimum and maximum temperature combined with sea level changes which intensify during the quaternary (~last 2.6 Ma) and happened in a periodicity of 100 ky (i.e. 10 timesteps) (Pillans, Chappell, and Naish 1998). This approximates earths eccentricity with a conservative periodicity (Shepard et al. 2018) and reflects interactions among global climate dynamics and changes in incoming solar radiation, likely influencing ecological and evolutionary patterns. We approximating empirical mean temperature and sea levels (Westerhold et al. 2020) (Hoffmann and Sgrò 2011). Our dynamic temperature oscillates at similar periodicity and temporal intensity, so that lower temperature periods match with the periods of lowest sea levels (*Figure 1*). Given the randomly attribute location on Earth, i.e. south hemisphere, The south sides of each patch were 2°C colder than the northern sides and were smoothed with a focal function of mean 3x3 sites (raster package). We derive T_{min} and T_{max} fluctuations though time decreasing 0.01°C (i.e. lapse rate 0.01°C/m) for each increase in altitude (m). We draw minimum and maximum temperature from site mean temperatures by respectively subtracting and adding the absolute values from a normal distribution with mean=0 and standard deviation $SD = \frac{E_i}{\max(E)}$. This means that the distance between T_{min} and T_{max} increases in likelihood the higher the scaled site elevation E_i (m) is. Lowest available elevation of all times was -115m and the highest elevation in all times was 803m from final timestep sea level (i.e. 0m). This result in temperature ranges of 0—5°C (Animation 1, *Figure 2*). In all our simulations we penalize connectivity though a cost multiplier of geographical distance (Hagen et al. 2021). We used a cost of four (4) for unsuitable sites (i.e. under sea level) and 1 for suitable sites with the addition of 0.1 per 100m slope difference between source and destination site. Empirical evidence suggest that for high elevation species, greater elevation equals greater dispersal barriers, as mountain peaks are often embedded in a low elevation matrix and thus creating an island-like system (Vasconcelos

et al. 2020). Moreover, by choosing a strong matrix resistance, i.e. four, we stress the effects of topography, geodynamics and sea-level changes considering habitat unsuitability within 10'000 years.

Our simulations started with three patches (i.e. A, B and C) which do not change in topography and end with four (i.e. A, B, C and D) patches (Figure 1). Patch A and B have their connectivity periodically increased as a result of a shallow land bridge that increases in connectivity depending on sea level changes (Figure 1, Figure 3, Figure 4) while patch C remains relatively isolated. Patch D starts appearing around 1.5 Ma as a result of topographic and sea level changes.

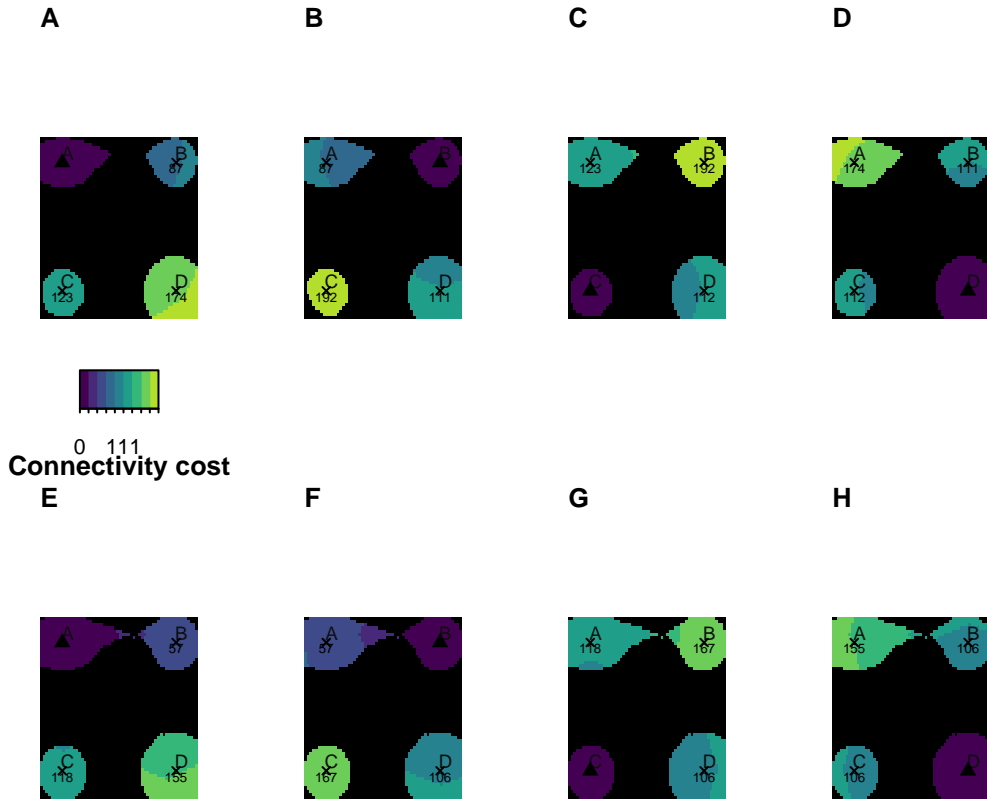


Figure 1: Connectivity costs in reference to the center of each patch (i.e. A,B,C and D) for two timesteps, i.e. Present (0 Ma, resp. A,B,C and D) and for 130'000 years ago (0.13 Ma, resp. E,F,G and H). Note the changes in connectivity due to sea level changes between the present and the lowest seal level period (i.e. 0.13 Ma).

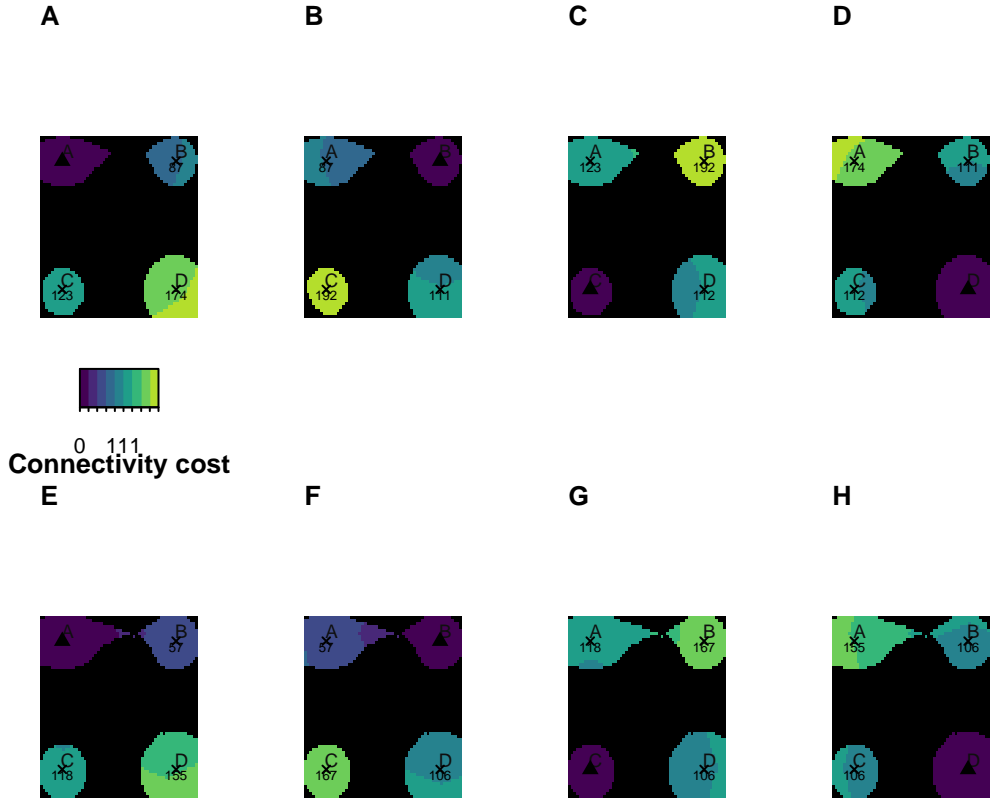


Figure 2: Connectivity costs in reference to the center of each patch (i.e. A,B,C and D) for two timesteps, i.e. Present (0 Ma, resp. A,B,C and D) and for 130'000 years ago (0.13 Ma, resp. E,F,G and H). Note the changes in connectivity due to sea level changes between the present and the lowest seal level period (i.e. 0.13 Ma).

Eco-evolutionary models

In short, M0 assume a fixed dispersal and competitive traits for all species within a simulation ($n=2000$). ME breaks this assumption by allowing dispersal and competitive traits to evolve freely, thus diverging with time between species ($n=2000$). MET adds a zero sum (i.e. a trade-off) between dispersal and competitive traits, assuming that no super species (i.e. $d_i = 1$, $l_i = 1$) are possible ($n=2000$). M0 serves as a reference and allowed the exploration of parameter ranges and sensitivity the system. The two alternative simulation scenarios (i.e. ME and MET), referred to as counterfactuals, investigate the effects of manipulating different components of the model. Specifically, these counterfactuals involved modifying the underlying biological model specifically referent to the evolution and trade-offs between dispersal and competitive abilities, focusing on how dispersal and species interactions affect colonization and other emergent properties in our eco-evolutionary models.

This automatically made species within a simulation not only diverge between each other on their temperature optime T_i and niche width ω_i (i.e. for M0, ME and MET), but also on dispersal d_i and competitive l_i traits (i.e. for ME and MET). For each counter-factual, we ran 2000 simulations with the same parameters for all models. This systematic exploration of alternative scenarios allowed us to assess the impact of specific model parameters on the resulting biodiversity patterns. We additionally run $XYZ = XYZ$. Specifically, we collected α , β and γ biodiversity metrics, colonization, speciation, extinction as well as trait proxies related to environmental and biotic suitability.

Initial conditions

All models, i.e. M0, ME and MET, were initiated at 5 Ma with three species, each with populations spread thought the suitable sites of each patch (i.e. sp1 on patch A, sp2 on patch B, and sp3 on patch C). Initial populations had thermal range $\omega_i = 0.4$ and thermal optimum equal to the local mean temperature $T_i = T_{mean}$.

We did a full factorial experiment ranging from extreme dispersal and competitive abilities $d_i = [0-1]$ $l_i = [0.9-1]$ and fixed $\Theta_s = 65$ (Figure 3). For model MET we impose the trade-off to the same parameters as in the other models, so that no initial species would have a “assumingly wrong” – meaning, wrong for consistency of MET. We randomized the seed at this stage, so that each single simulation could be reproduced.

Dispersal

Frequencies of dispersal are given according to a Weibull function that has scale changed by d resulting in concentrated short range dispersal events for small d with increasingly larger and longer tails for larger d (Figure 4).

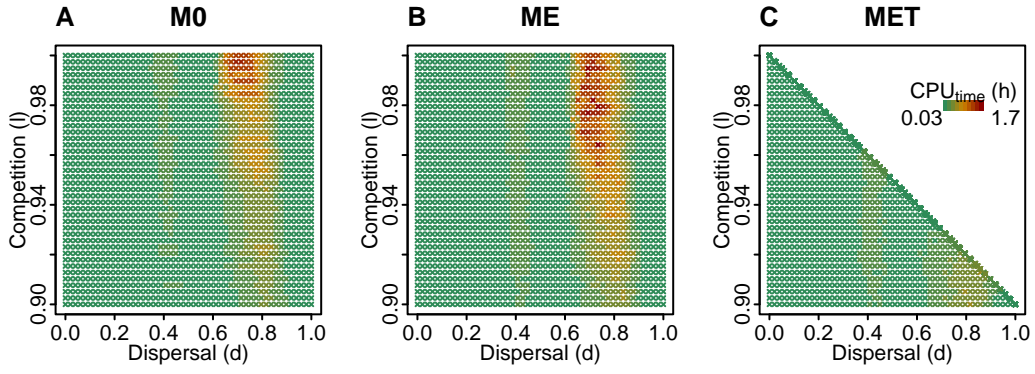


Figure 3: Initial competition and dispersal parameters for the main models and experiments.
Colors show the CPU time per simulation ($n=6000$).

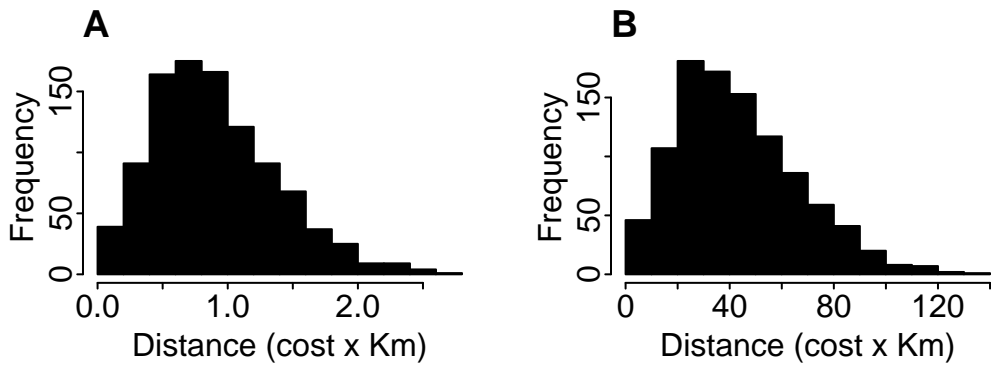


Figure 4: Histogram showing two extreme frequencies of 1000 dispersal events in a weibull distribution with shape of 2 and scale of 1 (A) and 50 (B). Note the difference of the x axis scales.

Ecological equilibrium

Ecological equilibrium was assumed for every site and for every timestep. Environmental fitness considered min and max temperature. Population size N_i changes according to local site conditions (i.e. T_{min}, T_{max} [9–26°C] and evolving species temperature optimum T_i and thermal range ω_i according to the geometric mean of a Gaussian environmental function at minimum and maximum site temperature (for an example, see Figure 5).

Relative growth rate decreases linearly with conspecific population size B_i in the site with a conspecific interaction coefficient α_{ff} and a heterospecific interaction coefficient α_{fh} . The conspecific interaction coefficient was fixed for all simulations (i.e. $\alpha_{ff} = 0.2$), since our focus was on components on intrerspecific competition, i.e. modulated though heterospecific tolerance trait (l). For an example, see the interactions between three (3) and thirteen (13) species though ODE (i.e. 30 interaction) in our Lotka-Volterra model type (Figure 6 AB and C respectively).

Equilibrium equations

We want to estimate the equilibrium of our Lotka-Volterra model that describes the dynamics of a focal species f in a given site, depending on other heterospecific species k :

$$\frac{dN_f}{dt} \frac{1}{N_f} = r_f - \alpha_{ff} N_f - \alpha_{fh} \sum_{k \neq f} N_k \quad (1)$$

with parameters r_f , α_{ff} and α_{fh} . We first estimate the carrying capacity of a local population of species f (that is the equilibrium for the case $\alpha_{fh} = 0$), that is determined by given by $N_f = r_f / \alpha_{ff}$ and by inserting the site-condition dependency of the maximal per capita growth rate r_f from equation 2 we obtain

$$K_f = \frac{r_f}{\alpha_{ff}} = \frac{g}{\alpha_{ff}} \times \sqrt{n_f(T_{min}) \times n_f(T_{max})} \quad (2)$$

The total population size of all species in the site is given by $J = \sum_{i=1}^S N_i$ where S is the total number of species in the site. Assuming zero-sum dynamics, which emerges if there is density dependence at the individual scale (e.g., through crowding competition), the number of heterospecifics at the site is given in good approximation by $\sum_{i \neq f} N_i = J - N_f$. Thus, equation 1 in equilibrium simplifies to

$$0 = r_f - \alpha_{ff} N_f^* + \alpha_{fh} N_f^* - \alpha_{fh} J \quad (3)$$

which leads to $r_f - \alpha_{fh} J = (\alpha_{ff} - \alpha_{fh}) N_f^*$, which yields the equilibrium

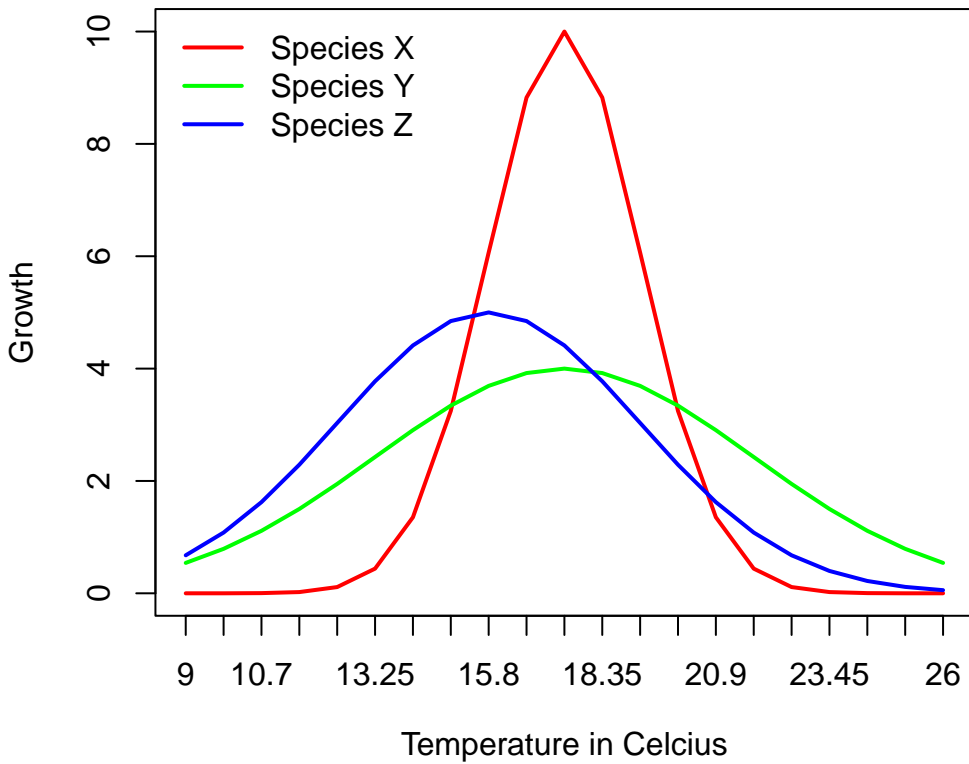


Figure 5: Population growth across a temperature gradient in °C for three different species with varying thermal optimum (T) and thermal range (ω) traits. Species X (dark red) has $T=18^\circ\text{C}$ and $\omega=0.1$; Species Y (green) has $T=18$ and $\omega=0.25$; Species Z (blue) has $T=16$ and $\omega=0.2$. Temperature-dependent growth is applied a constant and equal rate to all simulations. Maximal growth is proportional to the geometric mean of the fitness of the focal species at the minimal and maximal temperature in the site.

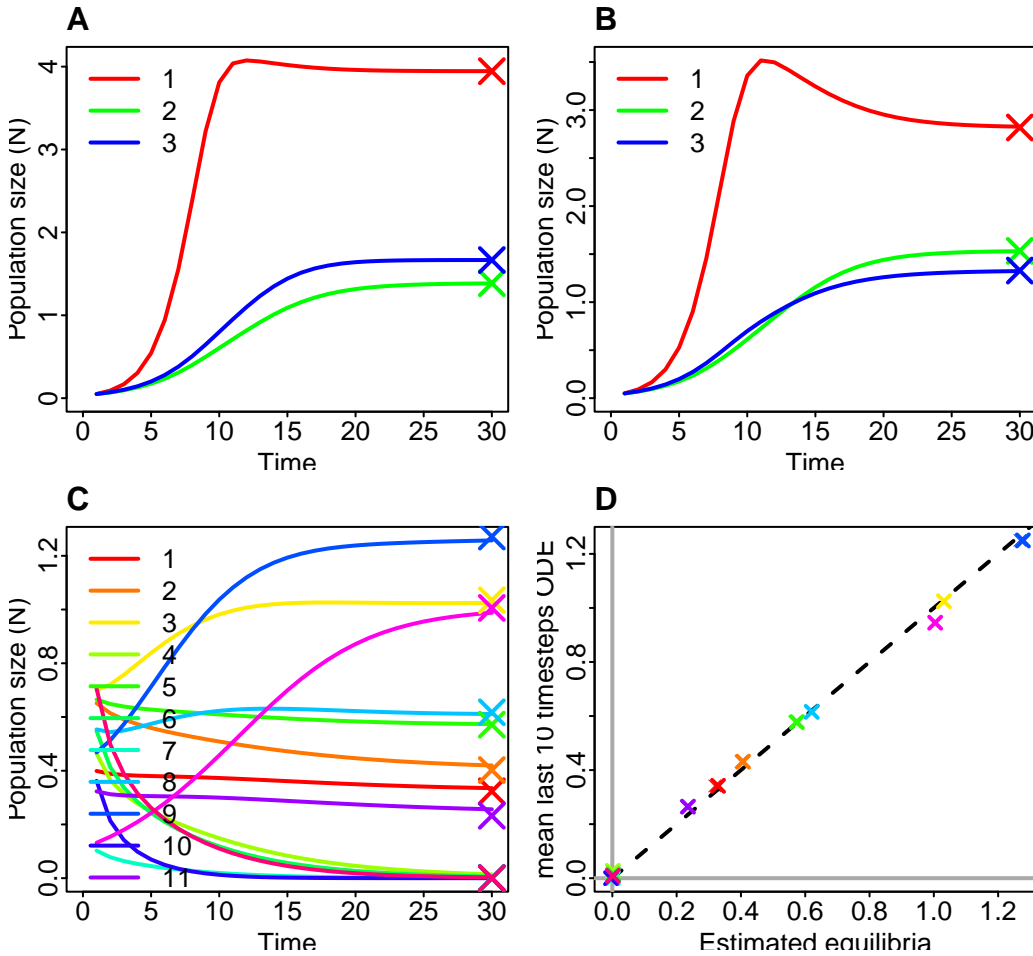


Figure 6: Local dynamics within 10'000 years showing population size changes for different communities (ABC) and comparison of mean last 10 timesteps of the ODE against estimated equilibria (D). Crosses show the estimated ecological equilibria. (A) Species 1 and 2 have a thermal optimum closer to the thermal optimum between site min and maximal temperatures than species 3. Moreover, species 1, 2 and 3 have thermal range of $\omega_1 = 0.1, \omega_2 = 0.25, \omega_3 = 0.2$ and same heterospecific tolerance ($l=0.98$). (B) we change heterospecific tolerance to ($l_1 = 0.9, l_2 = 0.98, l_3 = 0.96$). (C) Random community of 13 species. (D) Comparison of mean last 10 timesteps of ODE of community in (C) against estimated equilibria; grey lines show zero lines and dashed line show the 1-1 line. Note that we use here only 30 interactions though time and we increase in precision by increasing the number of interactions (ODE timesteps) and decreasing the number of coexisting species.

$$N_f^* = \frac{r_f - \alpha_{fh} J}{\alpha_{ff} - \alpha_{fh}} \quad (4)$$

Thus, besides the condition that $\alpha_{ff} > \alpha_{fh}$ (i.e. the conspecific interaction coefficient is larger than the heterospecific interaction coefficient), feasibility (i.e., a positive equilibrium N_f^*) requires that

$$\alpha_{fh} J < r_f \quad (5)$$

which also means that heterospecific competition must be sufficiently small to allow population growth at low populations sizes (this is the so called invasion criterion). Note that we obtain from equation 5 for small abundances of the focal species f the per-capita population growth rate $\frac{dN_f}{dt} \frac{1}{N_f} = r_f - \alpha_{fh} J$, which is positive if equation is satisfied. As explained in detail in Wiegand et al. (2021), the total population size J in one site at equilibrium can be then be estimated as

$$J = \frac{\sum_{f=1}^S \frac{\alpha_{ff} K_f}{\alpha_{ff} - \alpha_{fh}}}{(1 + \sum_{f=1}^S \frac{\alpha_{fh}}{\alpha_{ff} - \alpha_{fh}})} \quad (6)$$

In the special case where the interaction coefficients are the same for all species (as in our M0 model), we can derive a more detailed condition for the per capita population growth rates $r_f = \alpha_{ff} K_f$ to obtain positive abundances. In this case the community size J of the community in equilibrium can be estimated as

$$J = \frac{S \frac{1}{\alpha_{ff} \alpha_{fh}}}{(1 + S \frac{\alpha_{fh}}{\alpha_{ff} - \alpha_{fh}})} \frac{1}{S} \sum_{f=1}^S r_f \quad (7)$$

and with $\bar{r}_f = \frac{1}{S} \sum_{f=1}^S r_f$ being the community average maximal per capita population growth rate we find together with equation 4 the feasibility condition.

$$\frac{r_f}{\bar{r}_f} > \frac{S \alpha_{fh}}{\alpha_{ff} + \alpha_{fh}(S-1)} = \mu \quad (8)$$

The factor μ is always smaller than one and particularly small if the number of species (S) and the heterospecific interaction coefficient α_{fh} are small. It approaches a value of one if the species richness S becomes large and/or if heterospecific competition α_{fh} approaches the strength of conspecific competition α_{ff} . Equation 8 defines a minimum value for the growth rate r_f to allow for a positive equilibrium. Equation 8 thus tells us that a species will go extinct in a given site (i.e. having a negative equilibrium abundance) if its maximal per capita population growth rate r_f is too small, compared to the average per capita population growth

rate \bar{r}_f of all species at the site. Importantly, the environmental conditions, leading to lower growth rate r_f , can be poorer if there are fewer species at the site and/or if heterospecific competition is weaker.

To estimate equilibrium in the context of competition dynamics, we implement an iterative approach. Firstly, all species in a site are checked to determine if $a_{ff} > a_{hf}$ (condition 1, eq. 4). If not, the species is removed from consideration as conspecifics compete weaker than heterospecifics. Next, the carrying capacity (J^*) is estimated based on the values of K_f, a_{ff}, a_{fh} for each species f (eq. 2). Then, all species are checked again to see if the product of the intraspecific competition coefficient and carrying capacity is greater than the product of the interspecific competition coefficient $a_{ff}K > a_{fh}J^*$ (condition 2, eq. 4). Species that do not meet this condition, indicating a too low carrying capacity, are removed, and the estimation process returns estimating J^* (eq. 6). This is repeated until all remaining species satisfy the condition 2. Finally, the equilibrium of each species N_f^* is demonstrated using equation 6 (Figure 6).

Summary statistics

We conducted several statistics using custom and code from several R-packages [Kembel et al. (2010)](Bortolussi et al. 2006)(Castiglione et al. 2021), specifically, $\log_{10}(\bar{\alpha})$: Log 10 of mean alpha diversity (all sites) at final timestep. \overline{occup} Km²: Mean regional occupancy calculated in Km² according to the mean number of sites occupied by all species through time. $Occupancychange$: Proportion of occupancy change during the simulation. $\frac{Slope\ dispersal}{T_{start}/T_{end}}$: Rate of change in dispersal trait over time. $Dispersal(d)_{t_{start}}$: Dispersal trait value at the initial timestep. ϕ : Speciation threshold or time of isolation until reproductive isolation occurs. $l_{t_{start}}$: Competition trait value at the initial timestep. $Extinction\ prop.$: Proportion of extinction events in a simulation over final gamma diversity. $Speciation\ prop.$: Proportion of speciation events in a simulation over final gamma diversity. γ : Final gamma diversity, or final regional taxonomic richness (number of species alive at the last timestep). $Turnover$: Turnover between speciation and extinction. $Speciation\ invar.$: Temporal speciation invariability. $Extinction\ invar.$: Temporal extinction invariability. $Turnover\ invar.$: Temporal turnover invariability. $\bar{N}_{5\% t_{end}}$: Mean population size of its 5% quantile at final timestep. $\bar{N}_{50\% t_{end}}$: Mean population size at final timestep. $\bar{N}_{95\% t_{end}}$: Mean population size of its 95% quantile at final timestep. \bar{PD}_α : The Mean Faith's Phylogenetic Diversity at the site level. $\bar{\alpha}$: Mean alpha diversity of the entire archipelago. $\beta\%$: Proportional species turnover. βW : Whittaker beta diversity. $Zeta\ zeta$: Proportion of species that are common to all assemblages. $Eta\ eta$: Proportion of species that are not unique to an assemblage nor common to all assemblages. $Theta\ theta$: Species that are unique to an assemblage. PD_S : Standardized value of the unrooted Phylogenetic Diversity measure for species. MPD_S : Standardized value of the Mean Pairwise Distance measure. $MNTD_S$: Standardized value of the mean nearest taxon distance measure. CD_{X-Y} : Standardized Community Distance between two locations. $Mode\ d$: Number of modes at the dispersal trait distribution at final timestep.

$\bar{d}_{50\% t_{end}}$: Mean dispersal trait at final timestep. $\bar{T}_{50\% t_{end}}$: Mean thermal optimum trait at final timestep. $\bar{\omega}_{50\% t_{end}}$: Mean thermal range trait at final timestep. $\bar{l}_{50\% t_{end}}$: Mean tolerance to other species trait at final timestep. $Spread d t_{end}$: The range between the lowest and highest dispersal trait values at the final timestep. $\beta_{max split}$: The complete phylogenetic beta value derived from the Maximum Likelihood estimation within the Beta-splitting model. Additional recorded values include: *Finished*: Status of final simulation, if OK, simulation was finished. *CPU time (h)*: CPU time in hours for simulation.

M0

M0 diversity statistics reflected our expectations on general patterns of diversity, such as highest spetiation rates at intermediary diversity diversity levels Figure 7 . Meaning that peaks of γ diversity relate with the spatial structure of our landscape. After investigation, all speciation events of simulations with dispersal $d_i < 0.1$ happened within patches, and mostly during the dynamic phase (Figure 16 A). Speciation within patches was only observed in M0, as for ME and MET dispersal quickly evolved beyond the critical and small. We also can notice the qualitative changes in speciation events for intermediary dispersal $d_i = [0.15 - 0.55]$, which started involving speciation events between patches C and D, but for patch D only at the dynamic time phase, i.e. 2–0 Ma (Figure 16 C).

Investigating spatial dynamics for M0 during 4.5-0Ma (Figure 17 A-D) shows that mean occupancy increases with dispersal, while changes leave scale signatures and show that proportional change (i.e. $\frac{(increase-decrease)}{total occupancy}$). decreases with competition, while neutral models have higher proportional increase/decrease ratio. Moreover, we can see that this signature was stronger during the dynamic stage of this simulations (Figure 17 I-L).

Inspecting the community distances between all the patches, there is a clear effect of increase in community diversity with patch distance and dispersal ability Figure 14 . As expected [refs], competition tends to decrease community distance overall where communities reach maximum diversity. The combination of community distances between islands A, B, C, and D is depicted for M0 in Figure 15. Each line corresponds to simulations with the same competitive value. Community distance represents the standardized value of the community distance, akin to the beta diversity version of the Mean Pairwise Distance (MPD), which provides the average phylogenetic distance between two communities.

ME

Figure Figure 19 captures the evolving spatial patterns and occupancy dynamics of species from 4.5 million years ago (Ma) to the present. This visualization portrays a period of stability between 4.5 and 2.5 Ma, followed by a phase of significant change from 2 to 0 Ma, elucidating the evolutionary trajectory of species occupancy over millennia.

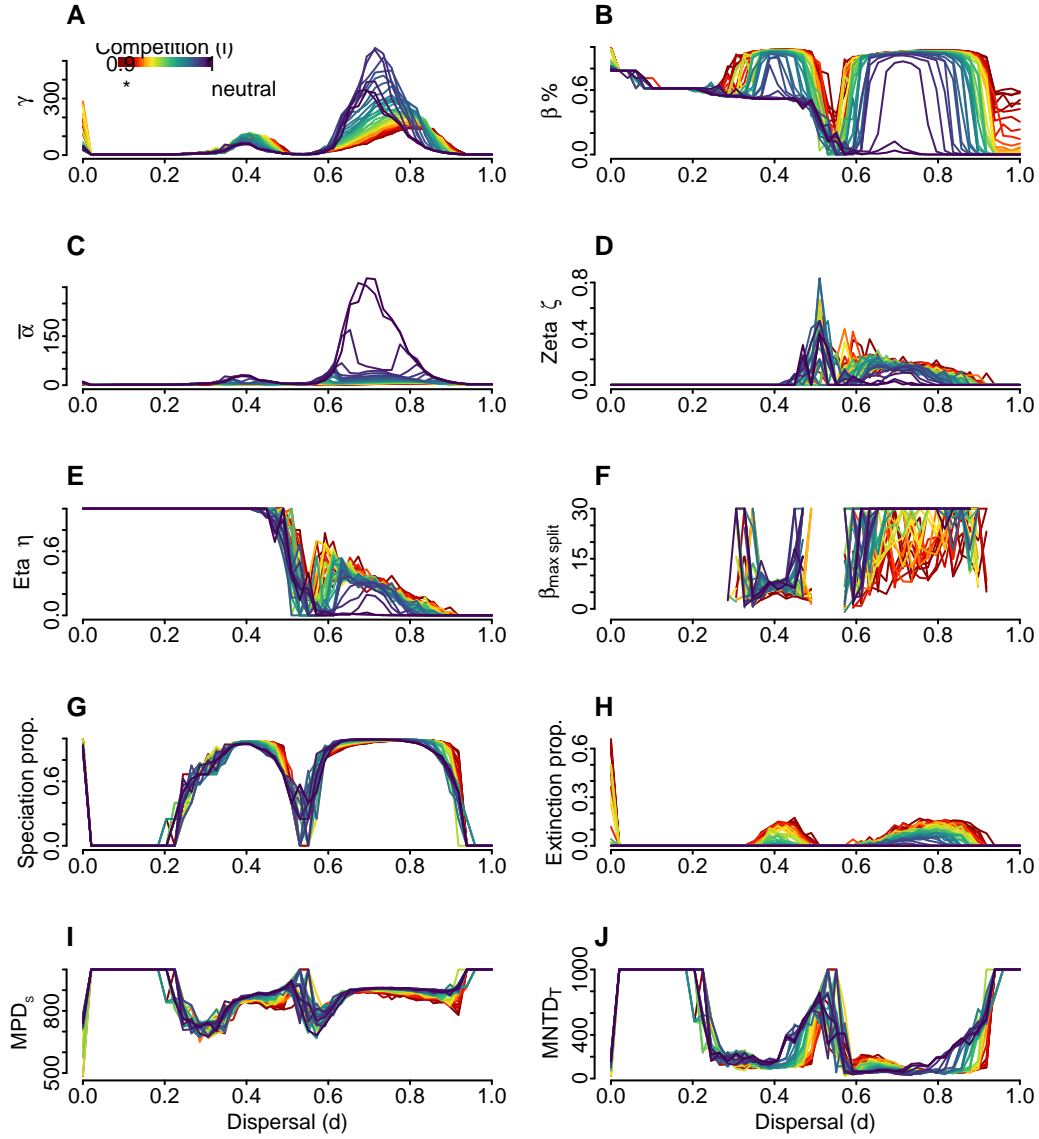


Figure 7: Summary statistics for M0 through dispersal. Each line corresponds to simulation within a same competitive value along dispersal ability at the initial timestep. (A) Final gamma diversity, or final regional taxonomic richness (number of species alive at the last timestep). (B) Proportional species turnover, i.e. $1 - \text{mean}(\alpha/\gamma)$ quantifies what proportion of the species diversity in the dataset that is not contained in an average site (C) Mean alpha diversity of the entire archipelago. (D) Proportion of species that are common to all assemblages. Zeta diversity sensu Hui and McGeoch (2014). (E) Proportion of species that are not unique to an assemblage nor common to all assemblages. (F) The complete phylogenetic beta value derived from the Maximum Likelihood estimation within the Beta-splitting model. This is computed using the `maxlik.betasplit` function from the `apTreeshape` package. (G) Proportion of speciation events in a simulation over final gamma diversity. (H) Proportion of extinction events in a simulation over final gamma diversity. (I) Standardized value of the Mean Pairwise Distance measure on the archipelago, calculated using the `mpd` function from the `picante` package. (J) Standardized value of the mean nearest taxon distance measure for the entire archipelago.

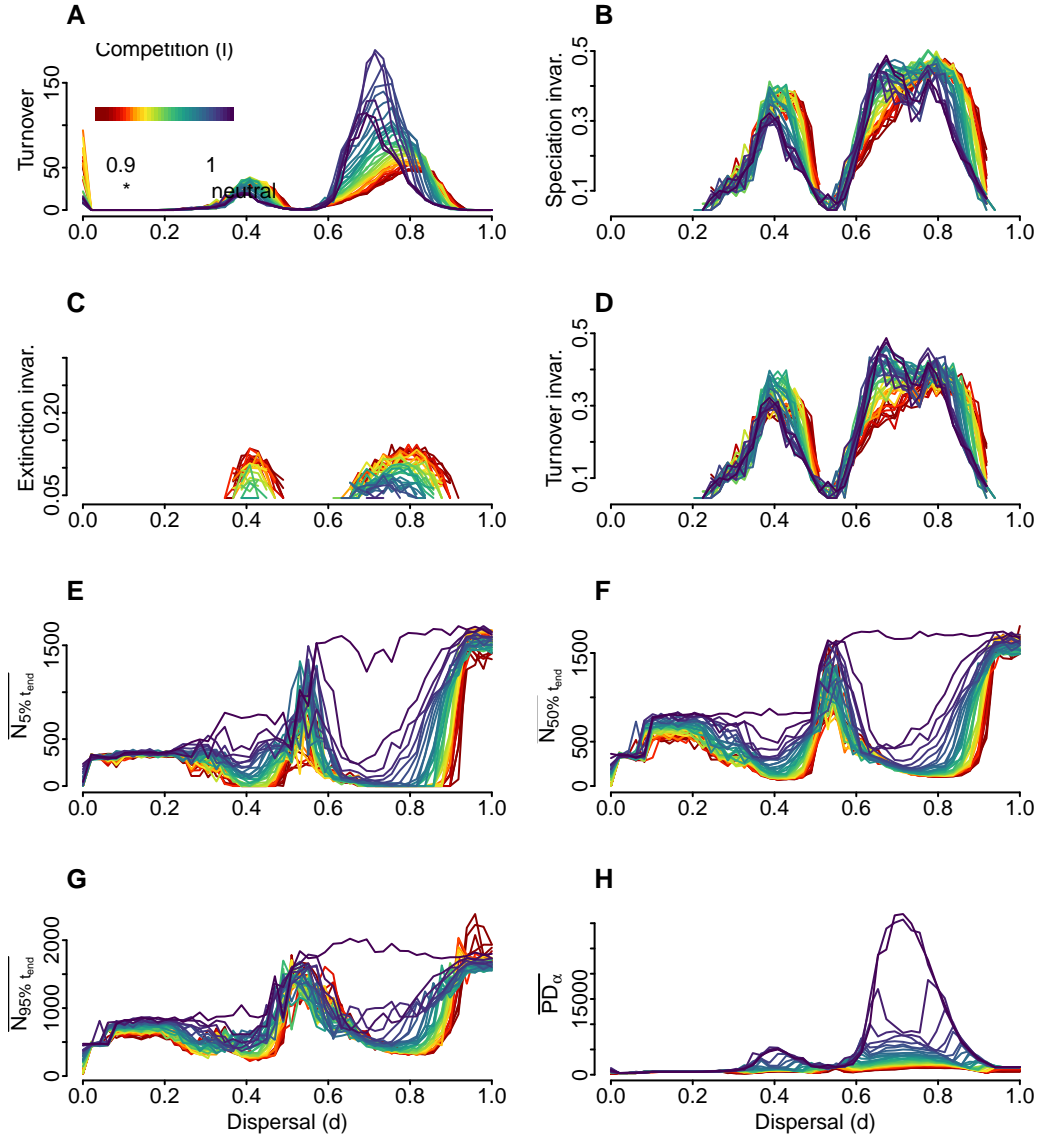


Figure 8: Additional summary statistics for M0 though initial dispersal values. Each line corresponds to simulations within a same competitive value, along dispersal ability. (A) Turnover between speciation and extinction. I.e. the sum of speciation - extinction for all timesteps divided by the number of initial species. (B) Temporal speciation invariability, also referred to as temporal stability of speciation events. (C) Temporal extinction invariability, also referred to as temporal stability of extinction events. (D) Temporal turnover invariability, also referred to as temporal turnover stability. (E) Mean population size of its 5% quantile at final timestep. (F) Mean population size at final timestep. (G) Mean population size of its 95% quantile at final timestep. (H) The Mean Faith's Phylogenetic Diversity (PD) at the site level, quantifies the total branch lengths and was calculated with the function PD from the picante package.

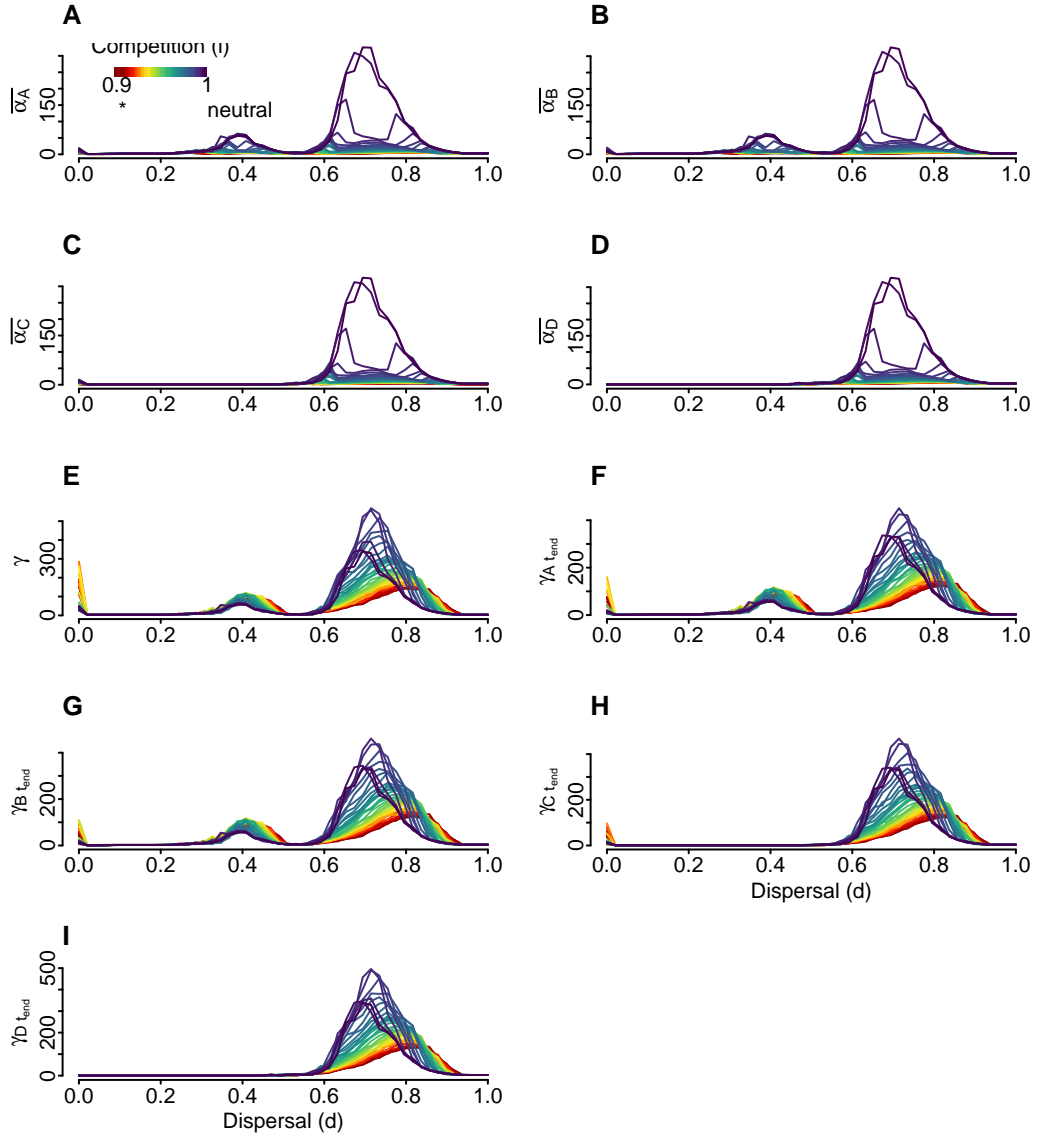


Figure 9: Additional summary statistics for M0 though initial dispersal values. Each line corresponds to simulations within a same competitive value, along dispersal ability. (A) Mean alpha diversity of sites on island A. (B) Mean alpha diversity of sites on island B. (C) Mean alpha diversity of sites on island C. (D) Mean alpha diversity of sites on island D. (E) Final gamma diversity, or final regional taxonomic richness (number of species alive at the last timestep). (F) Final gamma diversity of island A, or final regional taxonomic richness (number of species alive at the last timestep). (G) Final gamma diversity of island B. (H) Final gamma diversity of island C. (I) Final gamma diversity of island D.

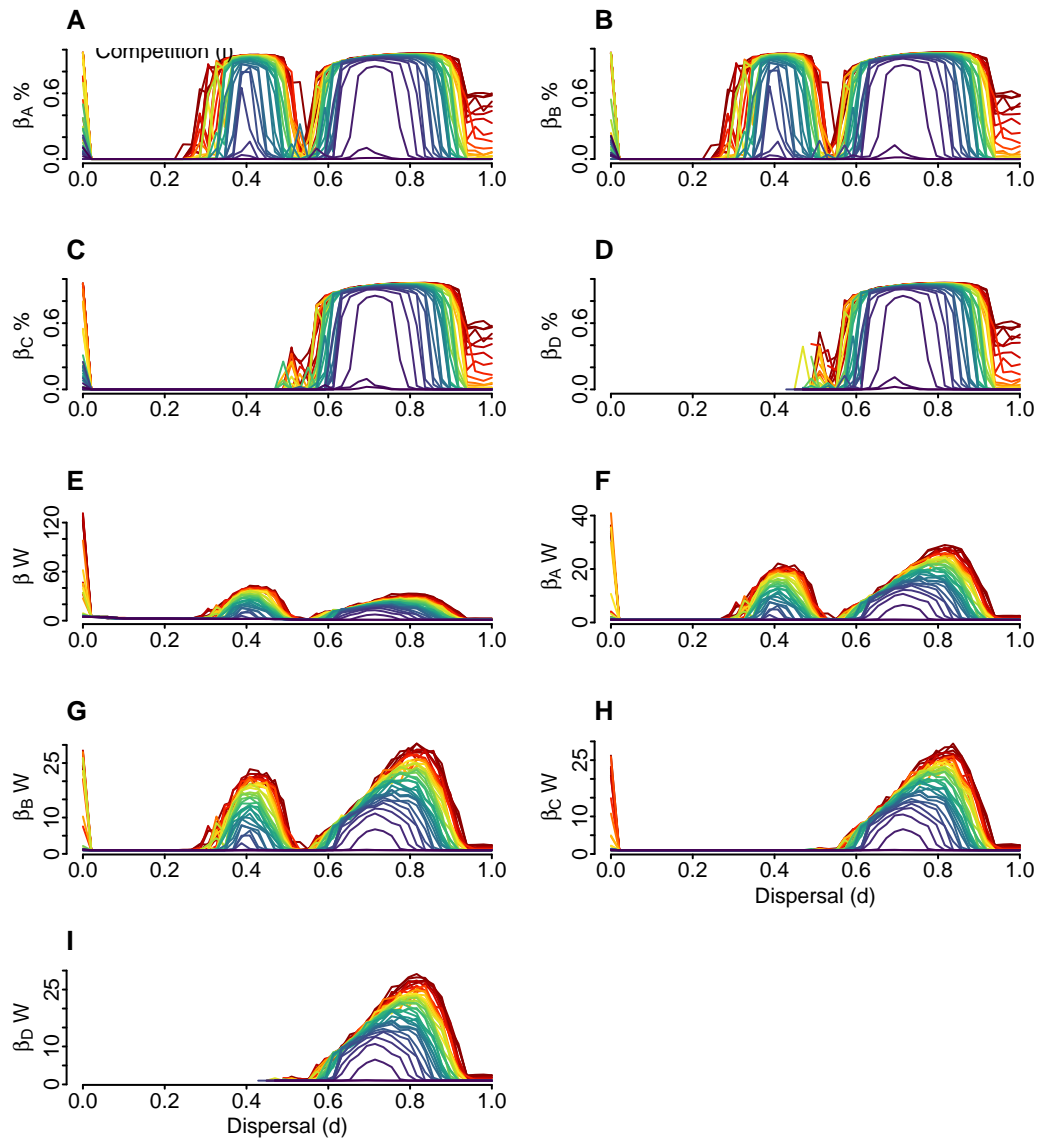


Figure 10: Additional summary statistics for M0 though initial dispersal values. Each line corresponds to simulations within a same competitive value, along dispersal ability. (A) Proportional species turnover in island A. (B) Proportional species turnover in island B. (C) Proportional species turnover in island C. (D) Proportional species turnover in island D. (E) Whittaker beta diversity, i.e. gamma/mean(alpha), how many subunits there would be if the total species diversity of the mean species diversity per subunit remained the same, but the subunits shared no species. (F) Whittaker beta diversity of island A. (G) Whittaker beta diversity of island B. (H) Whittaker beta diversity of island C. (I) Whittaker beta diversity of island D.

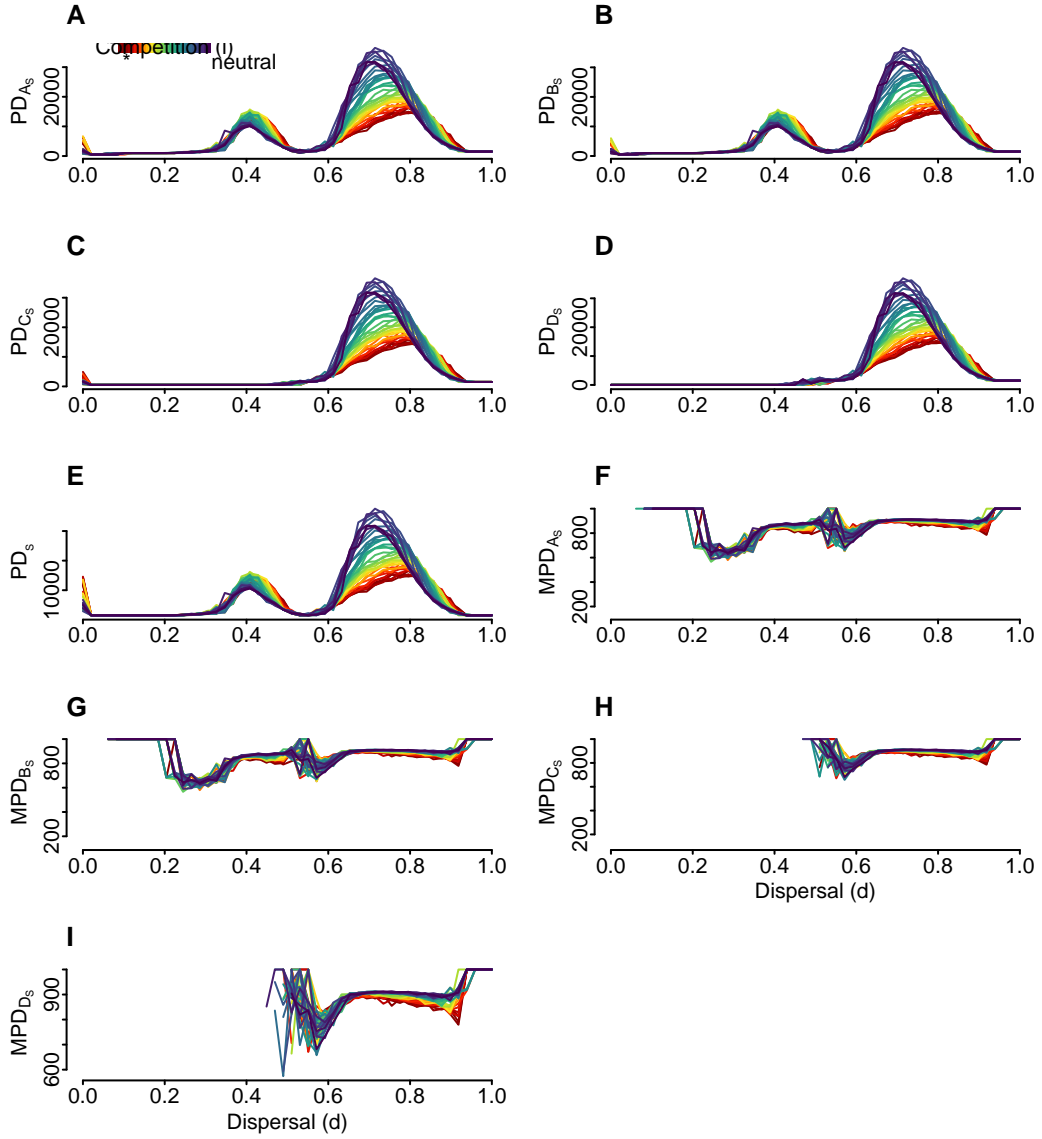


Figure 11: Additional summary statistics for M0 though initial dispersal values. Each line corresponds to simulations within a same competitive value, along dispersal ability. (A) Standardized value of the unrooted Phylogenetic Diversity measure for species in island A. (B) Standardized value of the unrooted Phylogenetic Diversity measure for species in island B. (C) Standardized value of the unrooted Phylogenetic Diversity measure for species in island C. (D) Standardized value of the unrooted Phylogenetic Diversity measure for species in island D. (E) Standardized value of the unrooted Phylogenetic Diversity measure for species on the archipelago, calculated using the `pd` function from the `picante` package. (F) Standardized value of the Mean Pairwise Distance measure in island A. (G) Standardized value of the Mean Pairwise Distance measure in island B. (H) Standardized value of the Mean Pairwise Distance measure in island C. (I) Standardized value of the Mean Pairwise Distance measure in island D.

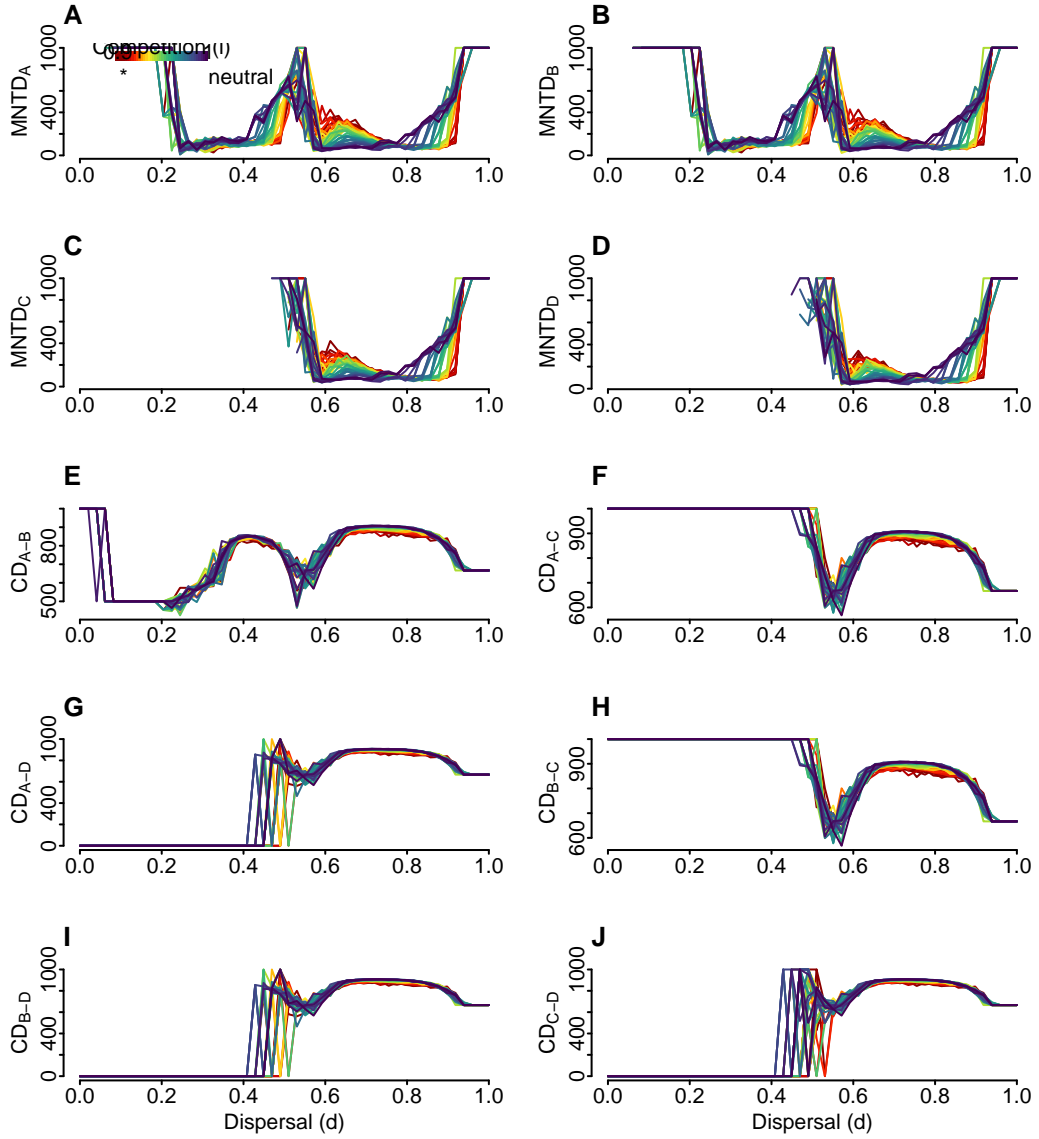


Figure 12: Additional summary statistics for M0 though initial dispersal values. Each line corresponds to simulations within a same competitive value, along dispersal ability. (A) Standardized value of the mean nearest taxon distance measure for the island A. (B) Standardized value of the mean nearest taxon distance measure for the island B. (C) Standardized value of the mean nearest taxon distance measure for the island C. (D) Standardized value of the mean nearest taxon distance measure for the island D. (E) Standardized Community Distance between island A and B. It is the beta diversity version of Mean Pairwise Distance (MPD), giving the average phylogenetic distance between two communities. (F) Standardized Community Distance between island A and C. (G) Standardized Community Distance between island A and D. (H) Standardized Community Distance between island B and C. (I) Standardized Community Distance between island B and D. (J) Standardized Community Distance between island C and D.

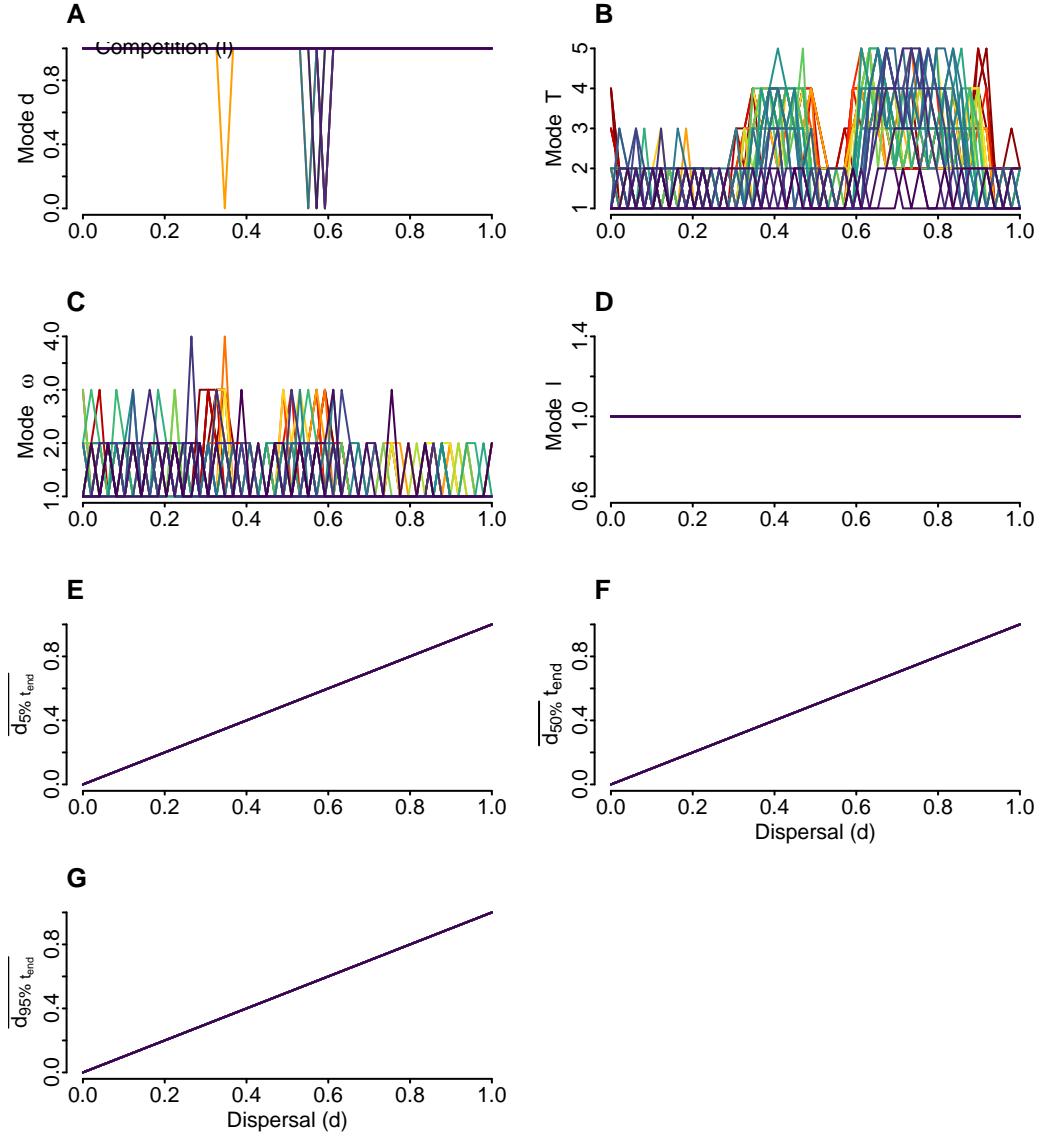


Figure 13: Additional summary statistics for M0 though initial dispersal values. Each line corresponds to simulations within a same competitive value, along dispersal ability. (A) Number of modes at the dispersal trait distribution at final timestep, i.e. no modes (such as in a uniform distribution), or more. Calculated with the function ‘Mode’ from package LaplacesDemon. (B) Number of modes at the thermal optimum distribution at final timestep. (C) Number of modes at the thermal range trait distribution at final timestep. (D) Number of modes at the competition trait (i.e. tolerance to other species) distribution at final timestep. (E) Mean dispersal trait of its 5% quantile at final timestep. (F) Mean dispersal trait at final timestep. (G) Mean dispersal trait of its 95% quantile at final timestep.

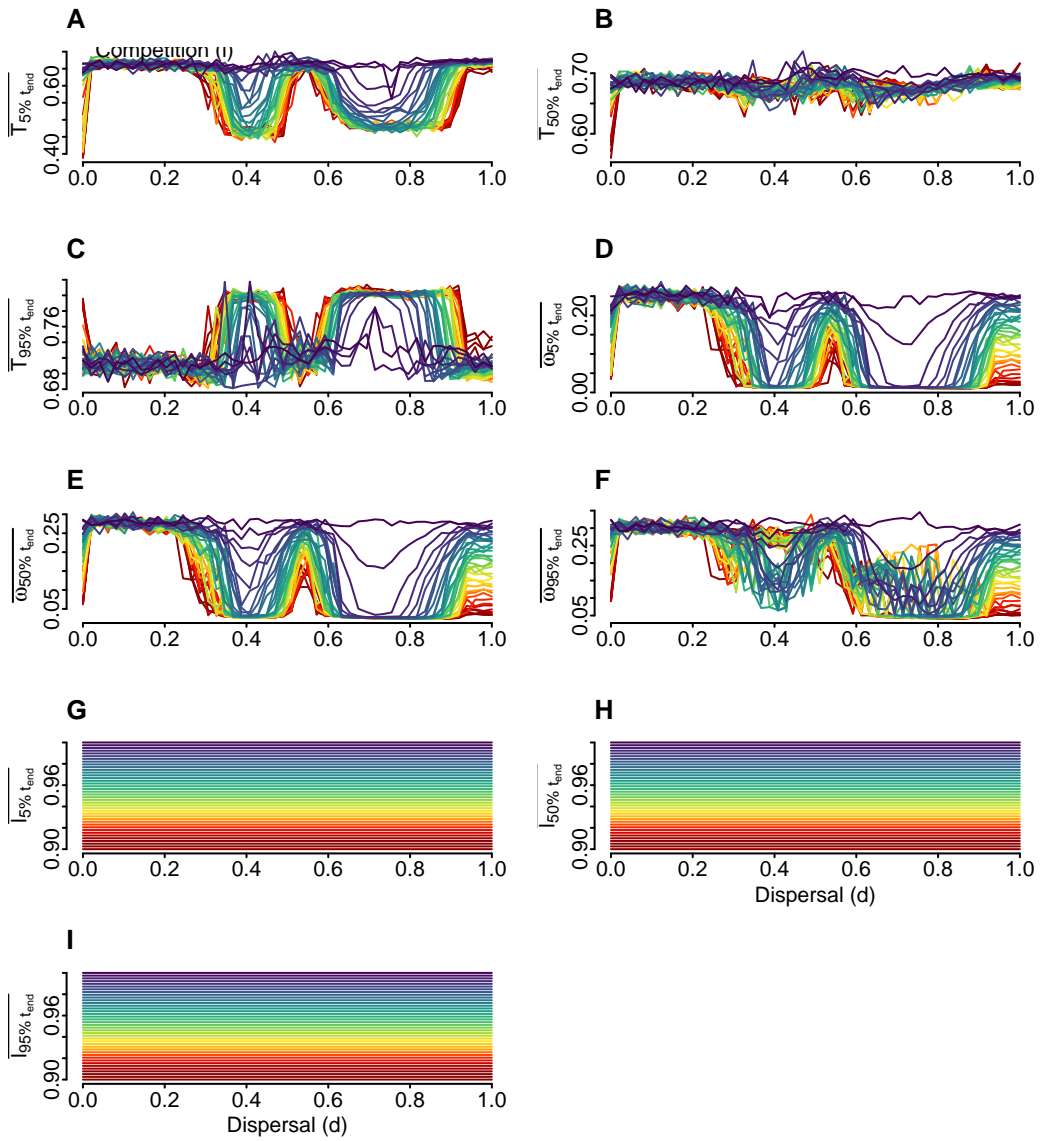


Figure 14: Additional summary statistics for M0 though initial dispersal values. Each line corresponds to simulations within a same competitive value, along dispersal ability. (A) Mean thermal optimum of its 5% quantile at final timestep. (B) Mean thermal optimum at final timestep. (C) Mean thermal optimum of its 95% quantile at final timestep. (D) Mean thermal range trait of its 5% quantile at final timestep. (E) Mean thermal range trait at final timestep. (F) Mean thermal range trait of its 95% quantile at final timestep. (G) Mean tolerance to other species trait of its 5% quantile at final timestep. (H) Mean tolerance to other species trait at final timestep. (I) Mean tolerance to other species trait of its 95% quantile at final timestep.

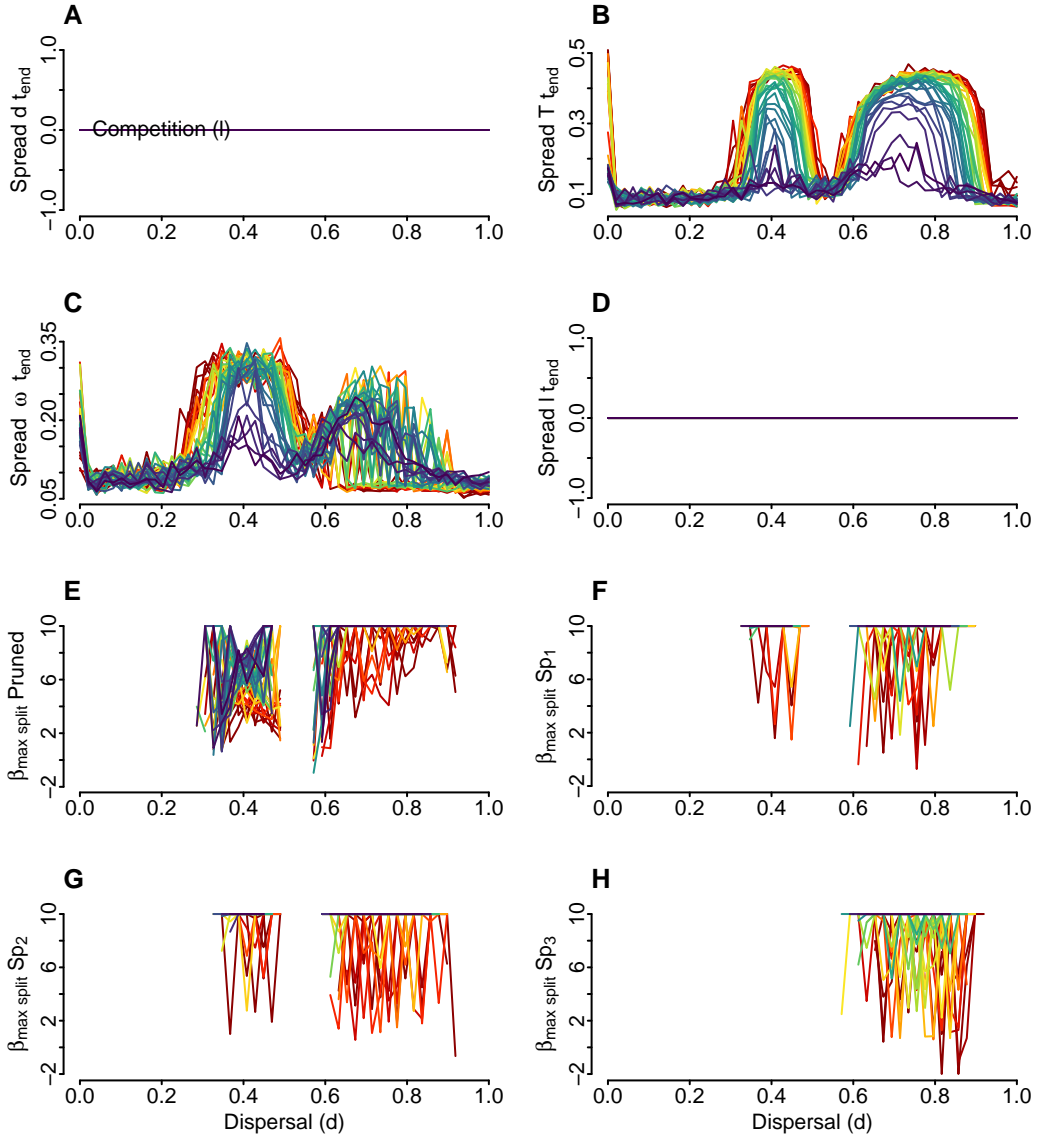


Figure 15: Additional summary statistics for M0 though initial dispersal values. Each line corresponds to simulations within a same competitive value, along dispersal ability. (A) The range between the lowest and highest dispersal trait values at the final timestep. (B) The range between the lowest and highest thermal optimum values at the final timestep. (C) The range between the lowest and highest thermal range trait values at the final timestep. (D) The range between the lowest and highest tolerance to other species trait values at the final timestep. (E) The pruned phylogeny beta value, excluding extinct branches, derived from the Maximum Likelihood estimation within the Beta-splitting model. (F) The pruned phylogeny beta value of species 1, excluding extinct branches. (G) The pruned phylogeny beta value of species 2, excluding extinct branches. (H) The pruned phylogeny beta value of species 3, excluding extinct branches.

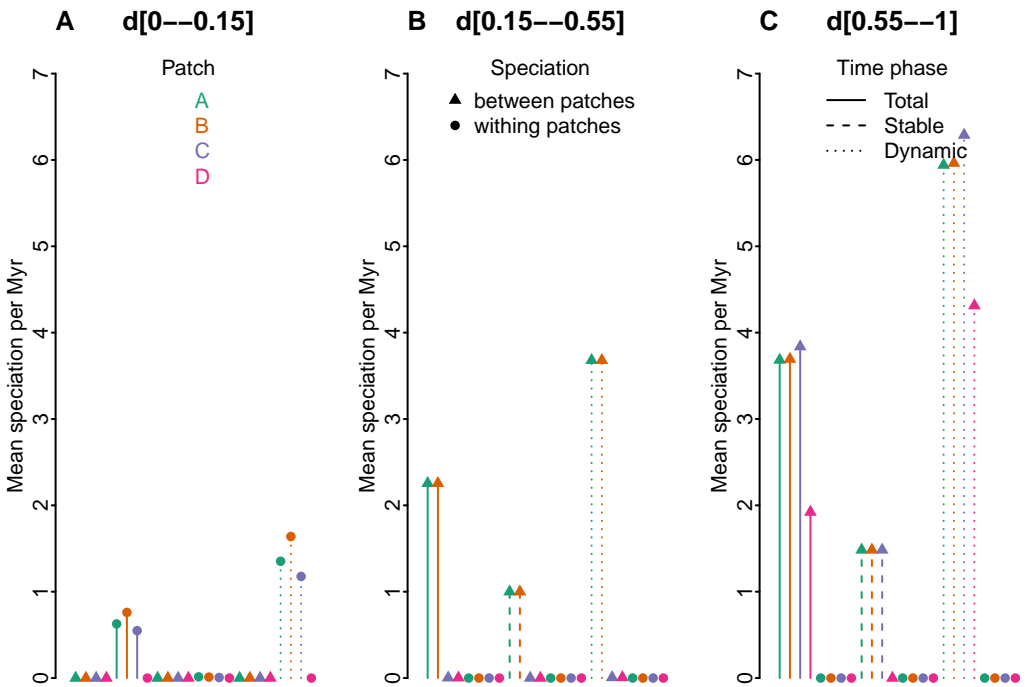


Figure 16: Mean speciation percentage for M0 with dispersal (A) smaller than, 0.15; (B) between 0.15 and 0.55; and (C) bigger than 0.55. We show for each patch (in different colors) and each phase (i.e. Total 4.5-0Ma, Stable 4.5-2.5Ma, Dynamic 2-0Ma) for speciation events between or within patches (respectively triangles and circles).

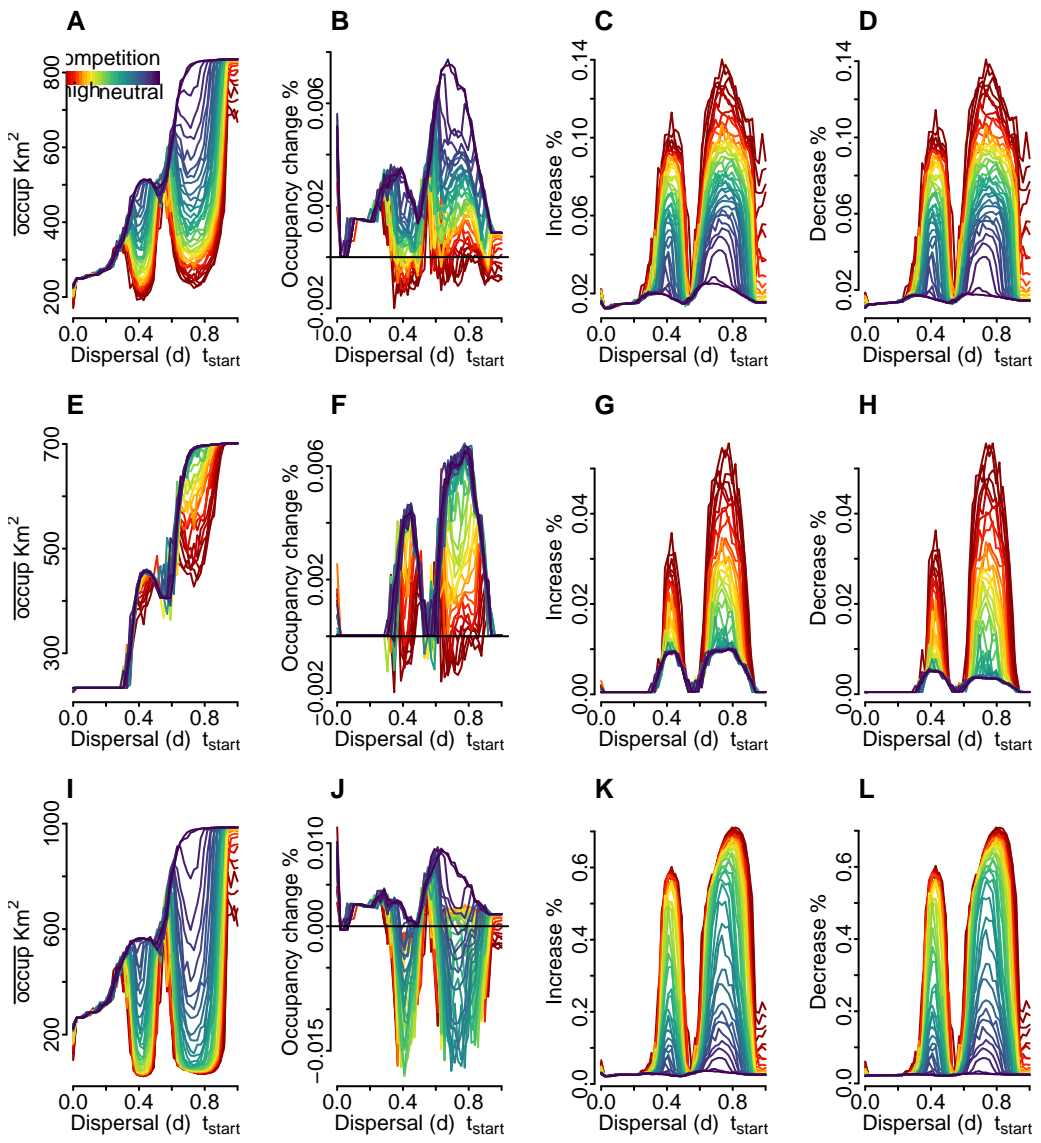


Figure 17: Spatial dynamics of M0 from 4.5 to 0 Ma (A-D), Stability from 4.5 to 2.5 Ma (E-H), and Dynamism from 2 to 0 Ma (I-L). Figures show the mean occupancy, proportional occupancy, and changes in isolated proportional increase and decrease of the number of occupied sites per species.

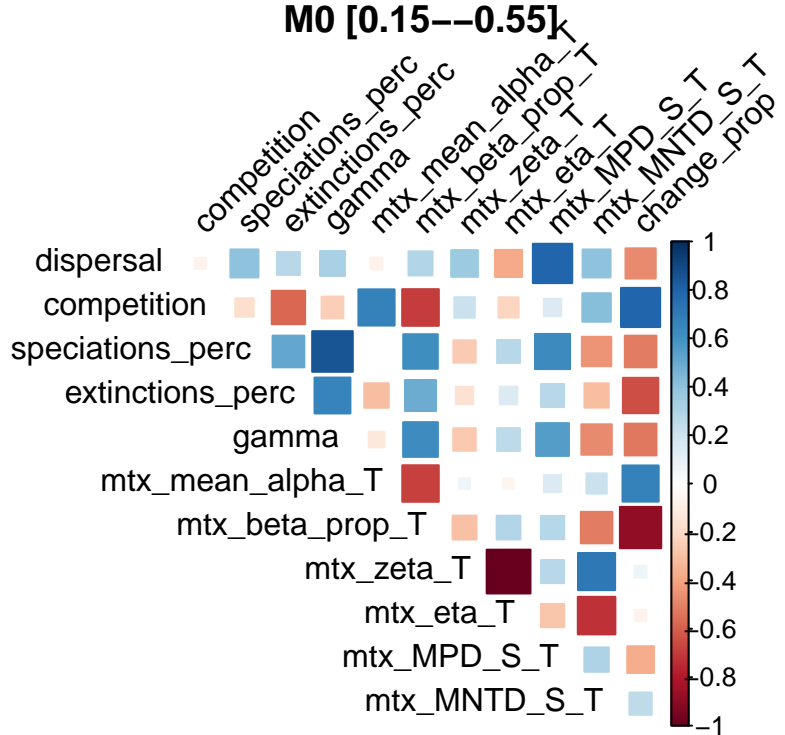
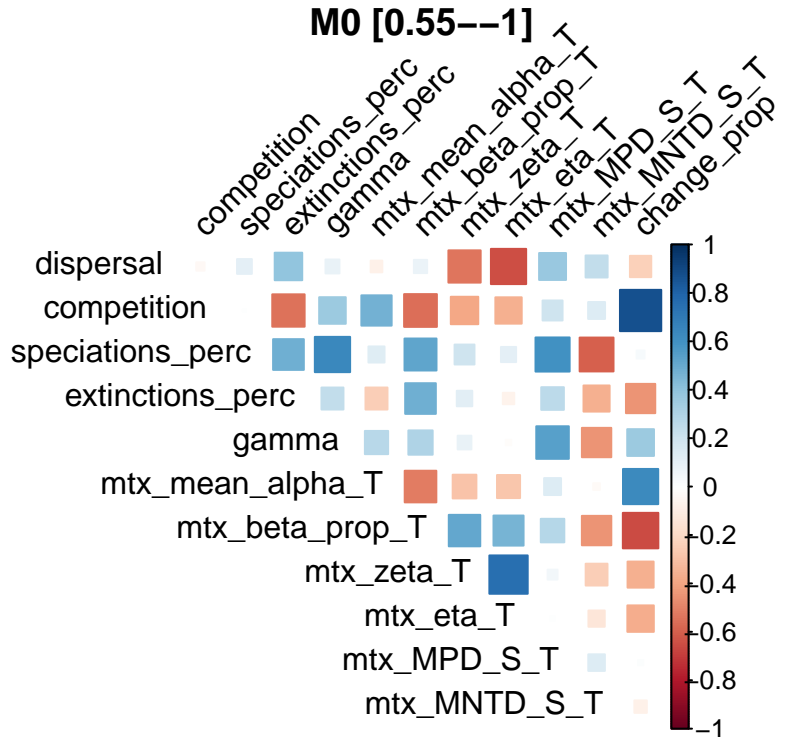
A**B**

Figure 18: Correlations for hand-picked summary statistics for M0 for different intervals of dispersal distance 0.15-0.55 (A) and 0.55-1 (B).

Figure Figure 20 delves into the intricate correlations between selected summary statistics across various dispersal distance intervals. This analysis sheds light on the complex interplay between dispersal, competition and landscape structure.

Furthermore, Figure 21, along with Figure 22, Figure 23, Figure 24, Figure 25, Figure 26, Figure 27, Figure 28 and Figure 29 present multiple statistical summaries along initial dispersal trait values. The depiction of competition is nuanced, with simulations regimes delineated by unique lines within the same initial competitive grouping, offering a comprehensive overview of the dispersal, competitive and landscape structure behind biodiversity dynamics.

MET

Figure Figure 30 captures the evolving spatial patterns and occupancy dynamics of species from 4.5 million years ago (Ma) to the present. This visualization portrays a period of stability between 4.5 and 2.5 Ma, followed by a phase of significant change from 2 to 0 Ma, elucidating the evolutionary trajectory of species occupancy over millennia.

Figure Figure 31 delves into the intricate correlations between selected summary statistics across various dispersal distance intervals. This analysis sheds light on the complex interplay between dispersal, competition, and landscape in molding the geographical distribution of species.

Furthermore, Figure 32, along with Figure 33, Figure 34, Figure 35, Figure 36, Figure 37, Figure 38, Figure 39 and Figure 40 present multiple statistical summaries along initial dispersal trait values. The depiction of competition is nuanced, with simulations regimes delineated by unique lines within the same initial competitive grouping, offering a comprehensive overview of the dispersal, competitive and landscape structure behind biodiversity dynamics.

Models Comparison

The correlation coefficients between the summary statistics and the mean final trait values for each model (M0, ME, MET) show how traits and species numbers are interrelated and vary across models (Figure 41). M0 Model had a positive correlation (0.35) between final richness γ and dispersal, indicating that an increase in dispersal trait values is associated with a higher number of species. The number of species and thermal range trait (ω) had negative correlation (-0.56), suggesting that wider temperature tolerance is associated with a lower number of species. ME Model had number of species and dispersal similarly correlated as to M0, a positive correlation (0.40) is observed, reinforcing the idea that higher dispersal capabilities are beneficial for species richness. Number of Species and thermal range: Again, a negative correlation (-0.43) is found, consistent with the M0 model's findings. Number of Species and Dispersal in MET Model shows a stronger positive correlation (0.56) compared to M0 and ME, indicating the assumed trade-off. The number of species and thermal range shows

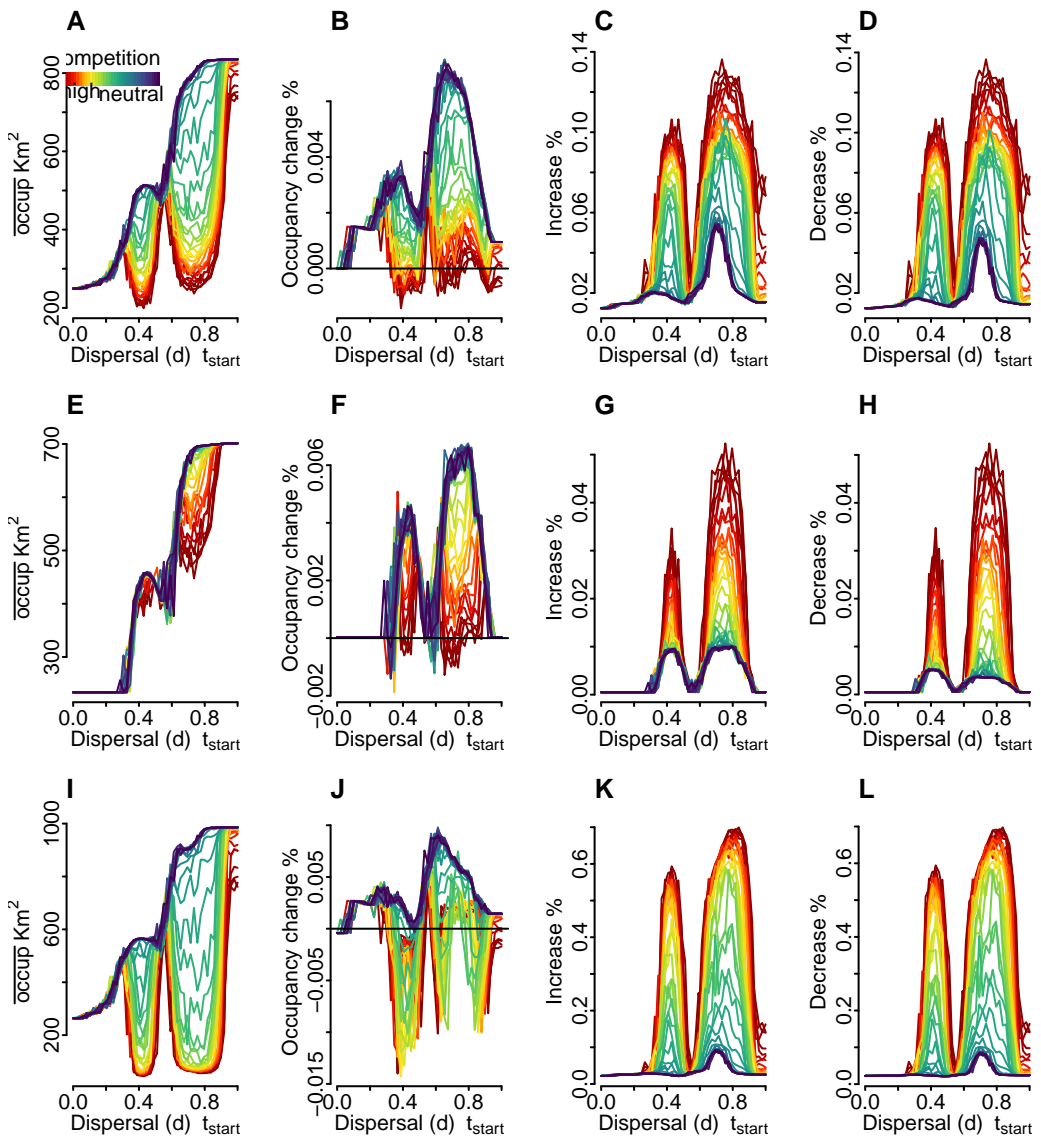


Figure 19: Spatial dynamics of ME from 4.5 to 0 Ma (A-D), Stability from 4.5 to 2.5 Ma (E-H), and Dynamism from 2 to 0 Ma (I-L). Figures show the mean occupancy, proportional occupancy, and changes in isolated proportional increase and decrease of the number of occupied sites per species.

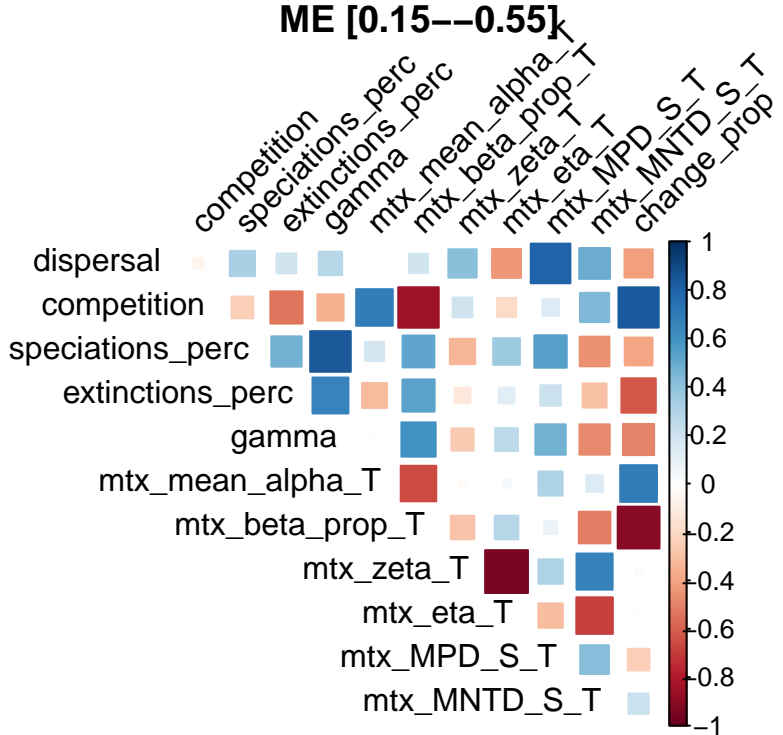
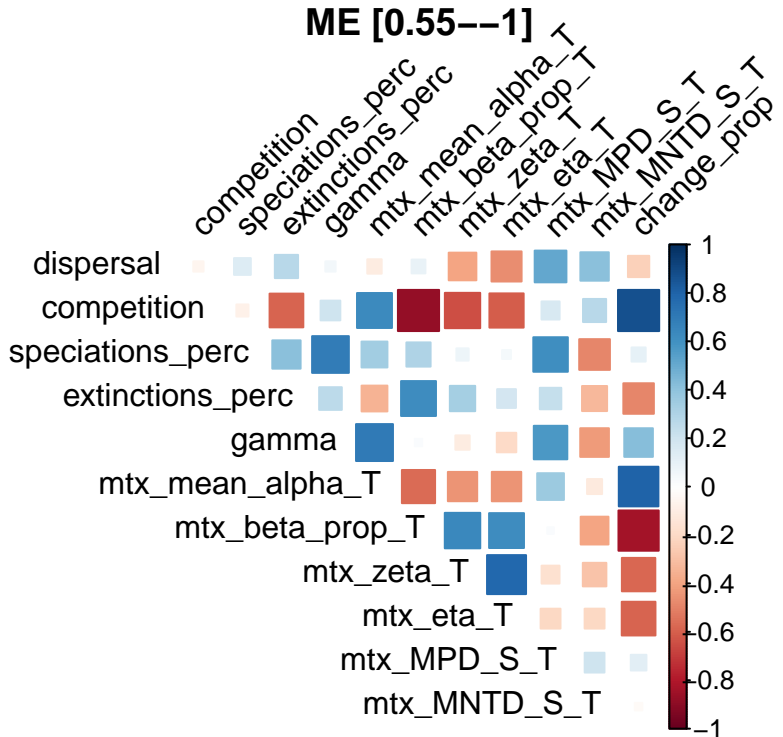
A**B**

Figure 20: Correlations for hand-picked summary statistics for ME for different intervals of dispersal distance 0.15-0.55 (A) and 0.55-1 (B).

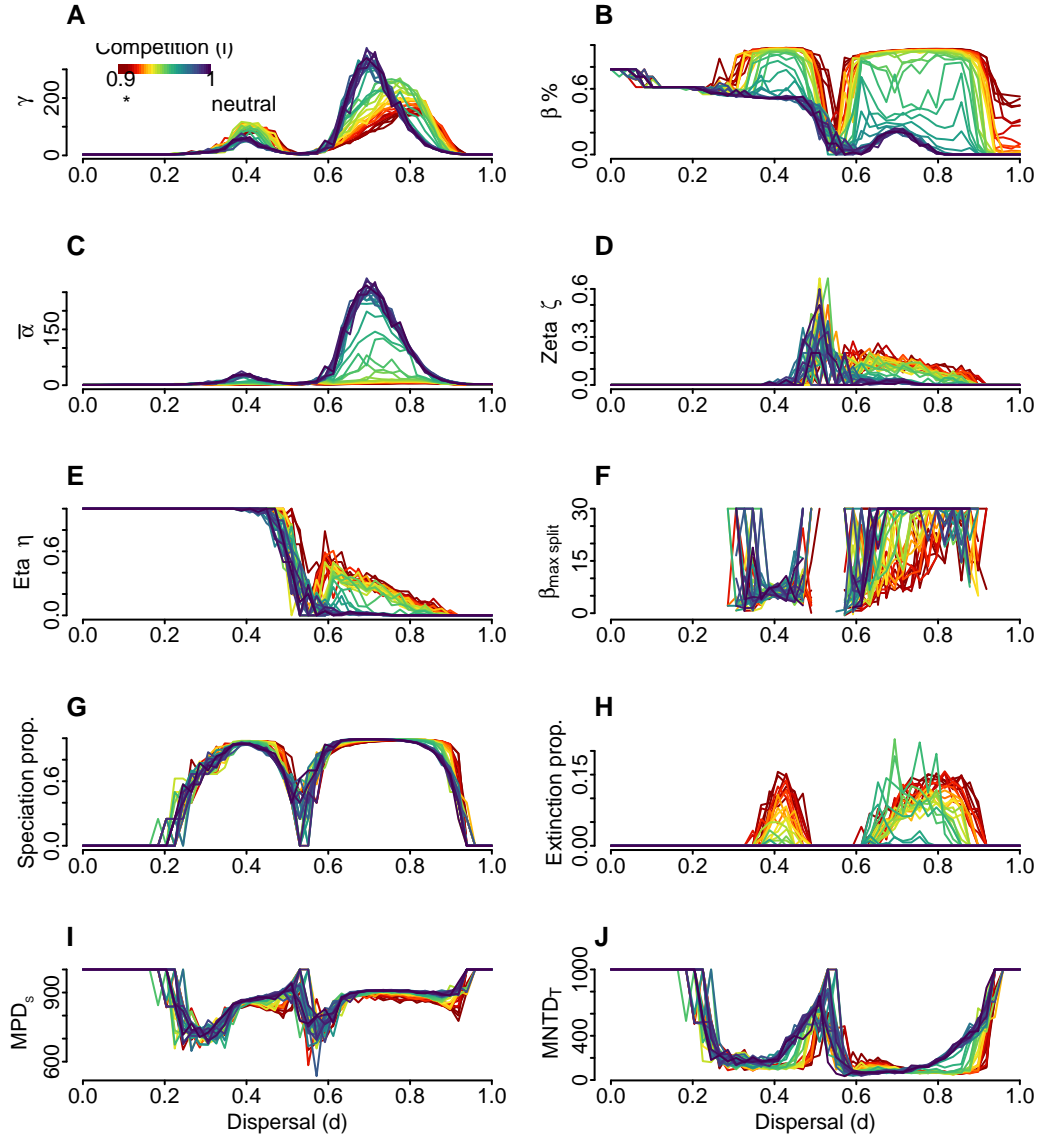


Figure 21: Summary statistics for ME through dispersal. Each line corresponds to simulation within a same competitive value along dispersal ability at the initial timestep. (A) Final gamma diversity, or final regional taxonomic richness (number of species alive at the last timestep). (B) Proportional species turnover, i.e. $1 - \text{mean}(\alpha/\gamma)$ quantifies what proportion of the species diversity in the dataset that is not contained in an average site (C) Mean alpha diversity of the entire archipelago. (D) Proportion of species that are common to all assemblages. Zeta diversity sensu Hui and McGeoch (2014). (E) Proportion of species that are not unique to an assemblage nor common to all assemblages. (F) The complete phylogenetic beta value derived from the Maximum Likelihood estimation within the Beta-splitting model. This is computed using the `maxlik.betasplit` function from the `apTreeshape` package. (G) Proportion of speciation events in a simulation over final gamma diversity. (H) Proportion of extinction events in a simulation over final gamma diversity. (I) Standardized value of the Mean Pairwise Distance measure on the archipelago, calculated using the `mpd` function from the `picante` package. (J) Standardized value of the mean nearest taxon distance measure for the entire archipelago.

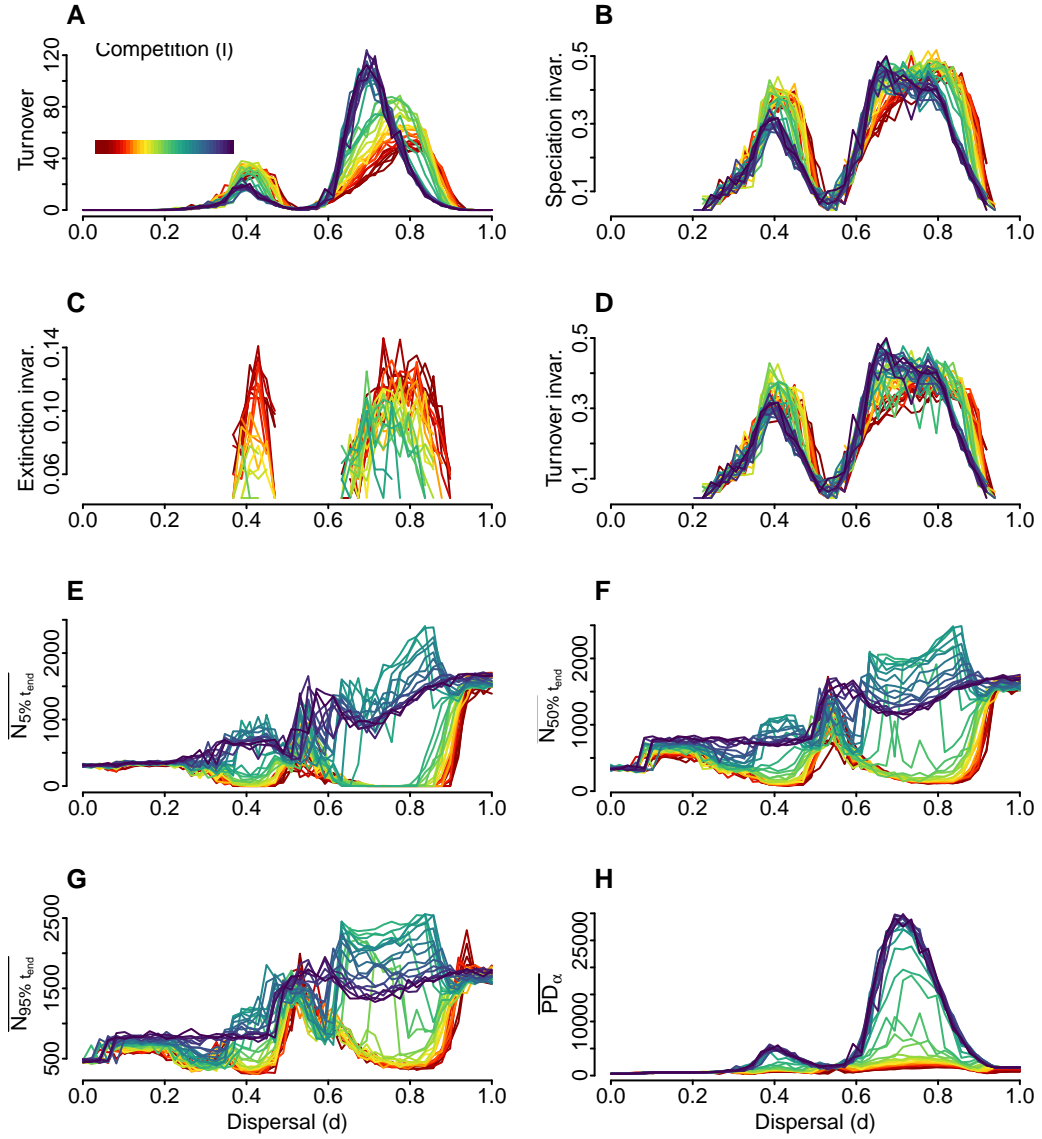


Figure 22: Additional summary statistics for ME though initial dispersal values. Each line corresponds to simulations within a same competitive value, along dispersal ability. (A) Turnover between speciation and extinction. I.e. the sum of speciation - extinction for all timesteps divided by the number of initial species. (B) Temporal speciation invariability, also refered to as temporal stability of speciation events. (C) Temporal extinction invariability, also refered to as temporal stability of extinction events. (D) Temporal turnover invariability, also referred to as temporal turnover stability. (E) Mean population size of its 5% quantile at final timestep. (F) Mean population size at final timestep. (G) Mean population size of its 95% quantile at final timestep. (H) The Mean Faith's Phylogenetic Diversity (PD) at the site level, quantifies the total branch lengths and was calculates with the function PD from the picante pacakge.

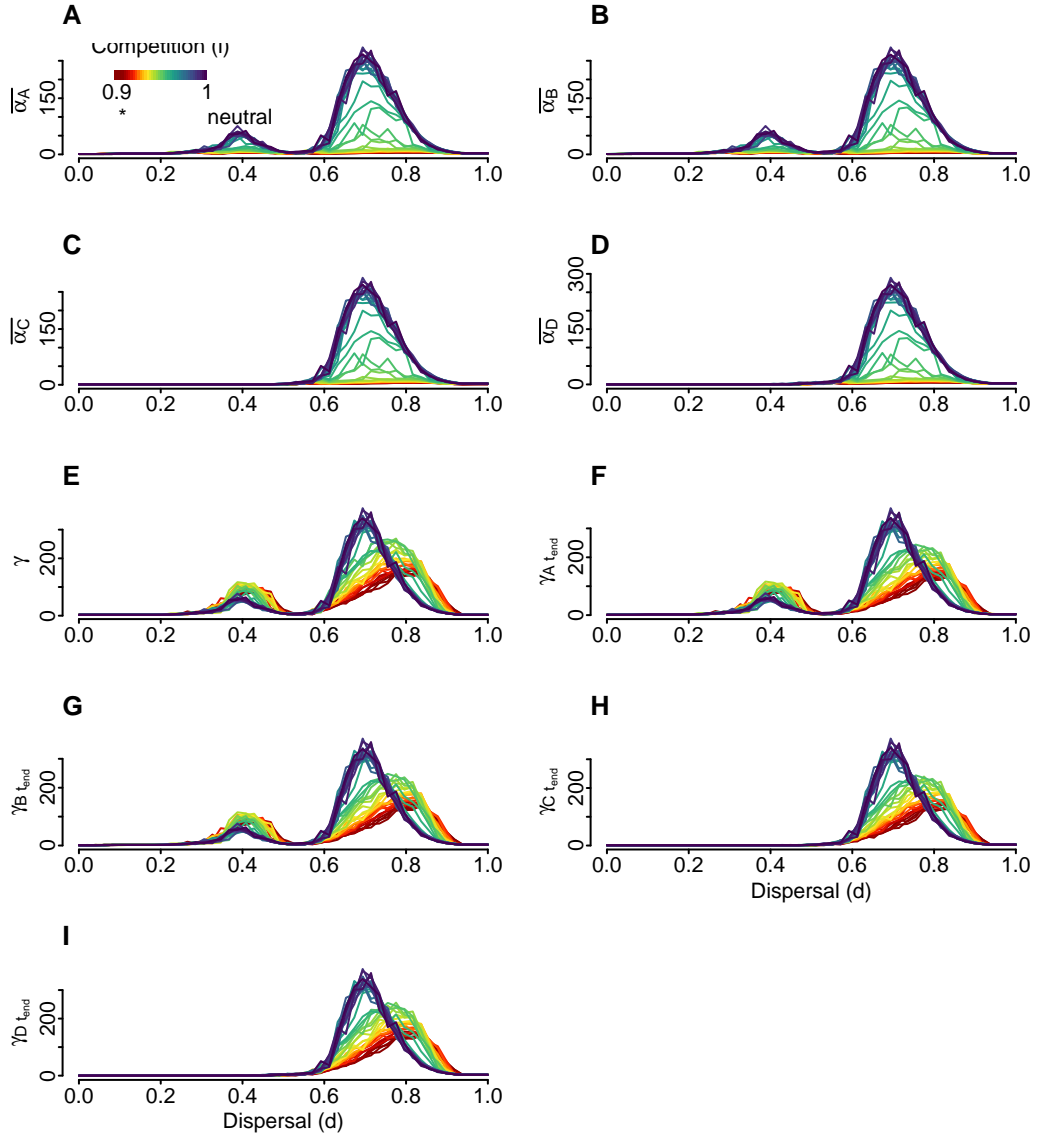


Figure 23: Additional summary statistics for ME though initial dispersal values. Each line corresponds to simulations within a same competitive value, along dispersal ability. (A) Mean alpha diversity of sites on island A. (B) Mean alpha diversity of sites on island B. (C) Mean alpha diversity of sites on island C. (D) Mean alpha diversity of sites on island D. (E) Final gamma diversity, or final regional taxonomic richness (number of species alive at the last timestep). (F) Final gamma diversity of island A, or final regional taxonomic richness (number of species alive at the last timestep). (G) Final gamma diversity of island B. (H) Final gamma diversity of island C. (I) Final gamma diversity of island D.

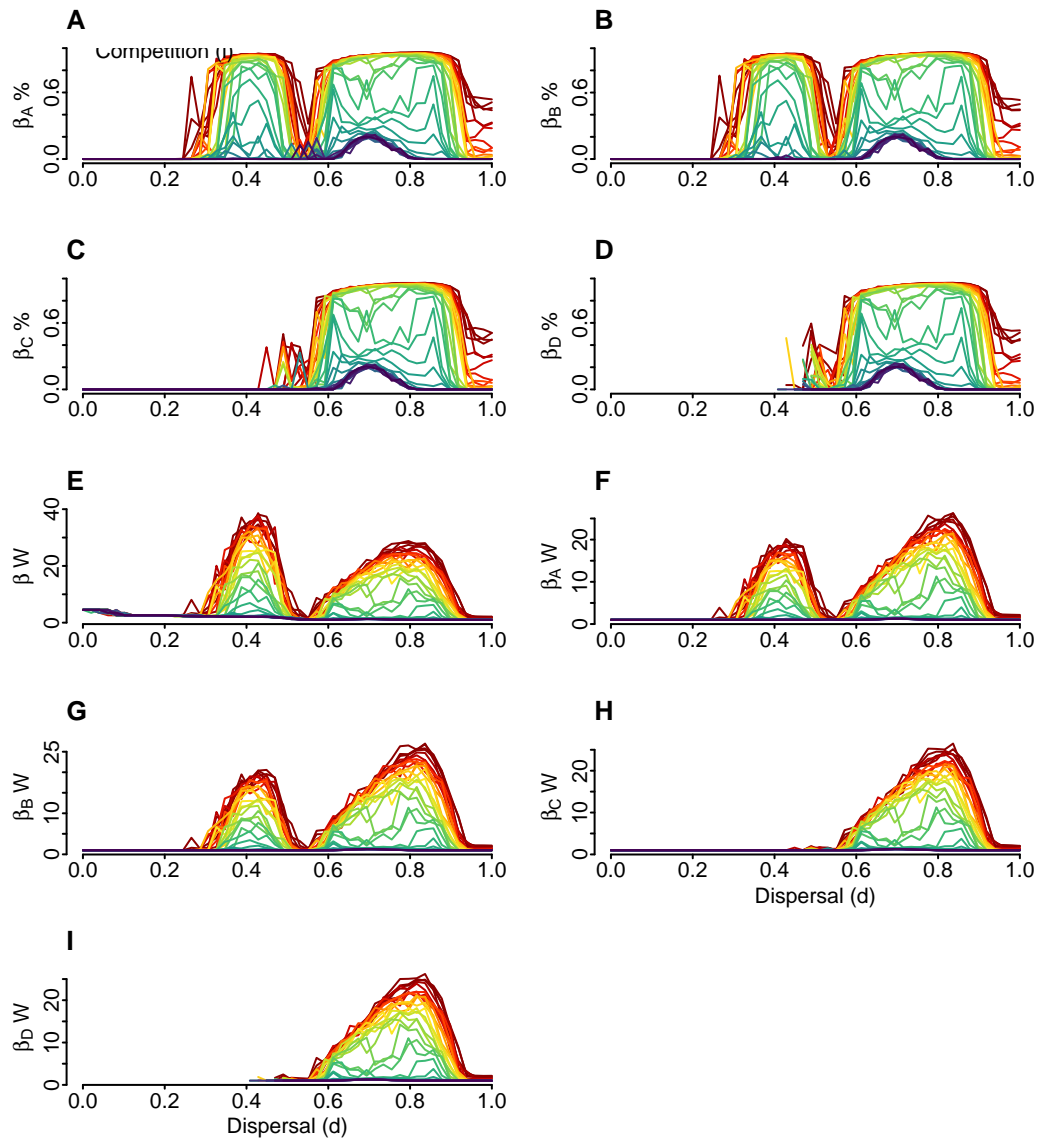


Figure 24: Additional summary statistics for ME though initial dispersal values. Each line corresponds to simulations within a same competitive value, along dispersal ability. (A) Proportional species turnover in island A. (B) Proportional species turnover in island B. (C) Proportional species turnover in island C. (D) Proportional species turnover in island D. (E) Whittaker beta diversity, i.e. gamma/mean(alpha), how many subunits there would be if the total species diversity of the mean species diversity per subunit remained the same, but the subunits shared no species. (F) Whittaker beta diversity of island A. (G) Whittaker beta diversity of island B. (H) Whittaker beta diversity of island C. (I) Whittaker beta diversity of island D.

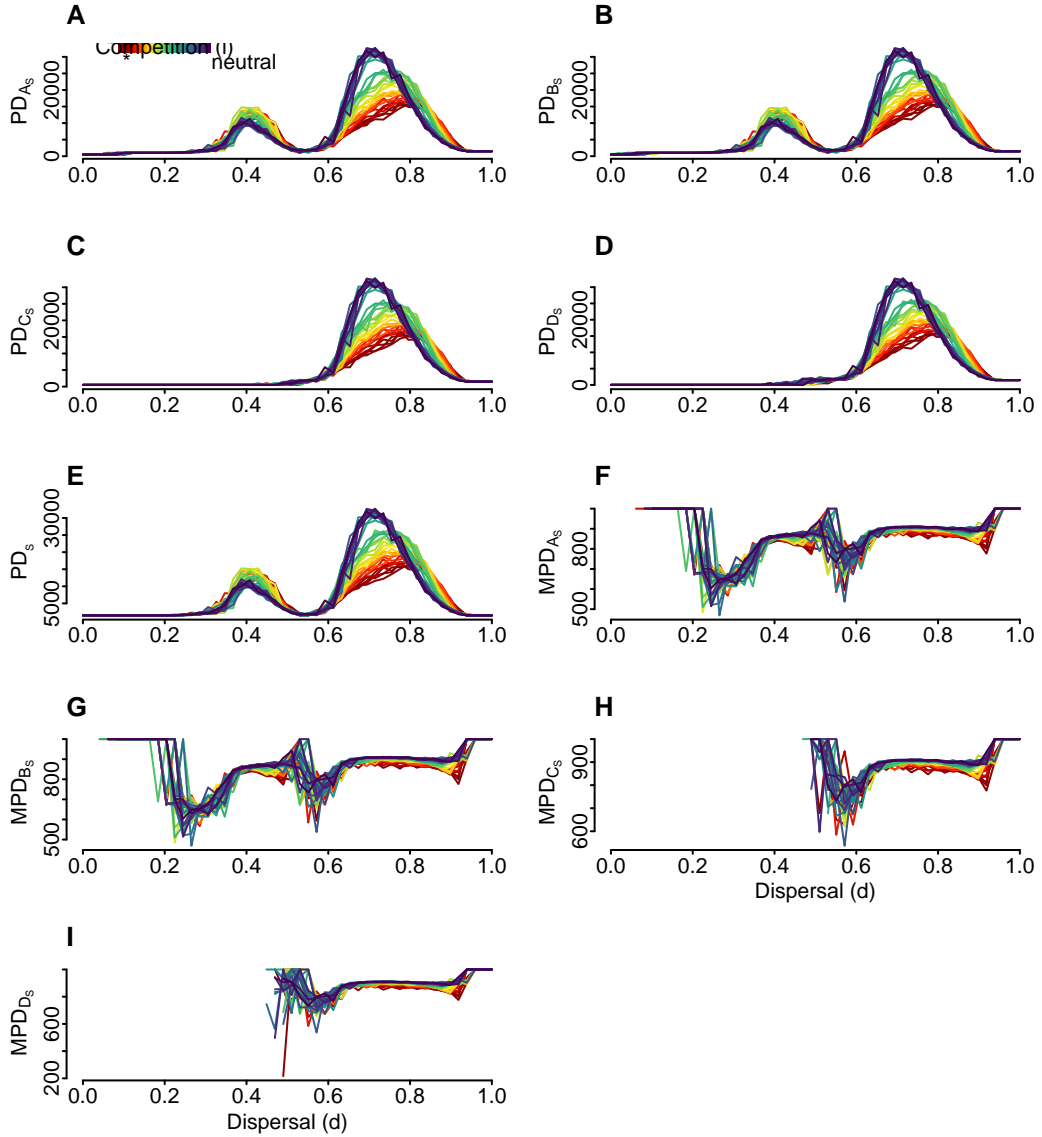


Figure 25: Additional summary statistics for ME though initial dispersal values. Each line corresponds to simulations within a same competitive value, along dispersal ability. (A) Standardized value of the unrooted Phylogenetic Diversity measure for species in island A. (B) Standardized value of the unrooted Phylogenetic Diversity measure for species in island B. (C) Standardized value of the unrooted Phylogenetic Diversity measure for species in island C. (D) Standardized value of the unrooted Phylogenetic Diversity measure for species in island D. (E) Standardized value of the unrooted Phylogenetic Diversity measure for species on the arquipelago, calculated using the `pd` function from the `picante` package. (F) Standardized value of the Mean Pairwise Distance measure in island A. (G) Standardized value of the Mean Pairwise Distance measure in island B. (H) Standardized value of the Mean Pairwise Distance measure in island C. (I) Standardized value of the Mean Pairwise Distance measure in island D.

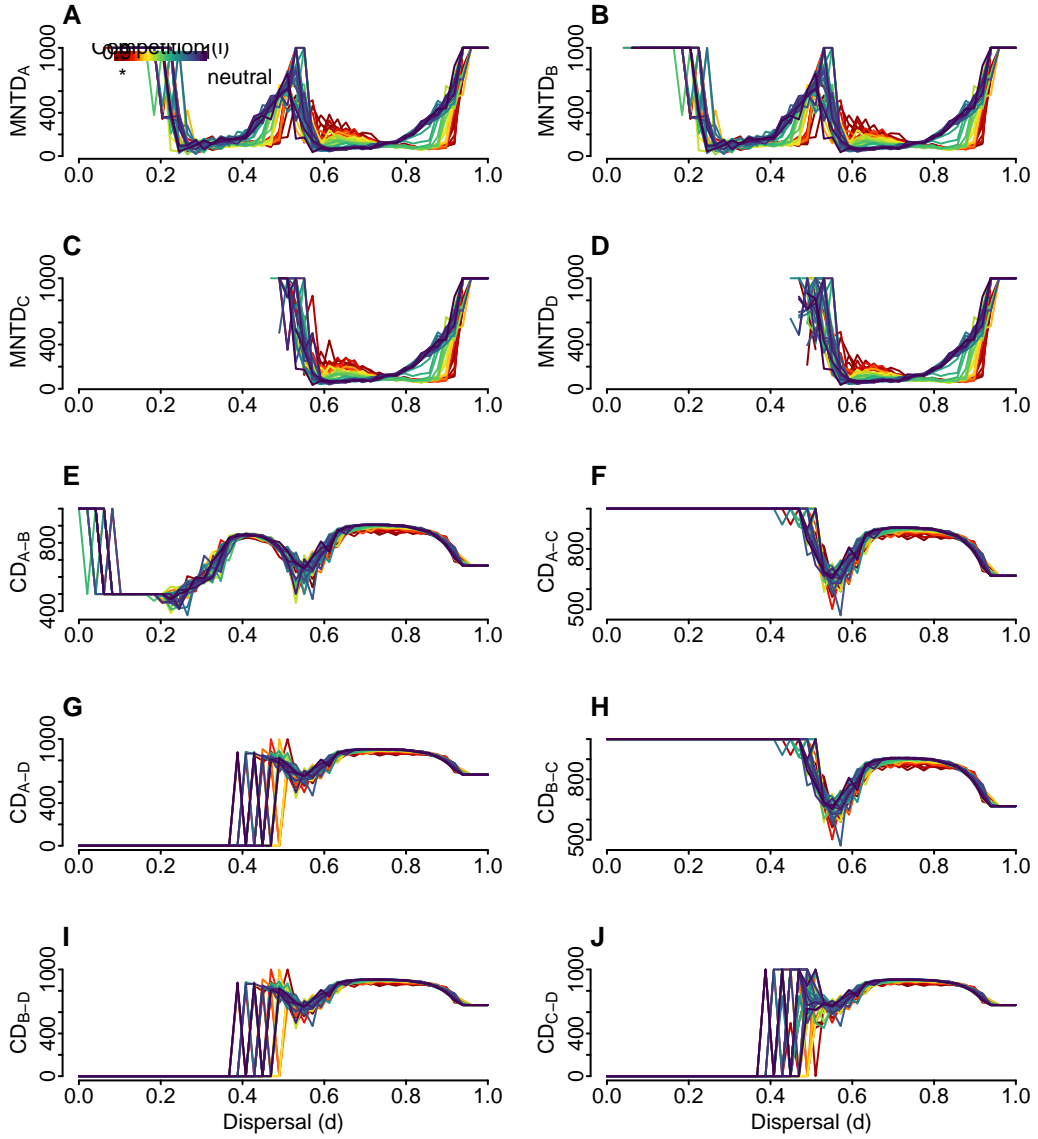


Figure 26: Additional summary statistics for ME though initial dispersal values. Each line corresponds to simulations within a same competitive value, along dispersal ability. (A) Standardized value of the mean nearest taxon distance measure for the island A. (B) Standardized value of the mean nearest taxon distance measure for the island B. (C) Standardized value of the mean nearest taxon distance measure for the island C. (D) Standardized value of the mean nearest taxon distance measure for the island D. (E) Standardized Community Distance between island A and B. It is the beta diversity version of Mean Pairwise Distance (MPD), giving the average phylogenetic distance between two communities. (F) Standardized Community Distance between island A and C. (G) Standardized Community Distance between island A and D. (H) Standardized Community Distance between island B and C. (I) Standardized Community Distance between island B and D. (J) Standardized Community Distance between island C and D.

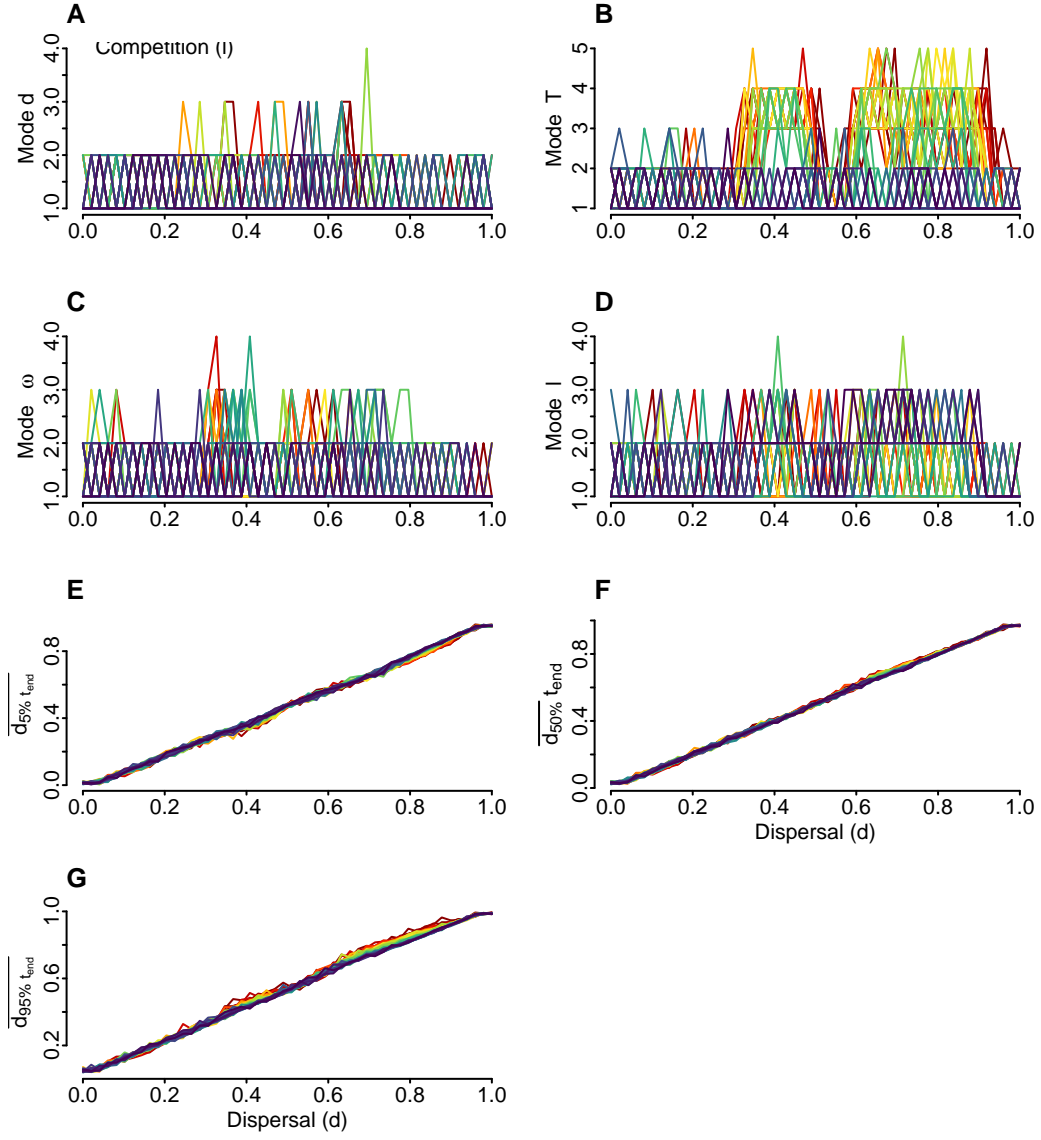


Figure 27: Additional summary statistics for ME though initial dispersal values. Each line corresponds to simulations within a same competitive value, along dispersal ability. (A) Number of modes at the dispersal trait distribution at final timestep, i.e. no modes (such as in a uniform distribution), or more. Calculated with the function ‘Mode’ from package LaplacesDemon. (B) Number of modes at the thermal optimum distribution at final timestep. (C) Number of modes at the thermal range trait distribution at final timestep. (D) Number of modes at the competition trait (i.e. tolerance to other species) distribution at final timestep. (E) Mean dispersal trait of its 5% quantile at final timestep. (F) Mean dispersal trait at final timestep. (G) Mean dispersal trait of its 95% quantile at final timestep.

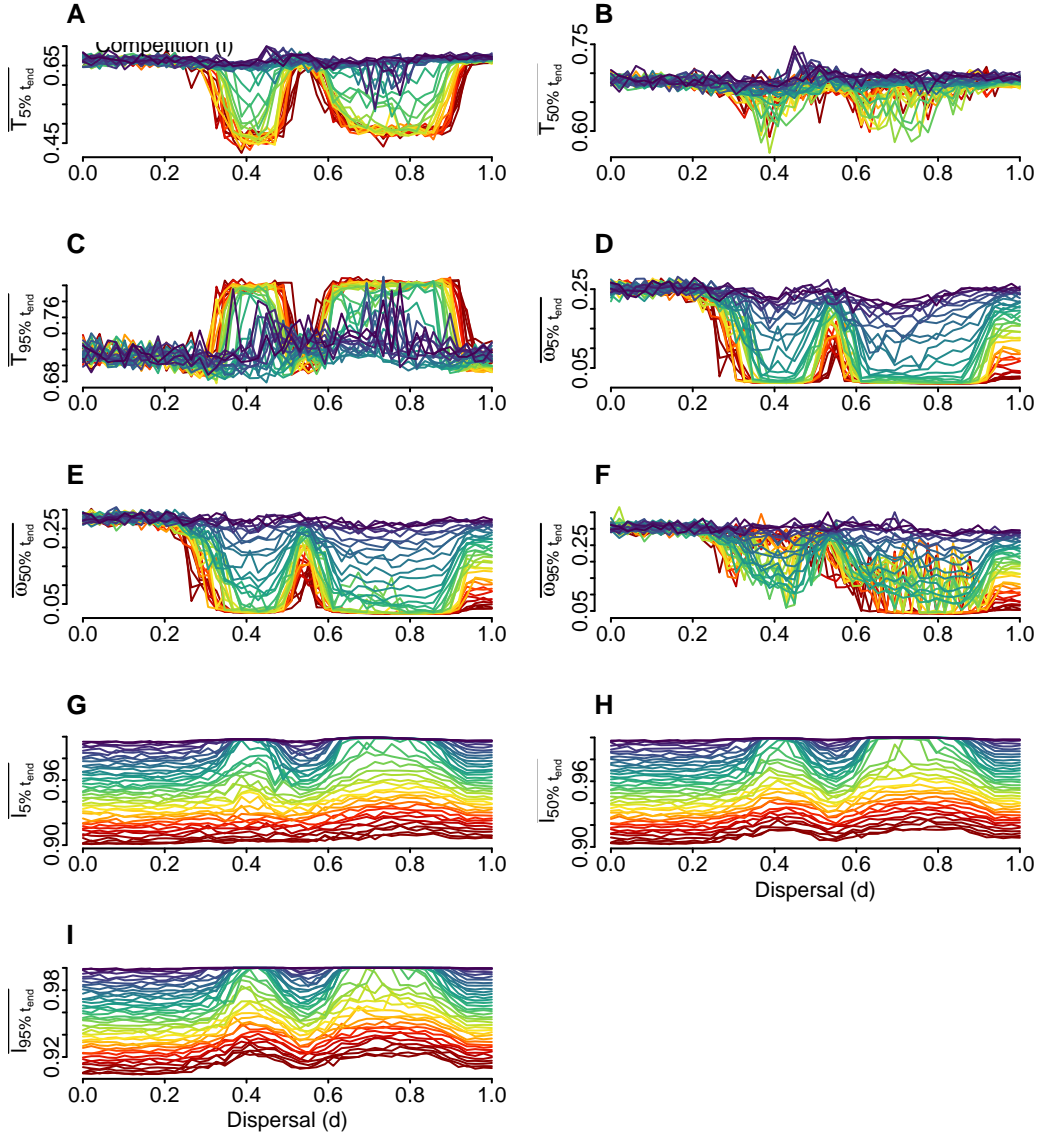


Figure 28: Additional summary statistics for ME though initial dispersal values. Each line corresponds to simulations within a same competitive value, along dispersal ability. (A) Mean thermal optimum of its 5% quantile at final timestep. (B) Mean thermal optimum at final timestep. (C) Mean thermal optimum of its 95% quantile at final timestep. (D) Mean thermal range trait of its 5% quantile at final timestep. (E) Mean thermal range trait at final timestep. (F) Mean thermal range trait of its 95% quantile at final timestep. (G) Mean tolerance to other species trait of its 5% quantile at final timestep. (H) Mean tolerance to other species trait at final timestep. (I) Mean tolerance to other species trait of its 95% quantile at final timestep.

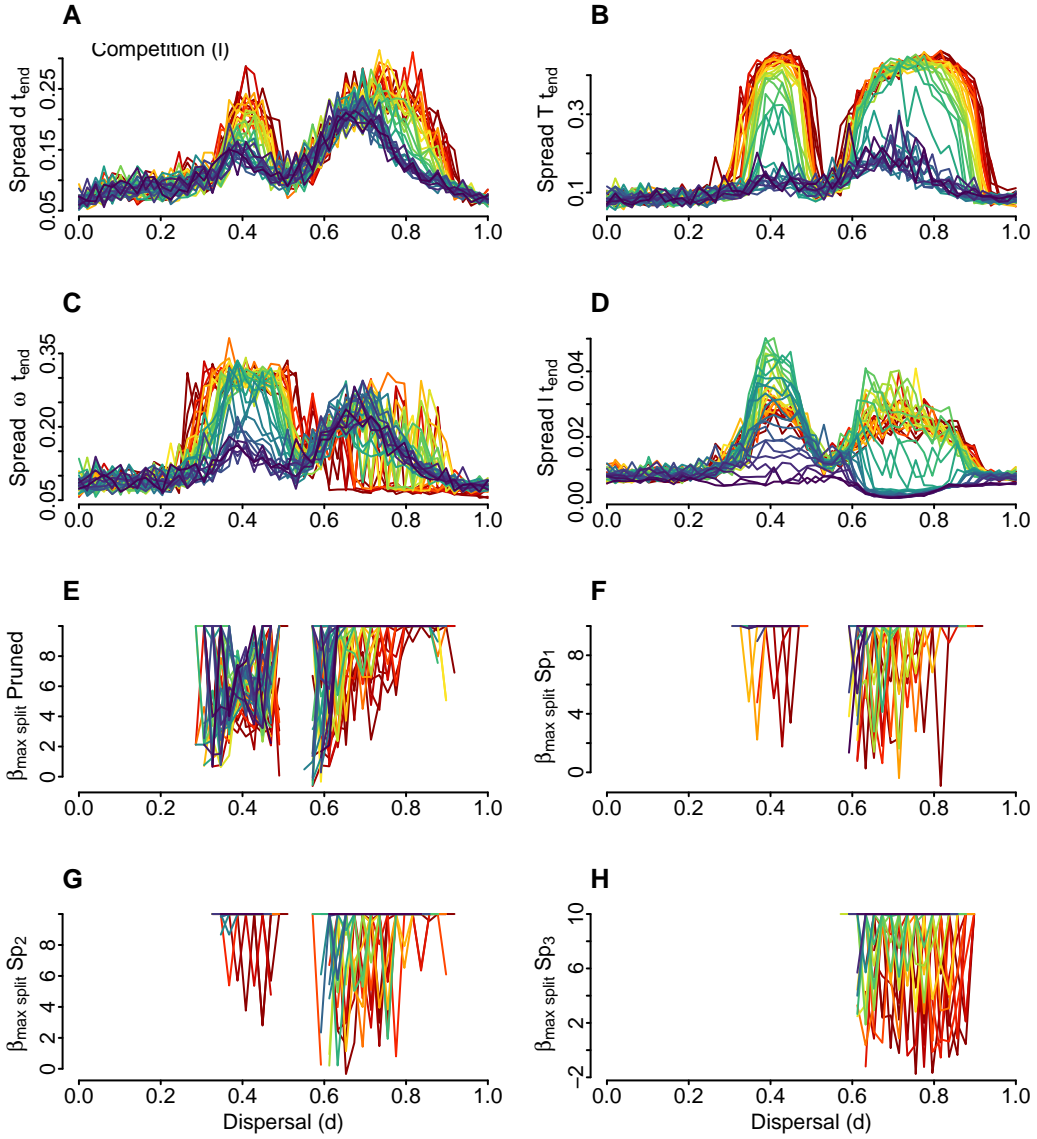


Figure 29: Additional summary statistics for ME though initial dispersal values. Each line corresponds to simulations within a same competitive value, along dispersal ability. (A) The range between the lowest and highest dispersal trait values at the final timestep. (B) The range between the lowest and highest thermal optimum values at the final timestep. (C) The range between the lowest and highest thermal range trait values at the final timestep. (D) The range between the lowest and highest tolerance to other species trait values at the final timestep. (E) The pruned phylogeny beta value, excluding extinct branches, derived from the Maximum Likelihood estimation within the Beta-splitting model. (F) The pruned phylogeny beta value of species 1, excluding extinct branches. (G) The pruned phylogeny beta value of species 2, excluding extinct branches. (H) The pruned phylogeny beta value of species 3, excluding extinct branches.

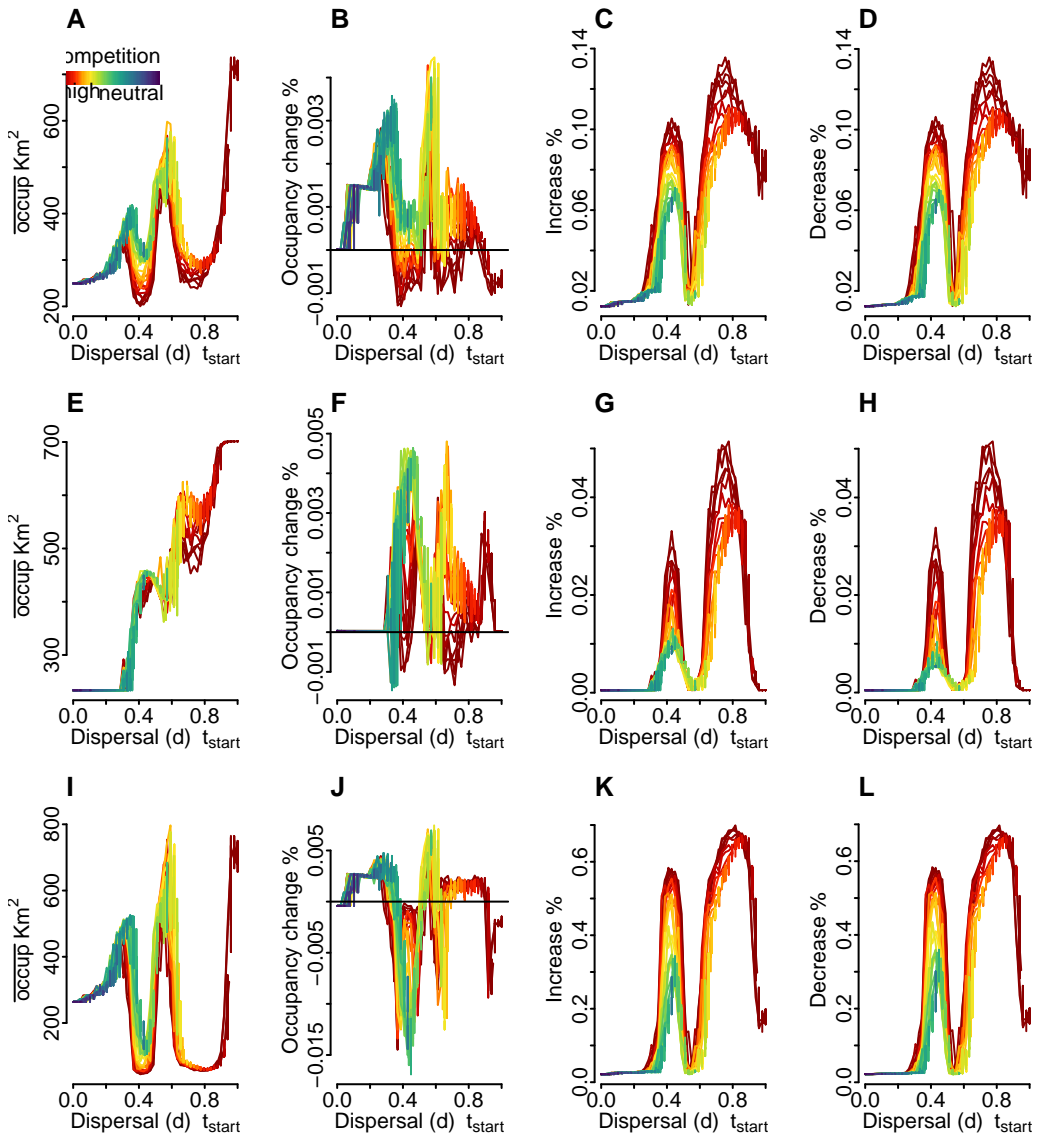


Figure 30: Spatial dynamics of MET from 4.5 to 0 Ma (A-D), Stability from 4.5 to 2.5 Ma (E-H), and Dynamism from 2 to 0 Ma (I-L). Figures show the mean occupancy, proportional occupancy, and changes in isolated proportional increase and decrease of the number of occupied sites per species.

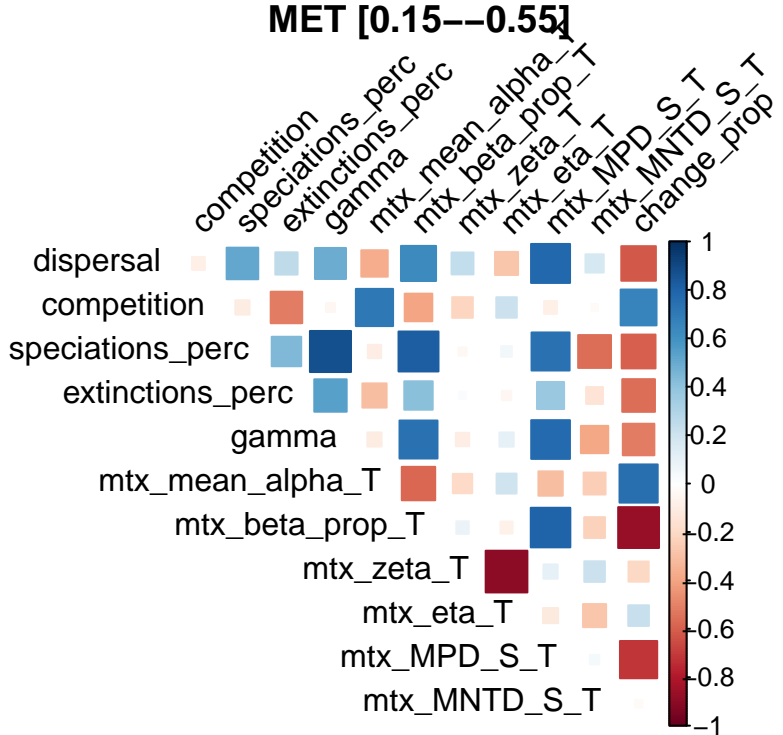
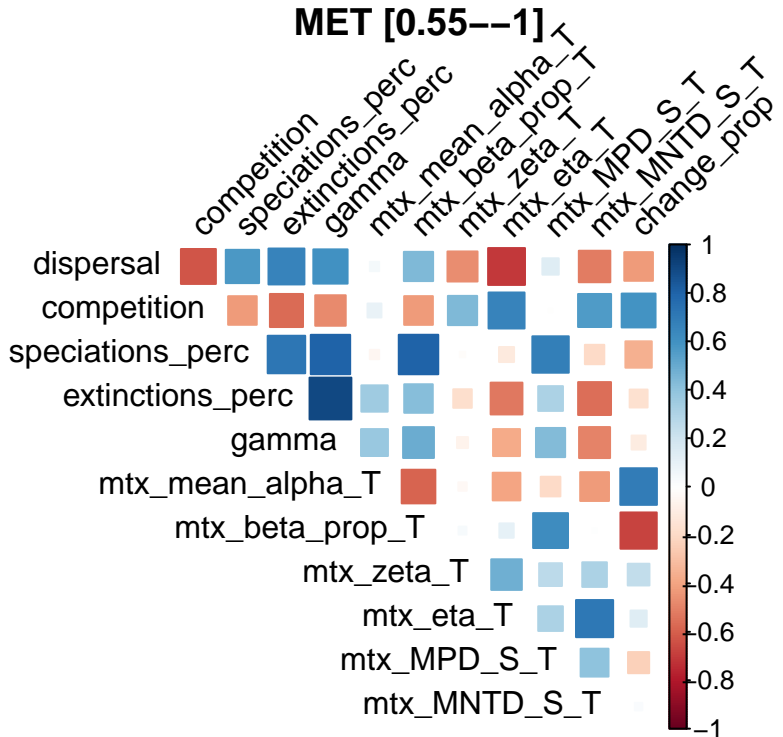
A**B**

Figure 31: Correlations for hand-picked summary statistics for MET for different intervals of dispersal distance 0.15-0.55 (A) and 0.55-1 (B).

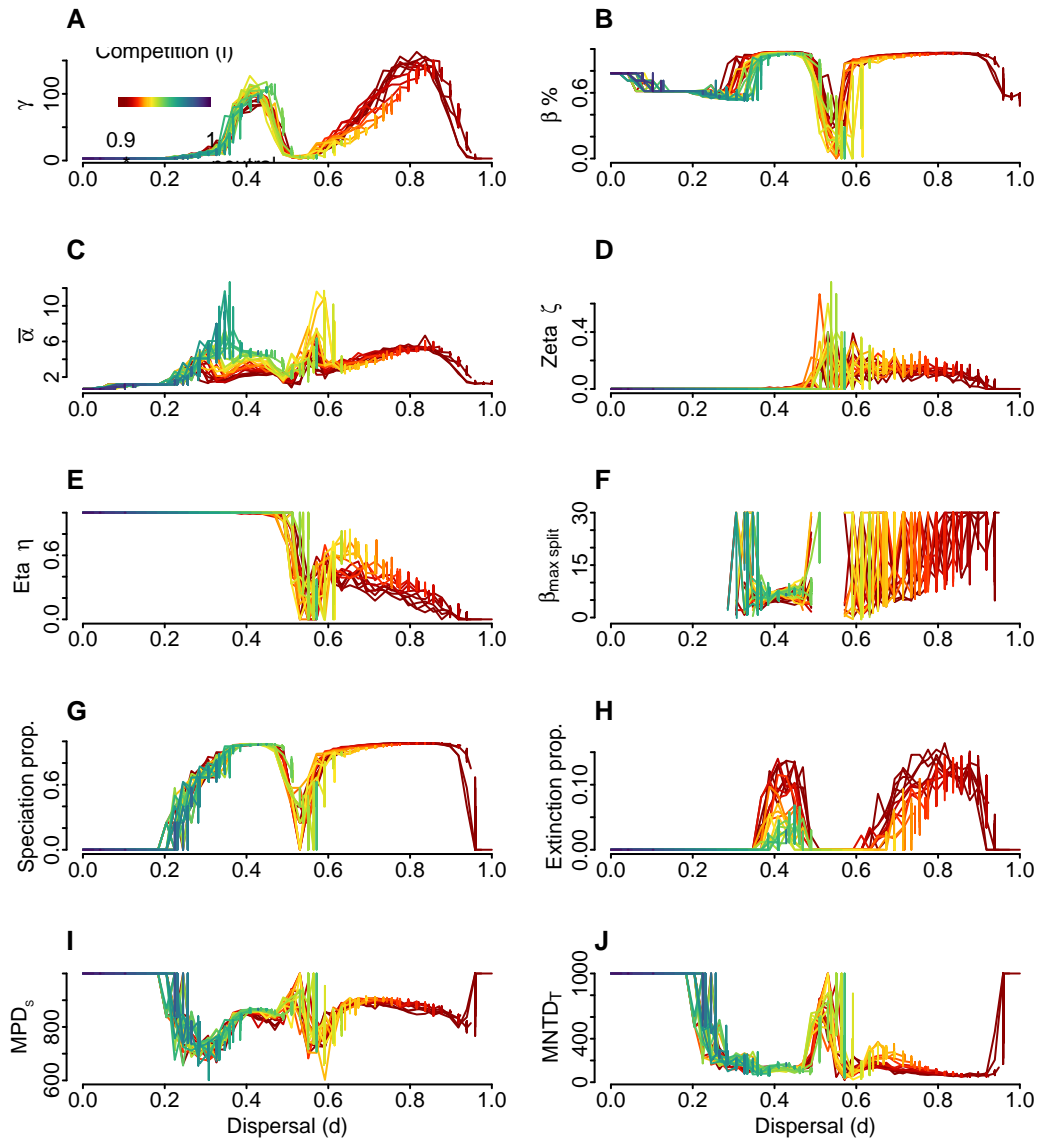


Figure 32: Summary statistics for ME through dispersal. Each line corresponds to simulation within a same competitive value along dispersal ability at the initial timestep. (A) Final gamma diversity, or final regional taxonomic richness (number of species alive at the last timestep). (B) Proportional species turnover, i.e. $1 - \text{mean}(\alpha/\gamma)$ quantifies what proportion of the species diversity in the dataset that is not contained in an average site (C) Mean alpha diversity of the entire archipelago. (D) Proportion of species that are common to all assemblages. Zeta diversity sensu Hui and McGeoch (2014). (E) Proportion of species that are not unique to an assemblage nor common to all assemblages. (F) The complete phylogenetic beta value derived from the Maximum Likelihood estimation within the Beta-splitting model. This is computed using the `maxlik.betasplit` function from the `apTreeshape` package. (G) Proportion of speciation events in a simulation over final gamma diversity. (H) Proportion of extinction events in a simulation over final gamma diversity. (I) Standardized value of the Mean Pairwise Distance measure on the archipelago, calculated using the `mpd` function from the `picante` package. (J) Standardized value of the mean nearest taxon distance measure for the entire archipelago.

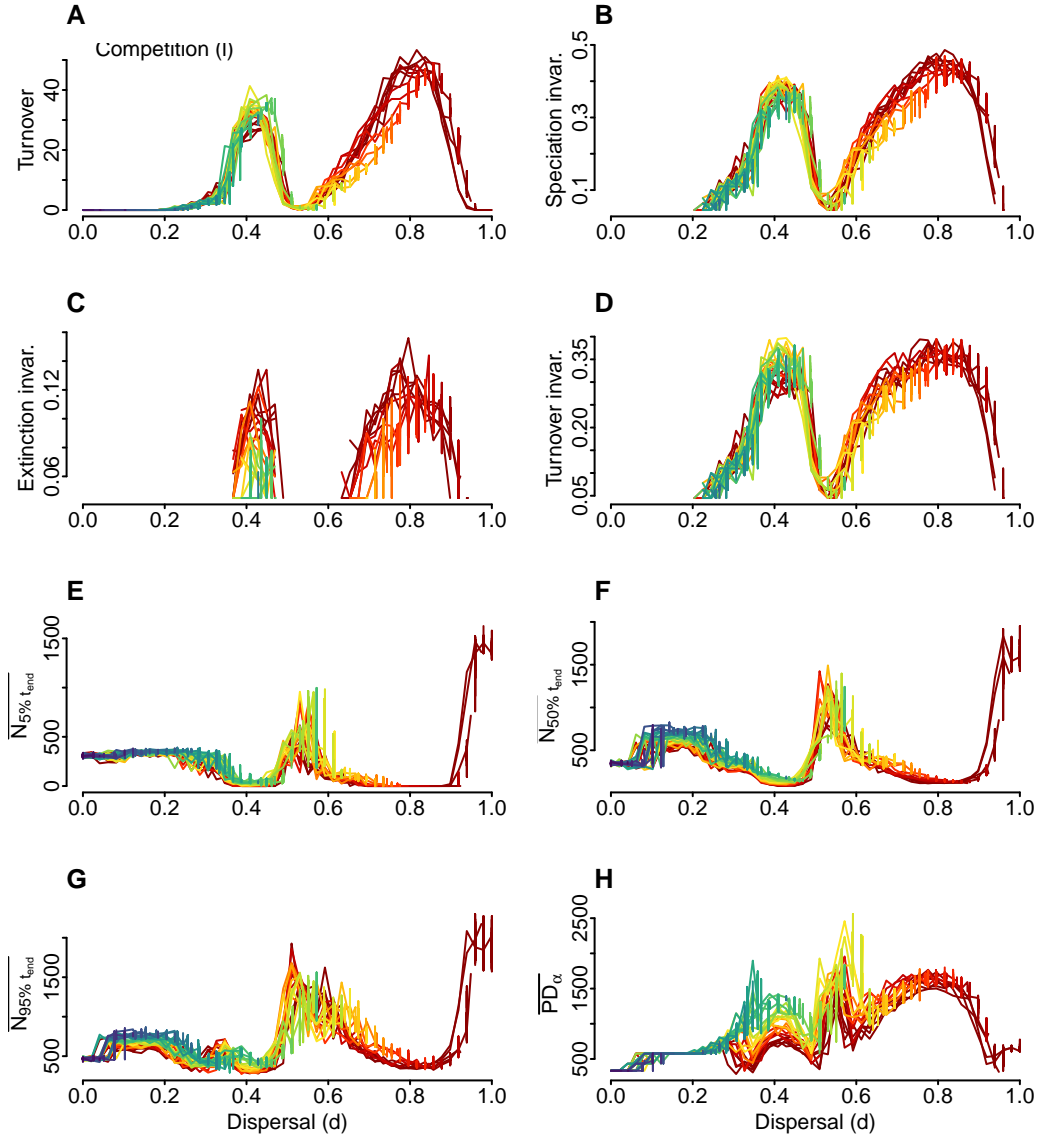


Figure 33: Additional summary statistics for MET through initial dispersal values. Each line corresponds to simulations within a same competitive value, along dispersal ability. (A) Turnover between speciation and extinction. I.e. the sum of speciation - extinction for all timesteps divided by the number of initial species. (B) Temporal speciation invariability, also referred to as temporal stability of speciation events. (C) Temporal extinction invariability, also referred to as temporal stability of extinction events. (D) Temporal turnover invariability, also referred to as temporal turnover stability. (E) Mean population size of its 5% quantile at final timestep. (F) Mean population size at final timestep. (G) Mean population size of its 95% quantile at final timestep. (H) The Mean Faith's Phylogenetic Diversity (PD) at the site level, quantifies the total branch lengths and was calculated with the function PD from the picante package.

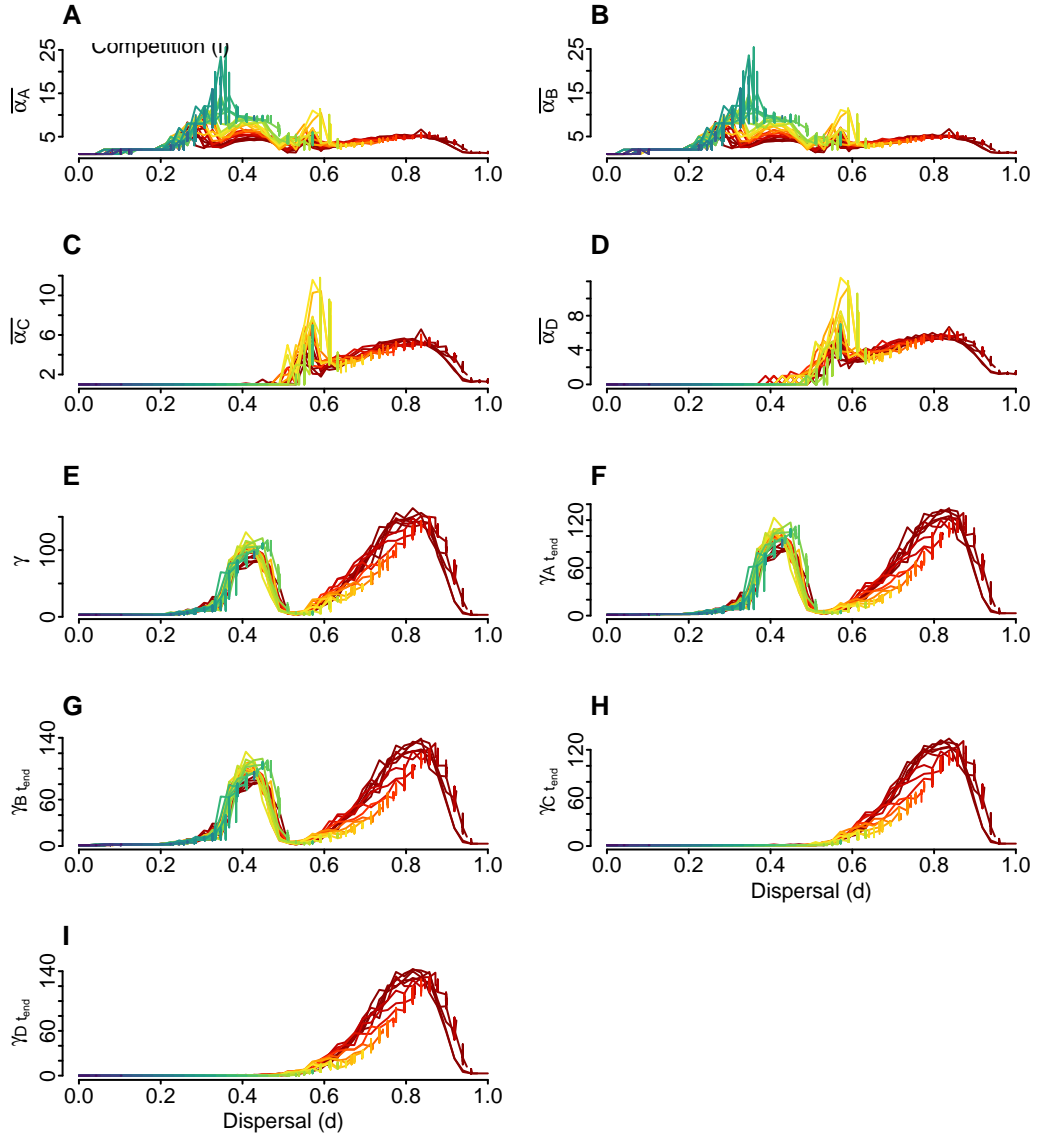


Figure 34: Additional summary statistics for MET though initial dispersal values. Each line corresponds to simulations within a same competitive value, along dispersal ability. (A) Mean alpha diversity of sites on island A. (B) Mean alpha diversity of sites on island B. (C) Mean alpha diversity of sites on island C. (D) Mean alpha diversity of sites on island D. (E) Final gamma diversity, or final regional taxonomic richness (number of species alive at the last timestep). (F) Final gamma diversity of island A, or final regional taxonomic richness (number of species alive at the last timestep). (G) Final gamma diversity of island B. (H) Final gamma diversity of island C. (I) Final gamma diversity of island D.

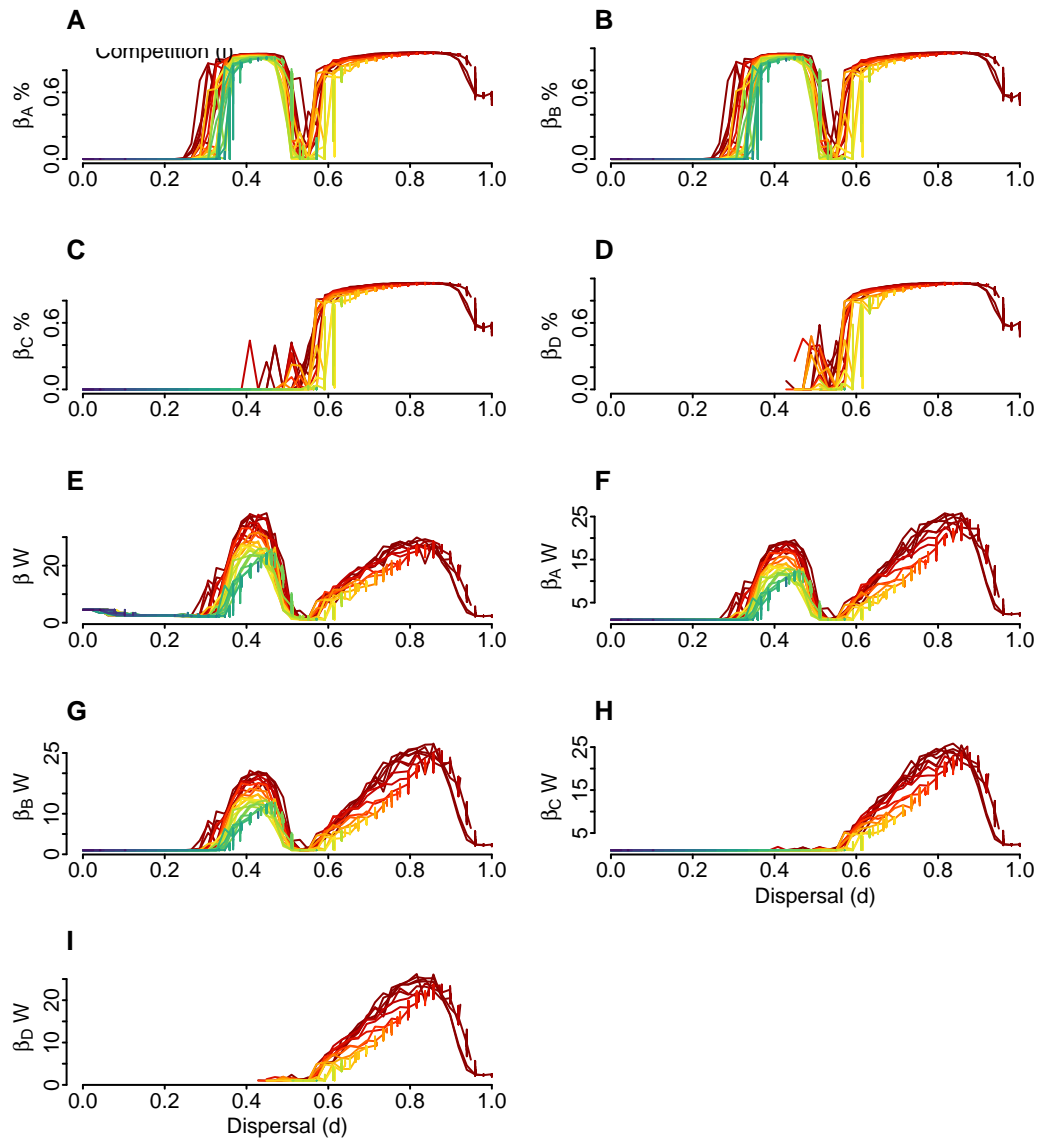


Figure 35: Additional summary statistics for MET though initial dispersal values. Each line corresponds to simulations within a same competitive value, along dispersal ability. (A) Proportional species turnover in island A. (B) Proportional species turnover in island B. (C) Proportional species turnover in island C. (D) Proportional species turnover in island D. (E) Whittaker beta diversity, i.e. gamma/mean(alpha), how many subunits there would be if the total species diversity of the mean species diversity per subunit remained the same, but the subunits shared no species. (F) Whittaker beta diversity of island A. (G) Whittaker beta diversity of island B. (H) Whittaker beta diversity of island C. (I) Whittaker beta diversity of island D.

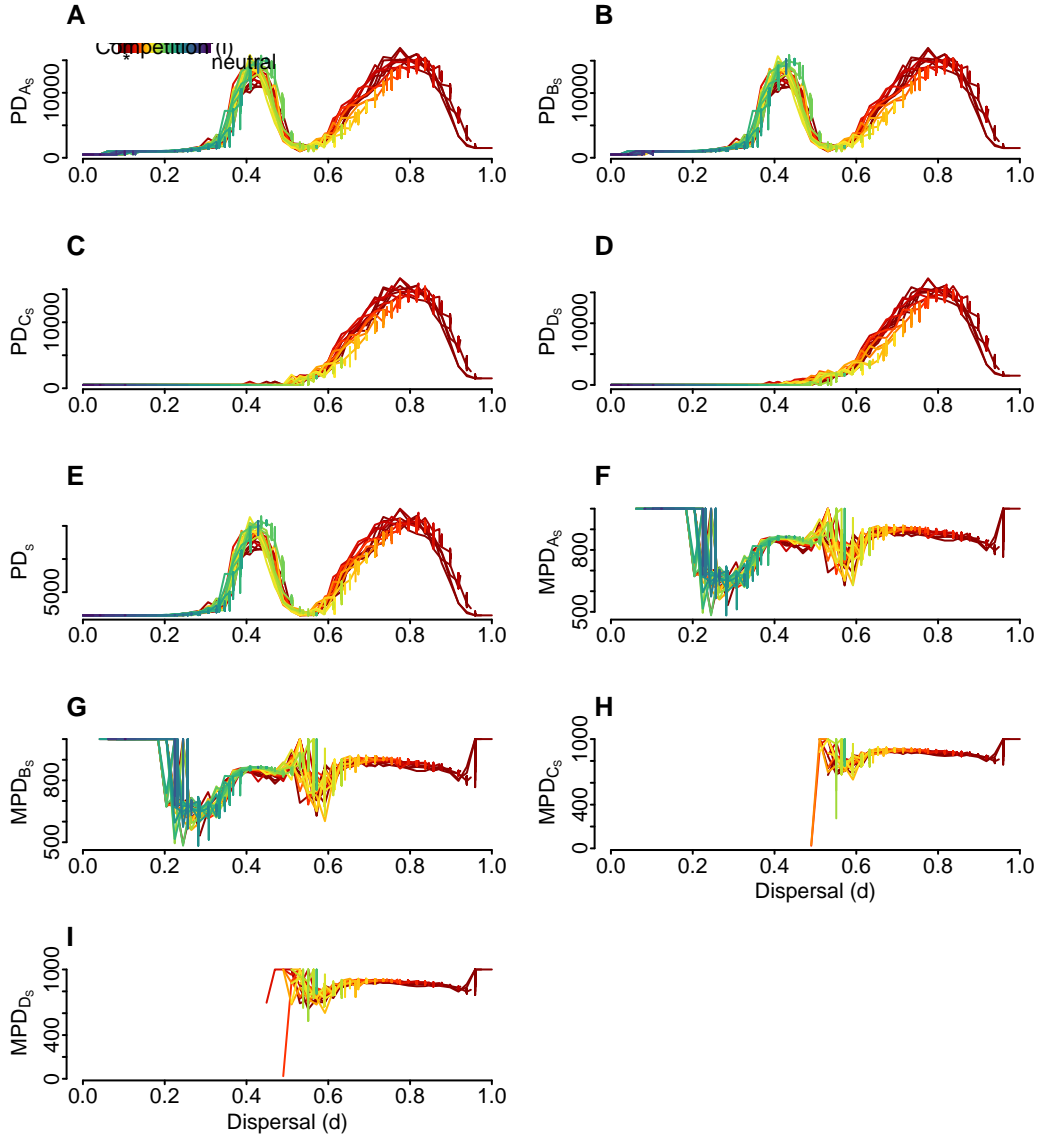


Figure 36: Additional summary statistics for MET through initial dispersal values. Each line corresponds to simulations within a same competitive value, along dispersal ability. (A) Standardized value of the unrooted Phylogenetic Diversity measure for species in island A. (B) Standardized value of the unrooted Phylogenetic Diversity measure for species in island B. (C) Standardized value of the unrooted Phylogenetic Diversity measure for species in island C. (D) Standardized value of the unrooted Phylogenetic Diversity measure for species in island D. (E) Standardized value of the unrooted Phylogenetic Diversity measure for species on the archipelago, calculated using the `pd` function from the `picante` package. (F) Standardized value of the Mean Pairwise Distance measure in island A. (G) Standardized value of the Mean Pairwise Distance measure in island B. (H) Standardized value of the Mean Pairwise Distance measure in island C. (I) Standardized value of the Mean Pairwise Distance measure in island D.

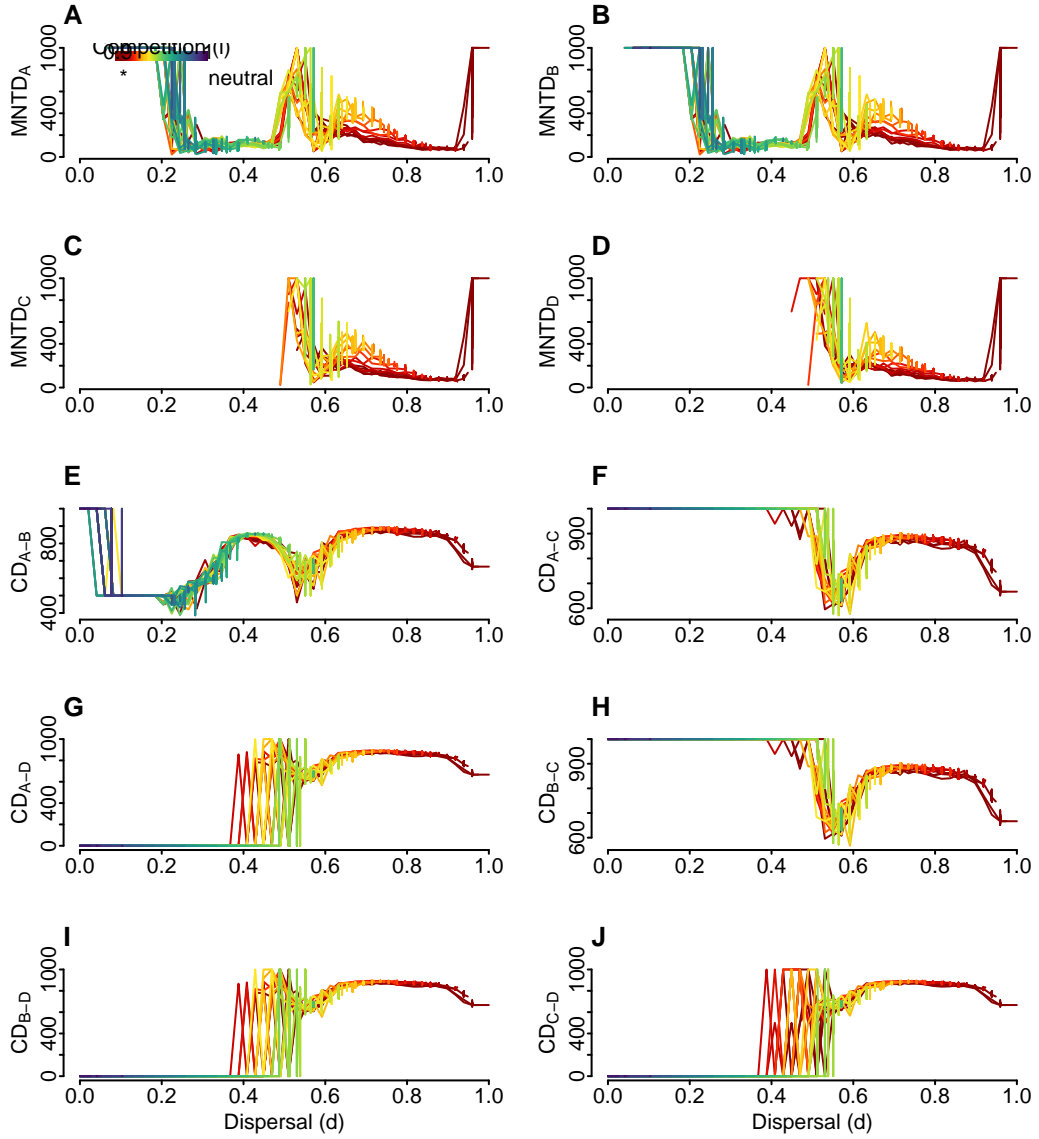


Figure 37: Additional summary statistics for MET through initial dispersal values. Each line corresponds to simulations within a same competitive value, along dispersal ability. (A) Standardized value of the mean nearest taxon distance measure for the island A. (B) Standardized value of the mean nearest taxon distance measure for the island B. (C) Standardized value of the mean nearest taxon distance measure for the island C. (D) Standardized value of the mean nearest taxon distance measure for the island D. (E) Standardized Community Distance between island A and B. It is the beta diversity version of Mean Pairwise Distance (MPD), giving the average phylogenetic distance between two communities. (F) Standardized Community Distance between island A and C. (G) Standardized Community Distance between island A and D. (H) Standardized Community Distance between island B and C. (I) Standardized Community Distance between island B and D. (J) Standardized Community Distance between island C and D.

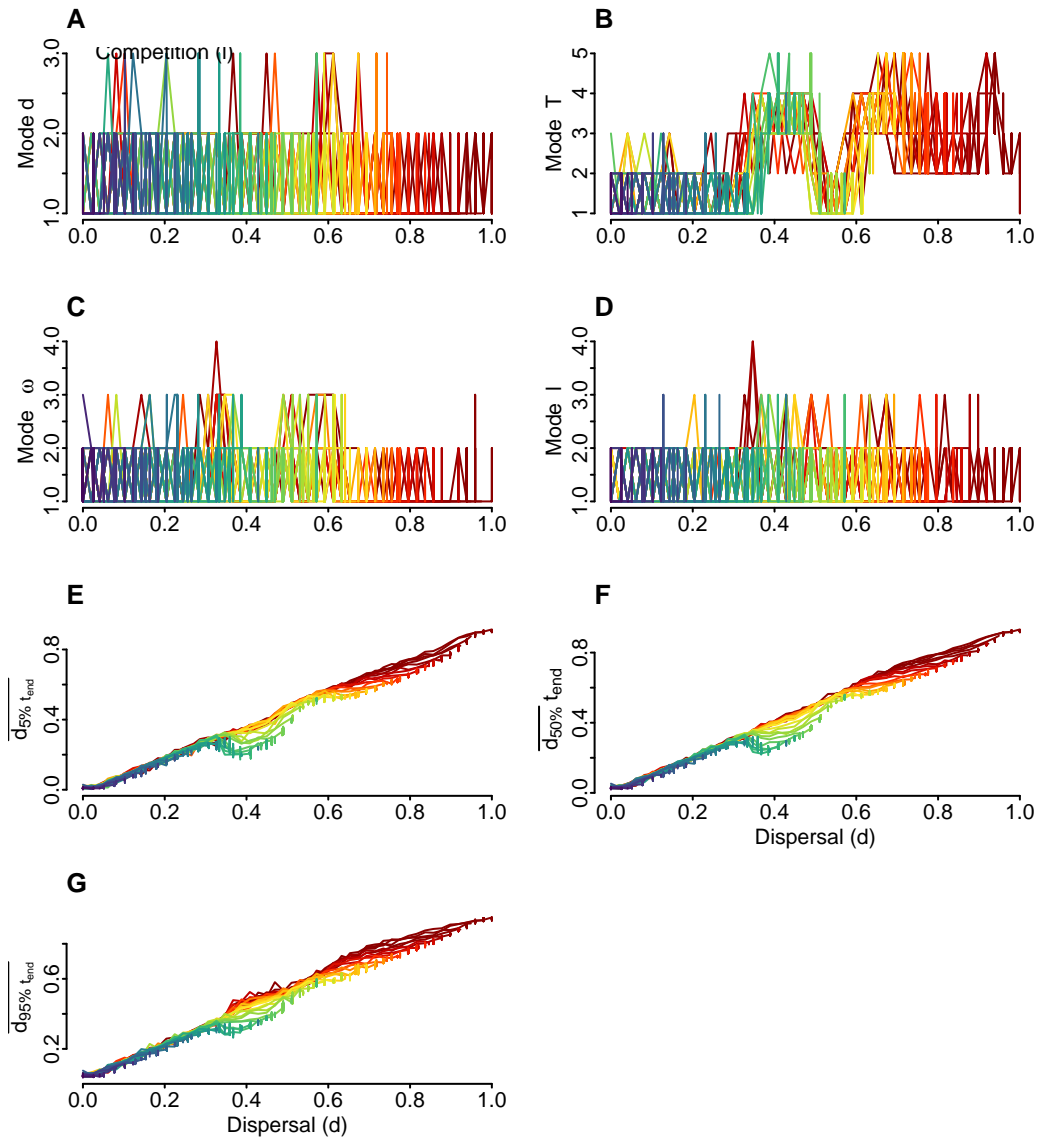


Figure 38: Additional summary statistics for MET through initial dispersal values. Each line corresponds to simulations within a same competitive value, along dispersal ability. (A) Number of modes at the dispersal trait distribution at final timestep, i.e. no modes (such as in a uniform distribution), or more. Calculated with the function ‘Mode’ from package LaplacesDemon. (B) Number of modes at the thermal optimum distribution at final timestep. (C) Number of modes at the thermal range trait distribution at final timestep. (D) Number of modes at the competition trait (i.e. tolerance to other species) distribution at final timestep. (E) Mean dispersal trait of its 5% quantile at final timestep. (F) Mean dispersal trait at final timestep. (G) Mean dispersal trait of its 95% quantile at final timestep.

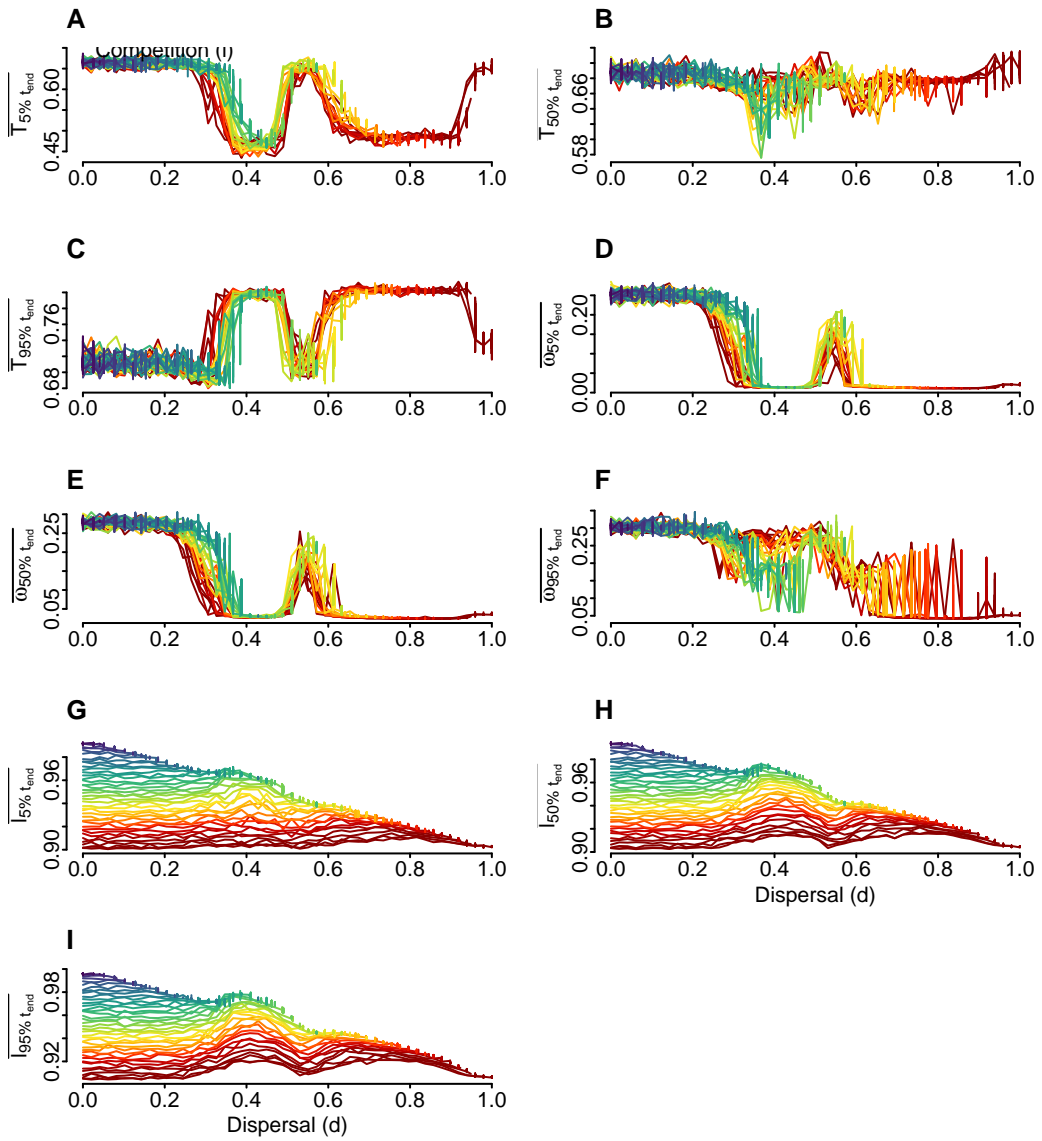


Figure 39: Additional summary statistics for MET through initial dispersal values. Each line corresponds to simulations within a same competitive value, along dispersal ability. (A) Mean thermal optimum of its 5% quantile at final timestep. (B) Mean thermal optimum at final timestep. (C) Mean thermal optimum of its 95% quantile at final timestep. (D) Mean thermal range trait of its 5% quantile at final timestep. (E) Mean thermal range trait at final timestep. (F) Mean thermal range trait of its 95% quantile at final timestep. (G) Mean tolerance to other species trait of its 5% quantile at final timestep. (H) Mean tolerance to other species trait at final timestep. (I) Mean tolerance to other species trait of its 95% quantile at final timestep.

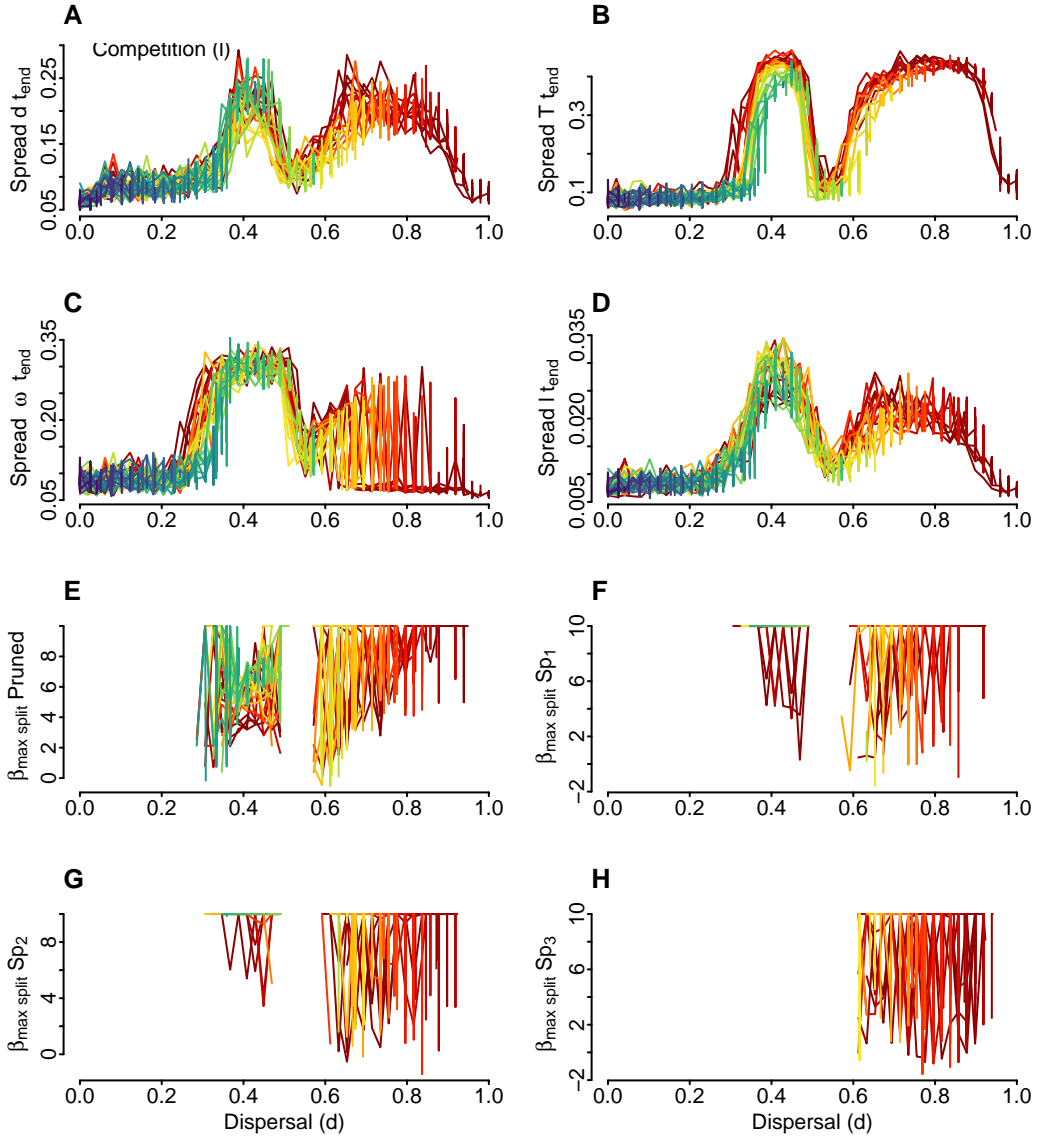


Figure 40: Additional summary statistics for MET through initial dispersal values. Each line corresponds to simulations within a same competitive value, along dispersal ability. (A) The range between the lowest and highest dispersal trait values at the final timestep. (B) The range between the lowest and highest thermal optimum values at the final timestep. (C) The range between the lowest and highest thermal range trait values at the final timestep. (D) The range between the lowest and highest tolerance to other species trait values at the final timestep. (E) The pruned phylogeny beta value, excluding extinct branches, derived from the Maximum Likelihood estimation within the Beta-splitting model. (F) The pruned phylogeny beta value of species 1, excluding extinct branches. (G) The pruned phylogeny beta value of species 2, excluding extinct branches. (H) The pruned phylogeny beta value of species 3, excluding extinct branches.

a very strong negative correlation (-0.74), suggesting that in the MET model, the impact of temperature tolerance on species numbers is even more significant.

Trait Changes

Figure 43 illustrates the variations in trait changes for the models M0, ME, and MET across different ecological parameters: dispersal, tolerance to other species, thermal range, and thermal optimum. Each model's (i.e. columns) shows the slope of trait change between the initial and final timesteps, offering insights into how these traits evolve over time under different conditions and assumptions. The use of color gradients conveys the intensity of competition affecting these traits, with warmer colors indicating higher levels of competition. This visualization underscores the complex interplay between competition and trait adaptability in ecological models, highlighting how traits like dispersal capacity and temperature tolerance shift in response to environmental pressures and species interactions.

Figure 44 presents the final gamma richness in relation to various mean parameter values at the final timestep, including thermal range, dispersal, and heterospecific interaction coefficient, across the models M0, ME, and MET. The columns for each model demonstrate the impact of these parameters on biodiversity, utilizing color gradients to represent the strength of competition and dispersal. The analysis of these relationships stresses the critical roles that temperature tolerance, dispersal capabilities, and interactions with other species play in shaping community richness and diversity.

Figure 45 depicts the final gamma richness plotted against the mean trait changes, illustrating the slope between initial and final trait values for all species within the models M0, ME, and MET. It examines traits such as thermal range, dispersal, and heterospecific interaction coefficient, segmented by each model in separate columns. Two color gradients are used for the strength of competition and dispersal. This visualization effectively showcases the linkage between trait adaptability and community richness, emphasizing the importance of assumptions to evolutionary responses to environmental and interspecific pressures in determining ecological outcomes.

Further analysis

Additional, we explore the intricate dynamics of species interaction and environmental adaptation through a series of figures. Figure Figure 46 showcases the final mean dispersal trait (d), plotted against final the mean competitive trait (l) (i.e. tolerance to other species), thermal optimum (T), and thermal range (ω) across Models MO, ME, and MET (Figure 46 Figure A-I). Further expanding on ecological theories, Figure Figure 47 delves into the theory of limiting similarity, illustrating how signals for species diversity impacting average population sizes through competitive exclusion. Lastly, Figure Figure 48 juxtaposes speciation versus extinction percentages with temporal stability in macroevolutionary events. This figure not

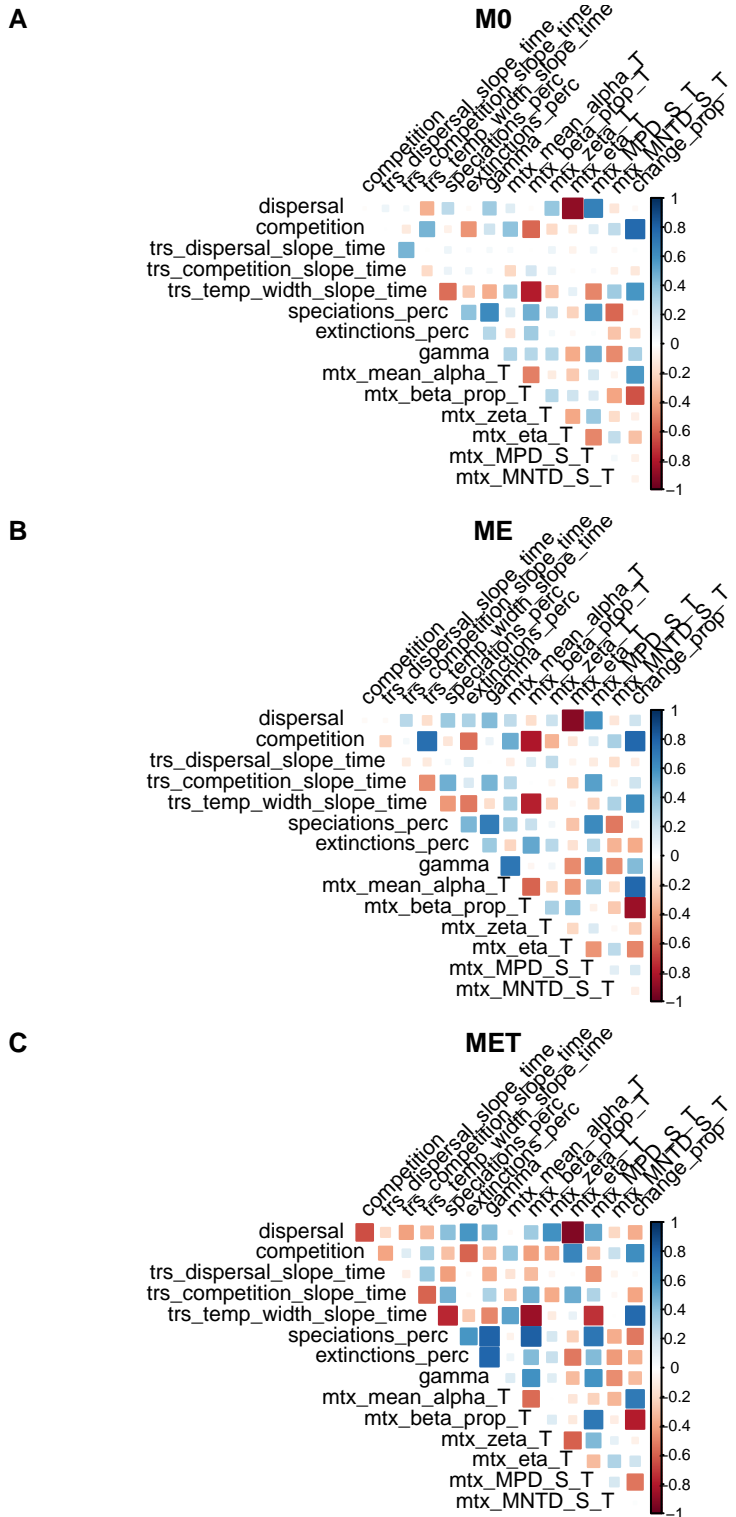


Figure 41: Correlations for hand-picked summary statistics for M0 (A); ME (B) and MET (C).

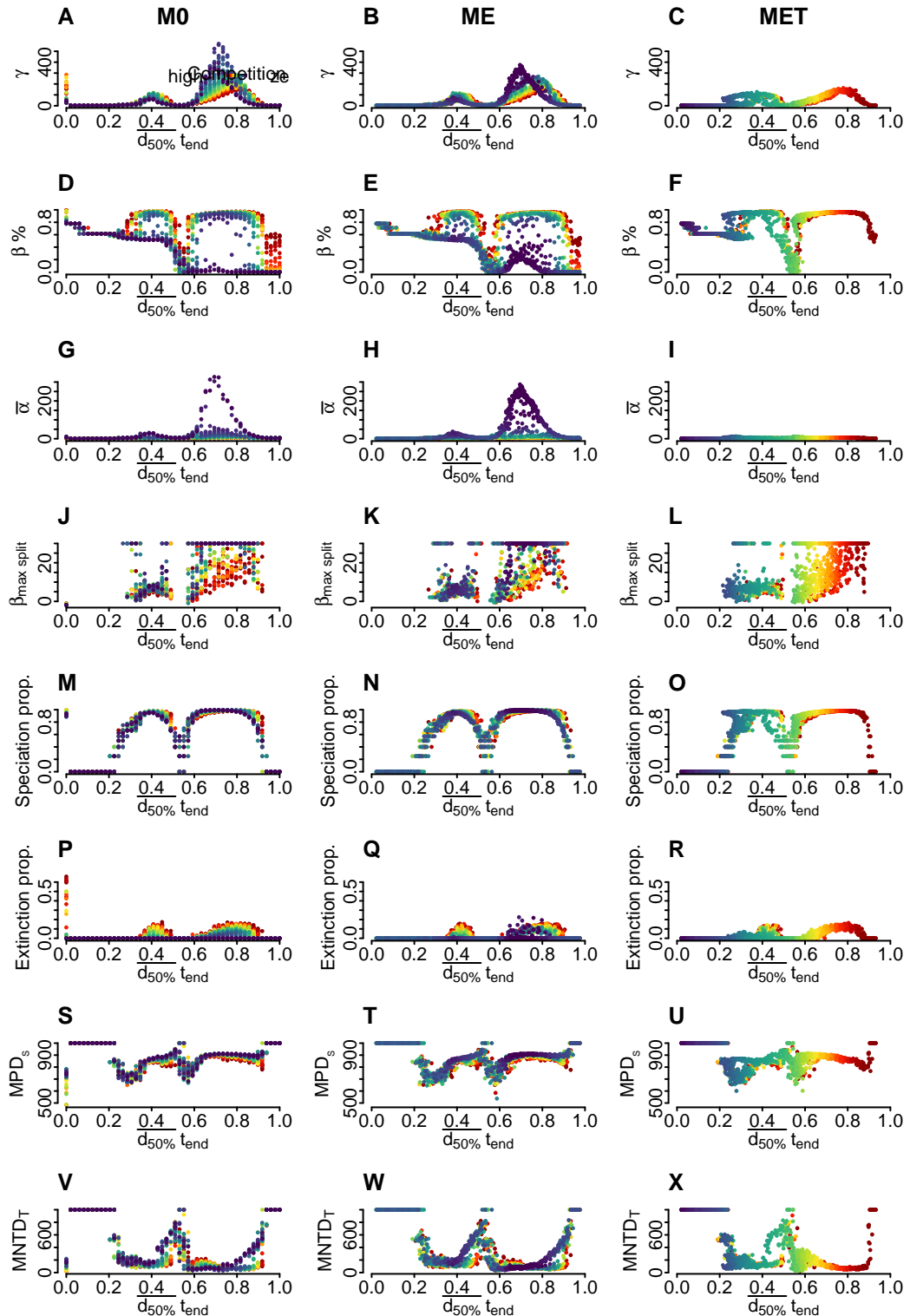


Figure 42: Comparison of M0, ME and MET for 8 summary statistics. Dispersal x axis plot the mean dispersal trait at the end of the simulation, rather than the initial dispersal parameter d . The same applies for the competition values that color the points

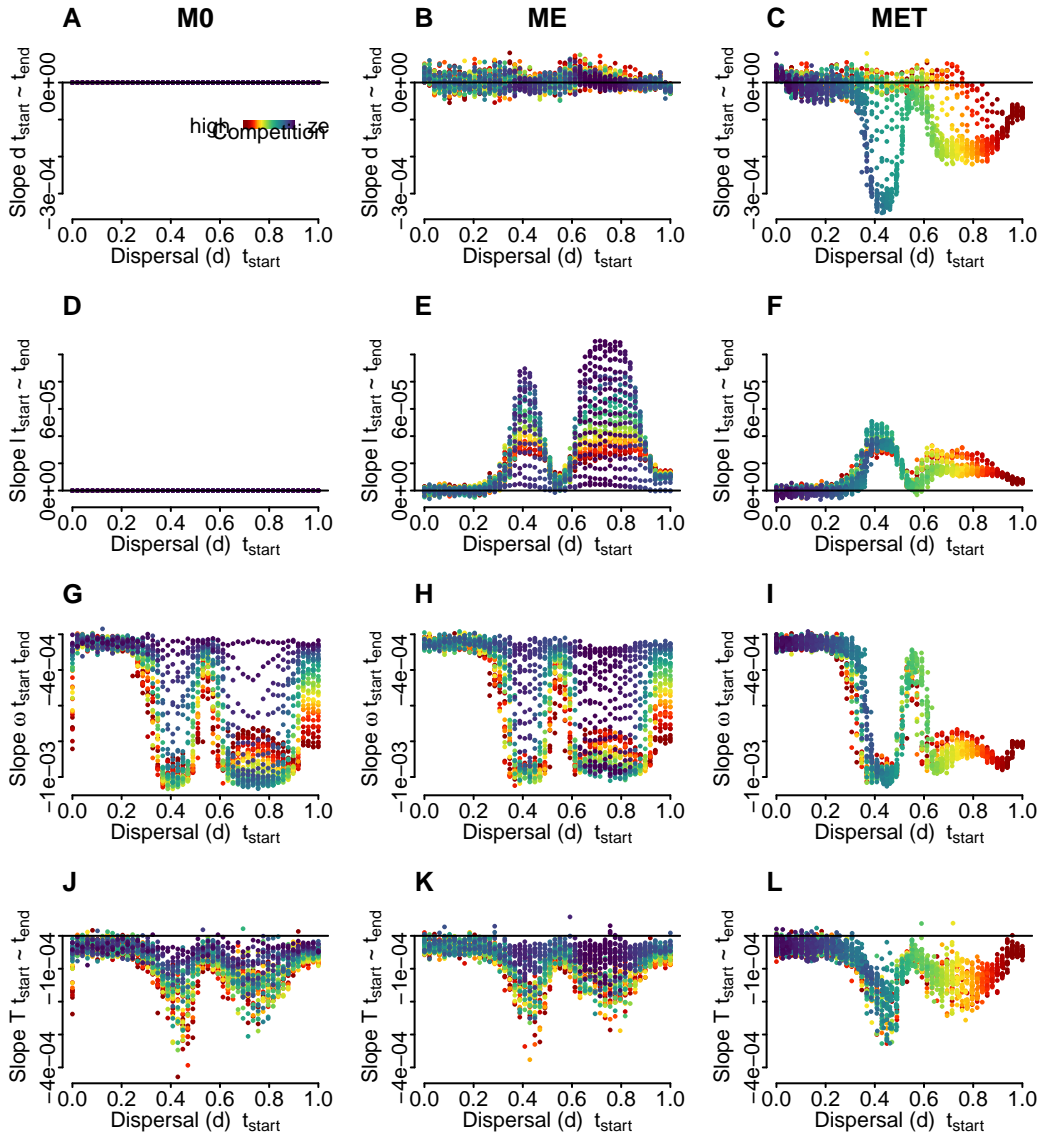


Figure 43: Slopes of trait change for M0, ME and MET (columns) between initial and final timestep, i.e. dispersal (A-C), tolerance to other species (D-F), thermal range (G-I), thermal optimum (J-L). The warmer the color the higher the competition.

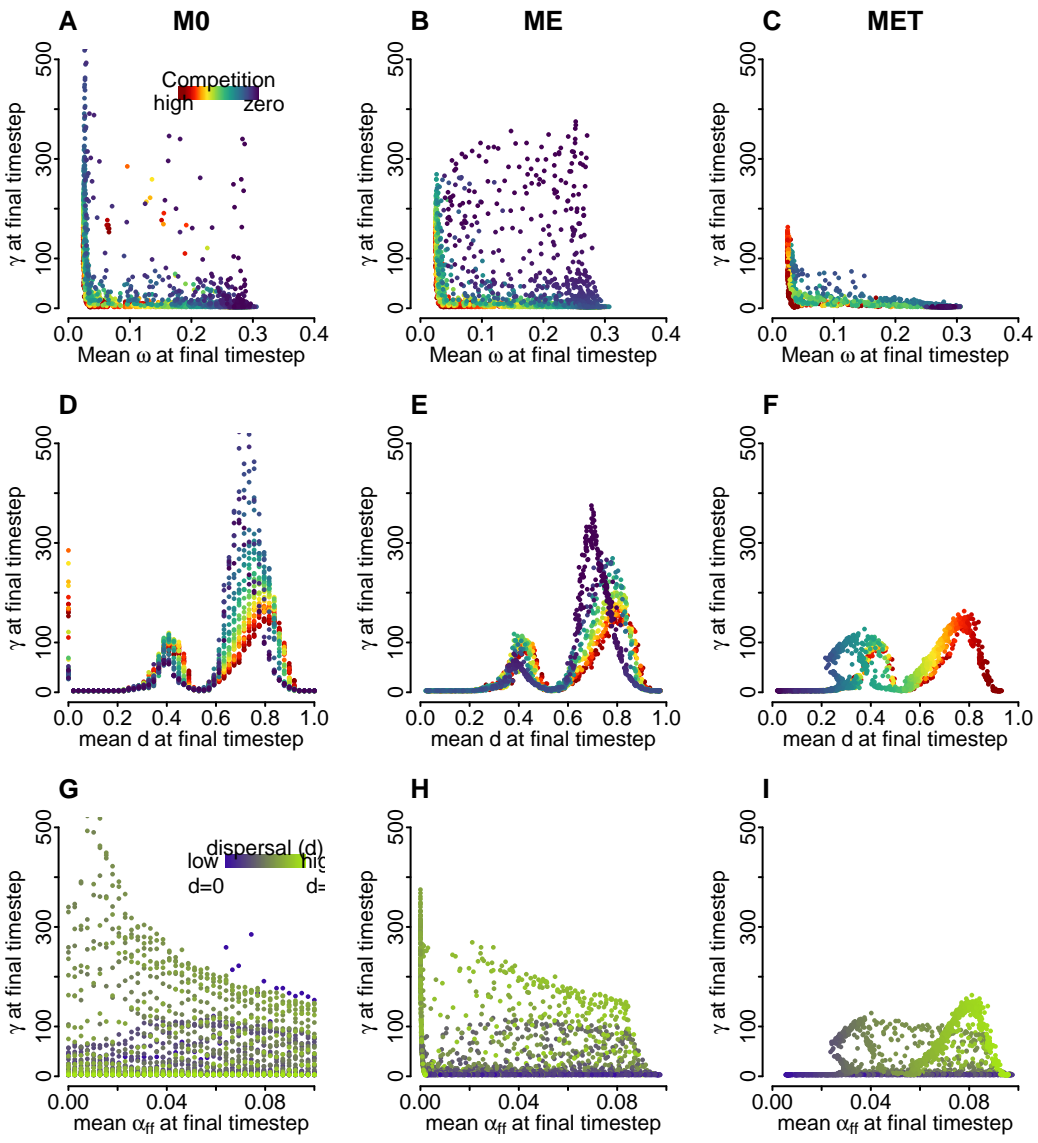


Figure 44: Final gamma richness at final timestep against different final mean parameter values (i.e. thermal range A-C, Dispersal D-F, Heterospecific interaction coefficient G-I) for Models MO, ME and MET on each column. Two color gradients are used, one for the strength of competition (A-F) and the other for the strength of dispersal (G-I).

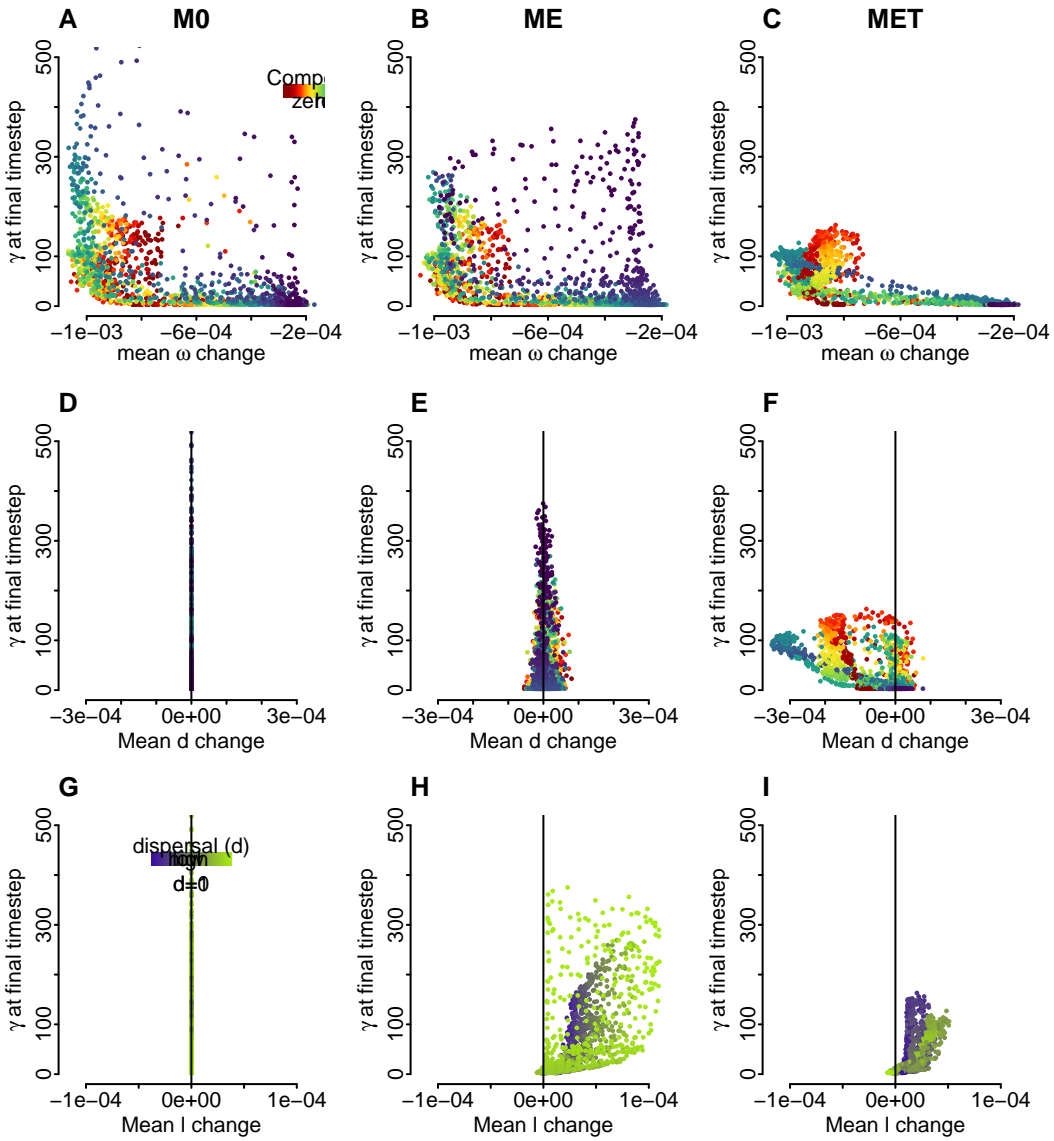


Figure 45: Final gamma richness at the last timestep plotted against the mean trait changes, which represent the slope between the initial and final trait values for all species. The mean trait is shown for thermal range A-C, dispersal D-F, and heterospecific interaction coefficient G-I for Models MO, ME, and MET in each column. Two color gradients are used, one for the strength of competition (A-F) and the other for the strength of dispersal (G-I).

only highlights the impact of interspecific competition on biodiversity outcomes but also shows temporal invariability fo the macroevolutionary processes (Figure 48 D-F).

Handpicked simulation

Examining a single simulation, specifically how trait changed though time for each species enables us to closely investigate the implemented processes in action (Figure 50). We select a simulation with initial $l=9.56$ and $d=0.367$, thus sampling initial value of l that leads to moderate competition and within connectivity regime κ_1 . Moreover, in all simulations island C remained occupied by only one species, serving as a control on biodiversity while island D is never occupied (Figure 51). As implemented, l and d did not change though time for M0 (Figure 50 I,M). Note single black isolated line that corresponds to single species in island C (Figure 50 E,F,G,J,K,O).

All models exhibit rapid niche specialization around 1 Ma, characterized by a decrease in and the expansion of T. The inclusion of trait evolution (i.e. ME and MET) illustrates the swift evolution of tolerance to other species' traits (l) in the presence of other species. Note isolated species in island C, with clearly lower final l than species present in islands A and B (Figure 50 J,K). However, this tolerance is less pronounced when a trade-off exists between d and l . Furthermore, the ME and MET simulations reveal a less abrupt decrease in niche width, though thermal range, compared to M0, as the latter only allows for species to escape competition in this form (i.e. no l or d evolution). In MET simulations, the trade-off deviates d evolution from a more neutral case, i.e. ME. Spatial patterns diverge among the models, with biodiversity hotspots shifting towards the center of the island - at this specific simulation (Figure 51 A,B,C) while the frequency of local extinctions consistently rises during periods of increased environmental variability (i.e. 2.5-0 Ma), impacting α diversity but without any global extinction (Figure 51 G,H,I).

The described cycle can be depicted at Figure 49, where a flowchart illustrates eco-evolutionary dynamics observed in M0, ME, and MET, which are relevant to biodiversity. All processes depicted are strongly influenced by dispersal and landscape structure. Changes in diversity influence heterospecific competition. Subsequently, a transition occurs towards niche specialization, suggesting that species evolve to occupy specific ecological niches as they compete, such as a decrease in thermal range (ω). This specialization may lead to a reduction in species' geographical range (i.e. local extinctions). If global extinction happens, diversity is negatively impacted (red arrow Figure 49). Conversely, if extinction is averted, the flow progresses to isolation, suggesting that species may become isolated in particular habitats or environments. From isolation, there arises potential for speciation though isolation fostering the emergence of new species (if they global extinction is avoided). If speciation unfolds, the flow completes a loop, contributing to diversity (blue arrow Figure 49). Overall, Figure 49 exemplifies the interconnectedness of ecological and evolutionary processes and the delicate balance between

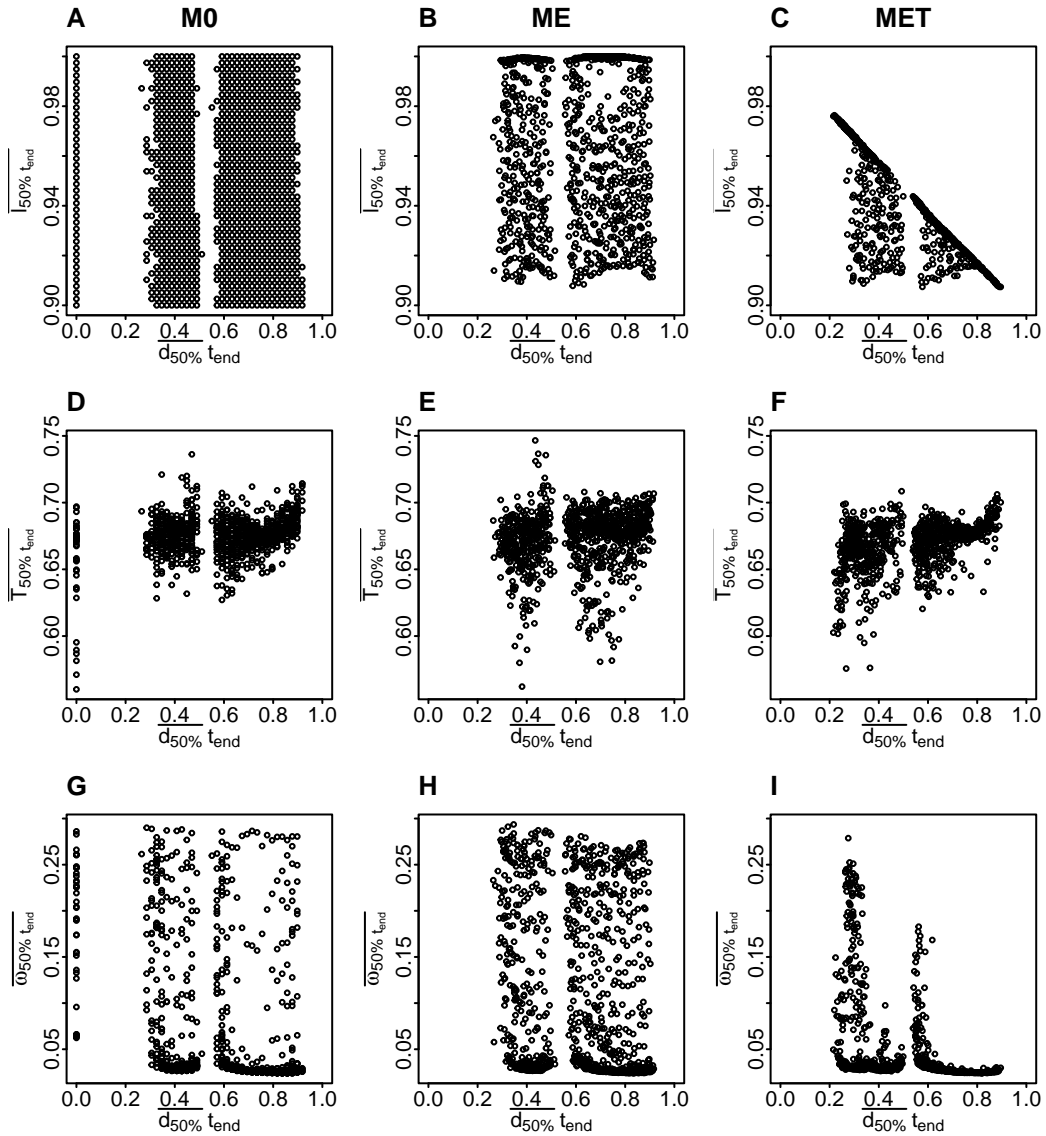


Figure 46: Final mean traits at last timestep are plotted against the mean trait changes. The mean trait is shown for tolerance to other species A-C, thermal optimum D-F, and thermal range G-I for Models MO, ME, and MET in each column.

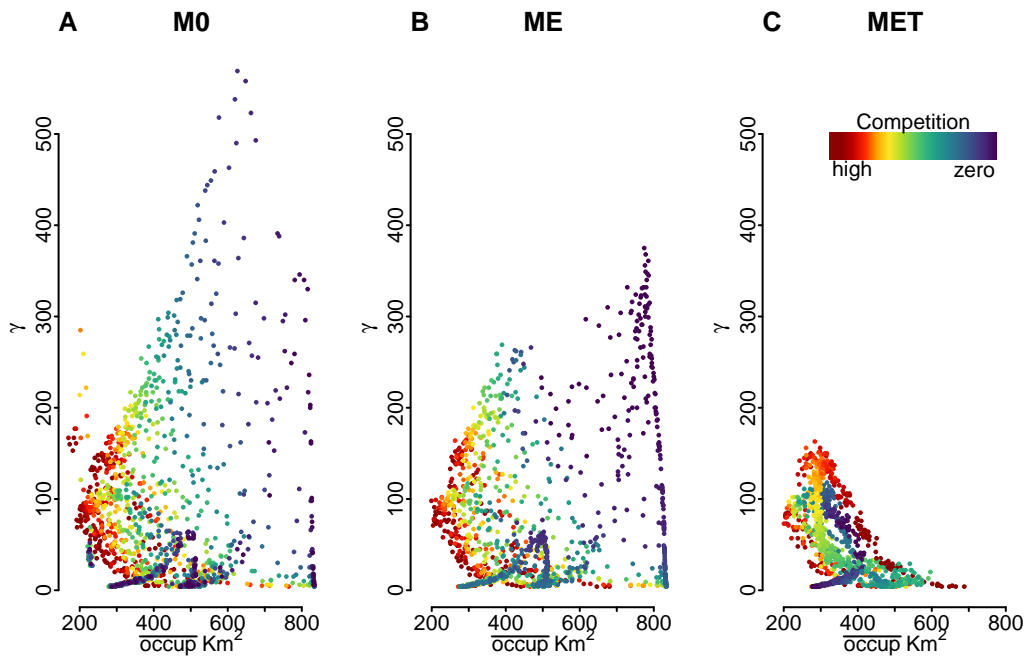


Figure 47: The theory of limiting similarity predicts that as species diversity increases, the average occupation decreases due to the need for coexisting species to be sufficiently different to coexist, resulting in lower occupation, as well as population sizes, when higher competition is present.

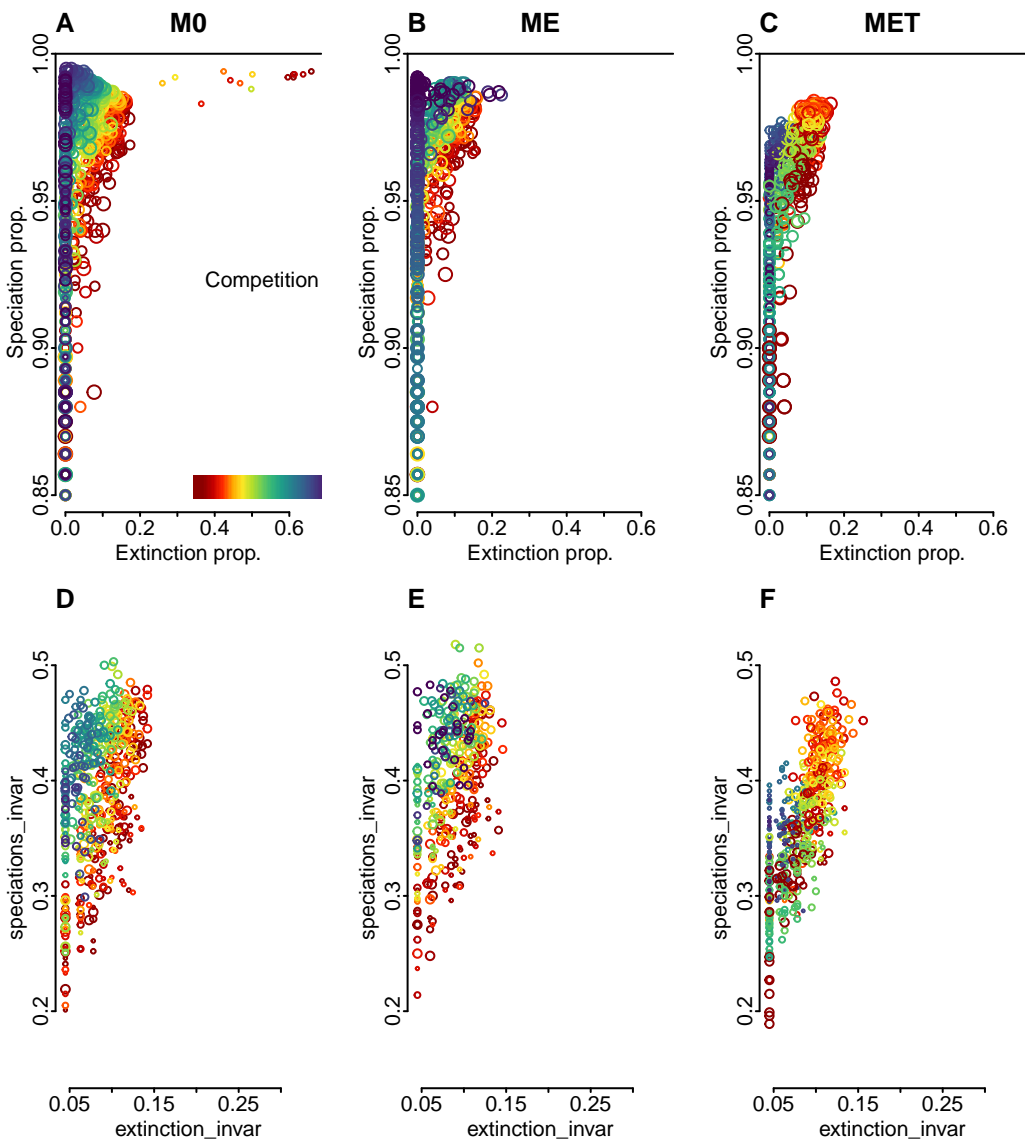


Figure 48: Speciation versus extinction percentage (A-C) and temporal invariability (i.e. temporal stability of macroevolutionary events) (D-F). Circles size are relative to mean dispersal trait at the final timestep. MET was the only model that show increased interspecific competition enhancing extinction and speciation.

competition, niche specialization, geographical range changes, extinction, isolation, and speciation in shaping biodiversity dynamics. It highlights a cyclic pattern in a delicate balance where local extinction can stimulate renewed diversity.

References

- Bortolussi, N., E. Durand, M. Blum, and O. Francois. 2006. “apTreeshape: Statistical Analysis of Phylogenetic Tree Shape.” *Bioinformatics* 22 (3): 363–64. <https://doi.org/10.1093/bioinformatics/bti798>.
- Castiglione, Silvia, Carmela Serio, Martina Piccolo, Alessandro Mondanaro, Marina Melchionna, Mirko Di Febbraro, Gabriele Sansalone, Stephen Wroe, and Pasquale Raia. 2021. “The Influence of Domestication, Insularity and Sociality on the Tempo and Mode of Brain Size Evolution in Mammals.” *Biological Journal of the Linnean Society* 132 (1): 221–31. <https://doi.org/10.1093/biolinmean/blaa186>.
- Hagen, Oskar, Benjamin Flück, Fabian Fopp, Juliano S. Cabral, Florian Hartig, Mikael Pontarp, Thiago F. Rangel, and Loïc Pellissier. 2021. “Gen3sis: A General Engine for Eco-Evolutionary Simulations of the Processes That Shape Earth’s Biodiversity.” *PLoS Biology* 19 (7): e3001340. <https://doi.org/10.1371/journal.pbio.3001340>.

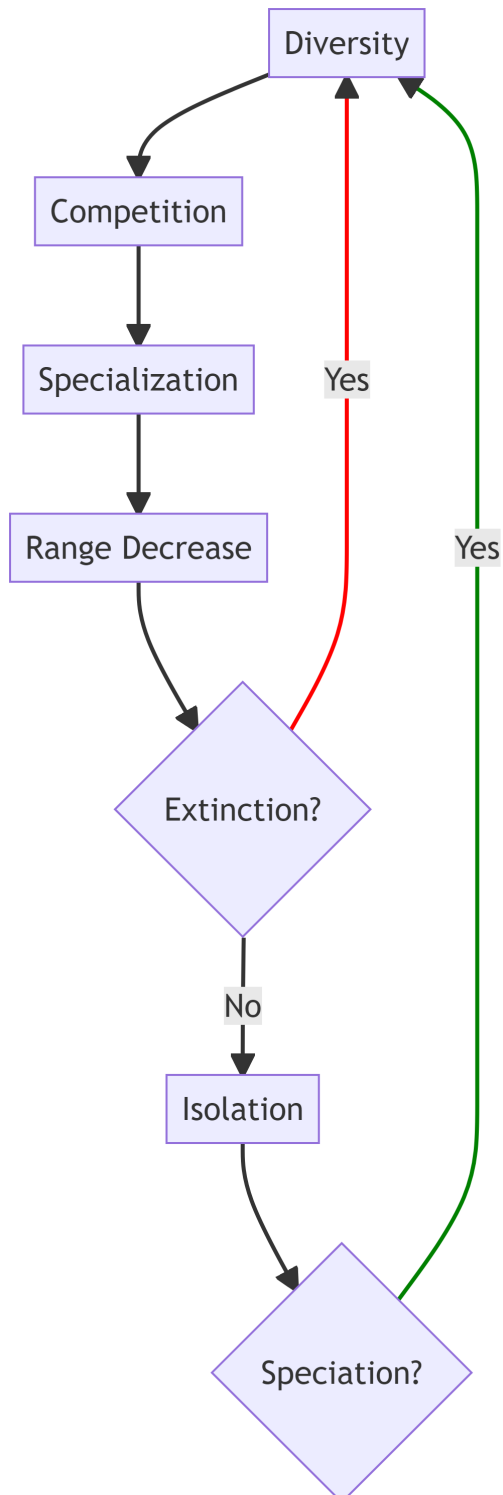


Figure 49: Flowchart of general eco-evolutionary dynamics in M0, ME, and MET, showing one simulated feedback loop relevant to biodiversity when competition is present and there is appropriate environmental structure and dispersal ability.

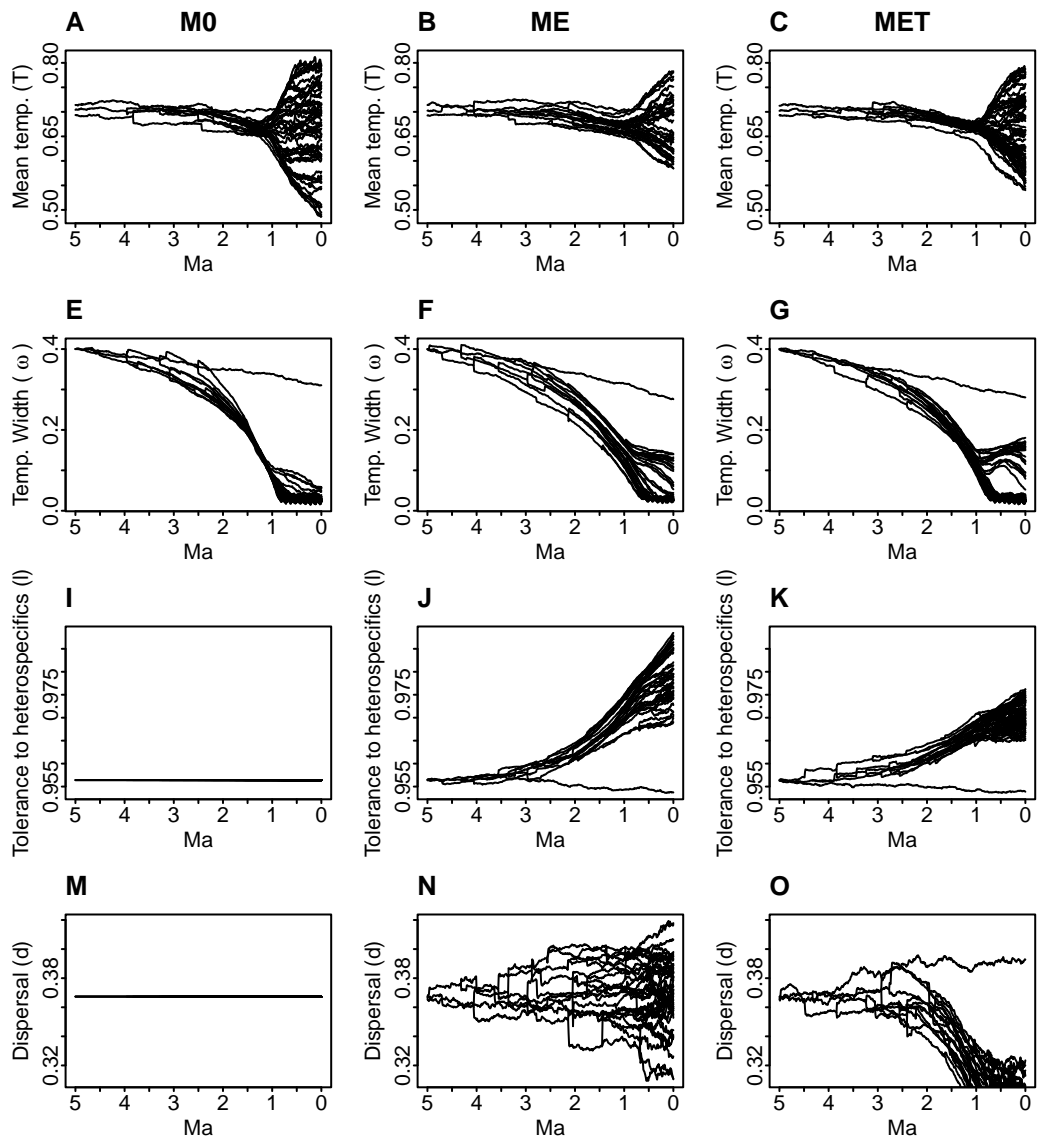


Figure 50: Trait change through time for a single simulation, i.e. config_1119, with same initial parameters $d=0.367$, $l=0.956$ for M0, ME and MET, respectively with 63, 46 and 69 species alive at the final timestep.

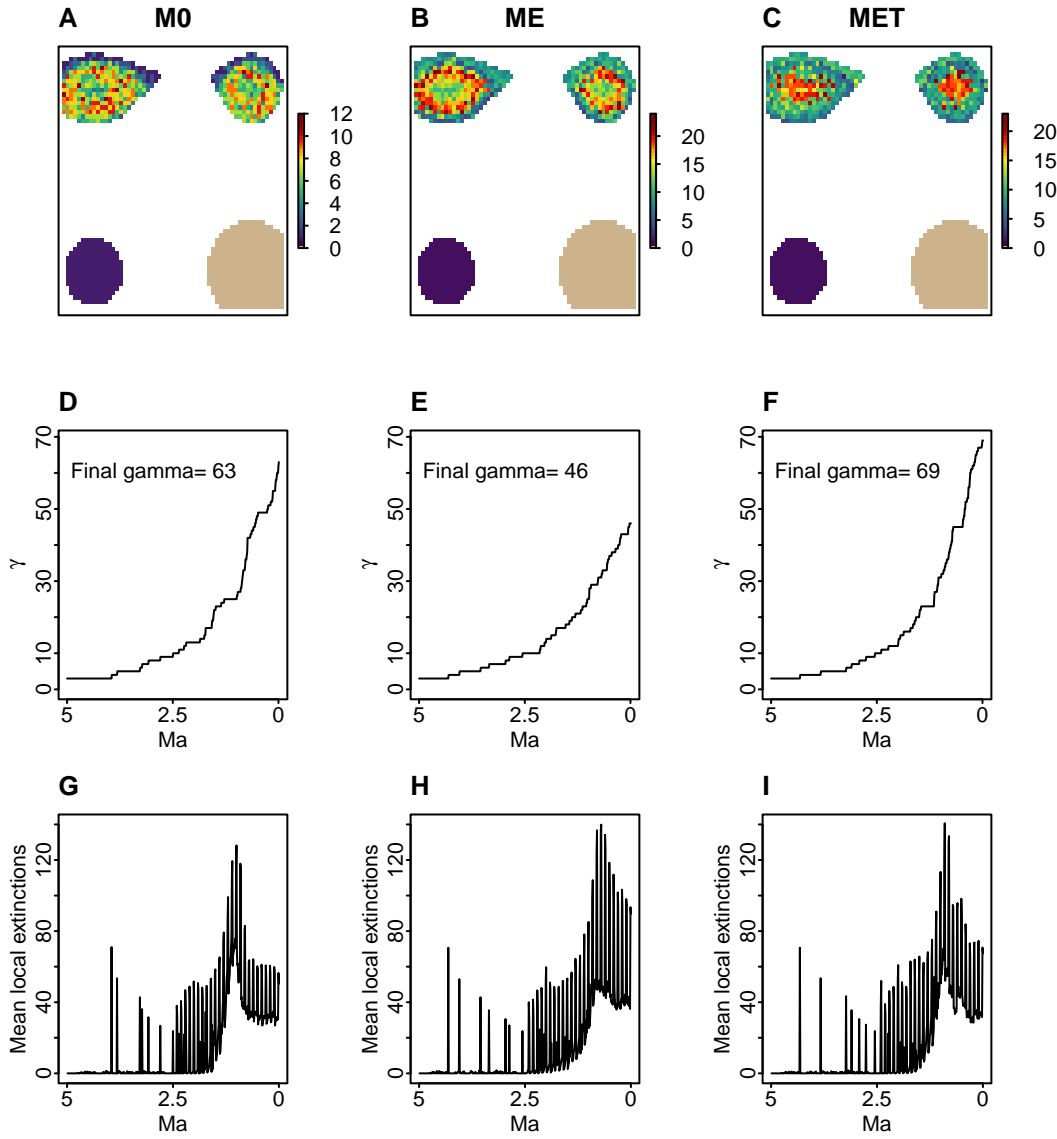


Figure 51: Trait change through time for a single simulation, with same initial parameters $d=0.367$, $l=0.956$ for ME and MET, respectively with 63, 46 and 69 species alive at the final timestep.

- Hoffmann, Ary A., and Carla M. Sgrò. 2011. “Climate Change and Evolutionary Adaptation.” *Nature* 470 (7335): 479–85. <https://doi.org/10.1038/nature09670>.
- Kembel, S. W., P. D. Cowan, M. R. Helmus, W. K. Cornwell, H. Morlon, D. D. Ackerly, S. P. Blomberg, and C. O. Webb. 2010. “Picante: R Tools for Integrating Phylogenies and Ecology.” *Bioinformatics* 26 (11): 1463–64. <https://doi.org/10.1093/bioinformatics/btq166>.
- Pillans, Brad, John Chappell, and Tim R. Naish. 1998. “A Review of the Milankovitch Climatic Beat: Template for Plio–Pleistocene Sea-Level Changes and Sequence Stratigraphy.” *Sedimentary Geology* 122 (1-4): 5–21. [https://doi.org/10.1016/S0037-0738\(98\)00095-5](https://doi.org/10.1016/S0037-0738(98)00095-5).
- Shepard, Christopher, Jon D. Pelletier, Marcel G. Schaap, and Craig Rasmussen. 2018. “Signatures of Obliquity and Eccentricity in Soil Chronosequences.” *Geophysical Research Letters* 45 (20): 11, 147–11, 153. <https://doi.org/10.1029/2018GL078583>.
- Vasconcelos, T. N. C., S. Alcantara, C. O. Andrino, F. Forest, M. Reginato, M. F. Simon, and J. R. Pirani. 2020. “Fast Diversification Through a Mosaic of Evolutionary Histories Characterizes the Endemic Flora of Ancient Neotropical Mountains.” *Proceedings of the Royal Society B: Biological Sciences* 287 (1923): 20192933. <https://doi.org/10.1098/rspb.2019.2933>.
- Westerhold, Thomas, Norbert Marwan, Anna Joy Drury, Diederik Liebrand, Claudia Agnini, Eleni Anagnostou, James S. K. Barnet, et al. 2020. “An Astronomically Dated Record of Earth’s Climate and Its Predictability over the Last 66 Million Years.” *Science* 369 (6509): 1383–87. <https://doi.org/10.1126/science.aba6853>.